



# **The Use of Image Processing to Determine Cell Defects in Polycrystalline Solar Modules**

**By: Peter Banda**

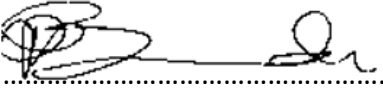
Submitted in fulfillment of the requirements for the degree of  
Master of Science, in the Faculty of Science  
at the Nelson Mandela University

Supervisor: **Dr. Lynette Barnard**. Co-Supervisor: **Dr. Frederik Vorster**

March 2019

# DECLARATION

I, Peter Banda, hereby declare that the dissertation for the degree Master of Science in Computer Science and Information Systems is my own work and that it has not previously been submitted for assessment of completion of any postgraduate qualification to another university or for another qualification.

A handwritten signature in black ink, consisting of a large, stylized initial 'P' followed by a series of loops and a final flourish, all resting on a dotted horizontal line.

Peter Banda

## **ACKNOWLEDGMENTS**

I would like to express my heartfelt gratitude to my supervisor, Dr Lynette Barnard, for her support, motivation and invaluable assistance throughout this research. I would also like to thank my Co-supervisor, Dr Frederik Vorster, for providing his expertise in Photovoltaics and for his interest in this project.

I would like to thank both staff and students in the Department of Computing Sciences for their support. Many thanks to the technical staff for stepping in whenever I encountered technical issues.

Lastly, I would like to thank my father for the financial support he provided during this research. I would like to express my gratitude to my family and friends for their much-needed support during the course of my research. For that, I am truly grateful.

## SUMMARY

This research aims to use image processing to determine cell defects in polycrystalline solar modules. Image processing is a process of enhancing images for different applications. One domain that seems to not yet utilise the use of image processing, is photovoltaics.

An increased use of fossil fuels is damaging the earth and a call to protect the earth has resulted in the emergence of pollutant-free technologies such as polycrystalline photovoltaic (PV) cells, which are connected to make up solar modules. However, defects often affect the performance of PV cells and consequently solar modules. Electroluminescence (EL) images are used to examine polycrystalline solar (PV) modules to determine if the modules are defective.

The main research question that this research addressed is *“How can an image processing technique be used to effectively identify defective polycrystalline PV cells from EL images of such cells?”*. The experimental research methodology was used to address the main research question.

The initial investigation into the problem revealed that certain sectors within industry, as well as the Physics Department at Nelson Mandela University (NMU), do not currently utilise image processing when examining EL images of solar modules. The current process is a tedious, manual process whereby solar modules are manually inspected. An analysis of the current processes enabled the identification of ways in which to automatically examine EL images of solar modules.

An analysis of literature provided a better understanding of the different techniques that are used to examine solar modules, and it was identified how image processing can be applied to EL images. Further analysis of literature provided a better understanding of image processing and how image classification experiments using Deep Learning (DL) as an image processing technique can be used to address the main research question. The outcome of the experiments conducted in this research were different adaptive models (LeNet, MobileNet, Xception) that can classify EL images of PV cells according to known standards used by the Physics Department at NMU. The known standards yielded four classes; normal, uncritical, critical and very critical, which were used for the classification of EL images of PV cells.

The adaptive models were evaluated to obtain the precision, recall and  $F_1$  – score of the models. The precision, recall, and  $F_1$  – score were required to determine how effective the models were in identifying defective PV cells from EL images. The results indicated that an image processing technique can be used to identify defective polycrystalline PV cells from EL images of such cells. However, further research needs to be conducted to improve the effectiveness of the adaptive models.

**Keywords**

Image Processing, Deep Learning, Photovoltaics, Electroluminescence

## GLOSSARY

<b>Term</b>	<b>Definition</b>
<i>Adam</i>	Adaptive Momentum Estimation
<i>AI</i>	Artificial Intelligence
<i>CNN</i>	Convolutional Neural Network
<i>DL</i>	Deep Learning
<i>EL</i>	Electroluminescence
<i>Epoch</i>	Number of times iterations are made through data when training an adaptive model
<i>ML</i>	Machine Learning
<i>NN</i>	Neural Network
<i>PV</i>	Photovoltaic

# CONTENTS

1 Introduction .....	1
1.1 Background.....	1
1.2 Problem Statement .....	2
1.3 Thesis statement .....	2
1.4 Research Questions.....	2
1.5 Project Goal.....	3
1.6 Project Scope and Risks.....	3
1.7 Research Methodology .....	4
1.8 Dissertation Structure .....	4
2 Research Design .....	6
2.1 Introduction.....	6
2.2 Research Onion .....	6
2.2.1 Research Philosophy .....	6
2.2.2 Approach.....	7
2.2.3 Strategy .....	10
2.2.4 Techniques .....	12
2.3 Research Methodology .....	13
2.4 Summary .....	14
3 Literature Review: Photovoltaics .....	16
3.1 Introduction.....	16
3.2 Photovoltaic (PV) Technologies.....	16
3.2.1 Single-crystalline Si.....	18
3.2.2 Multi-crystalline/Polycrystalline Si.....	18
3.2.3 Thin Film PV materials.....	18
3.3 Photovoltaic (PV) module design .....	19
3.4 Photovoltaic (PV) cell defects.....	20
3.5 Identifying Photovoltaic (PV) cell defects .....	21
3.5.1 Electroluminescence (EL) .....	21
3.5.2 Large-area laser beam induction current (LA-LBIC).....	22
3.5.3 Current-Voltage (I-V) characteristics .....	23
3.5.4 Light Infrared Imaging .....	24
3.6 Proposed integration.....	25
3.7 Summary .....	26
4 Literature Review: Computer Vision .....	28
4.1 Introduction.....	28
4.2 Computer Vision.....	29
4.3 Image Processing.....	31
4.3.1 Image Pre-processing.....	33
4.3.2 Deep Learning (DL).....	36
4.3.3 Image Classification.....	45
4.3.4 Pattern Recognition .....	49

4.4	Related Work.....	50
4.4.1	Medical Image Analysis.....	50
4.4.2	Feature Learning and Image Classification .....	51
4.5	Preliminary Investigation of Implementation Tools .....	52
4.6	Summary .....	53
5	Experimental Design and Implementation .....	55
5.1	Introduction.....	55
5.2	A proposed solution for automatic identification of defective photovoltaic (PV) cells .....	56
5.3	Experimental Design.....	58
5.3.1	Data processing.....	60
5.3.2	Experimental Setup.....	60
5.4	Experiment Implementation .....	64
5.5	Experimental Procedure.....	66
5.5.1	Learning Techniques and Experiment Groups .....	67
5.5.2	Performance – Phase One (Binary Classification).....	70
5.5.3	Performance – Phase Two (Multi-class classification).....	72
5.6	Evaluation Plan .....	74
5.7	Summary .....	76
6	Experimental Results.....	78
6.1	Introduction.....	78
6.2	Image Classification Results .....	79
6.2.1	Training from Scratch.....	80
6.2.2	Transfer Learning (TL) .....	83
6.2.3	Model Evaluation .....	84
6.3	Conclusion .....	89
7	Conclusion .....	90
7.1	Introduction.....	90
7.2	Research Achievements .....	91
7.3	Contribution of Research .....	92
7.3.1	Theoretical Contributions .....	93
7.3.2	Practical Contributions.....	93
7.4	Problems Encountered.....	94
7.5	Limitation and Recommendations for Future Research.....	94
7.6	Summary .....	95
	References.....	97
	Appendices.....	106
	Appendix A – Article.....	106
	Appendix B – Results.....	113



## LIST OF FIGURES

Figure 1-1: Dissertation structure .....	5
Figure 2-1: The research onion (Saunders et al., 2008).....	7
Figure 2-2: Research approach .....	9
Figure 2-3: Research strategy .....	11
Figure 2-4: Research methodology .....	14
Figure 3-1: Chapter overview.....	17
Figure 3-2: Images showing examples of PV devices a) Single-crystalline Si PV cell, b) multi-crystalline/polycrystalline Si PV cell, c) thin film PV device.....	18
Figure 3-3: Two PV cells connected in series .....	19
Figure 3-4: Scanned EL images of part of a PV modules a) The PV module without defects, b) non-functional PV module, c) PV module with cracked cells (Friedrischková & Horák, 2013).....	22
Figure 3-5: Laser beam induction current system (Rabha, Dimassi, Bouaïcha, Ezzaouia, & Bessais, 2009) .....	23
Figure 3-6: I-V characteristic curve of a PV cell.....	23
Figure 3-7: I-V curve of a normal PV cell from normal PV module vs an I-V curve of a defective PV cell in defective PV module (Schill, Brachmann, & Koehl, 2015).....	24
Figure 3-8: A greyscale thermal image of a string of PV modules with a single defective cell .....	25
Figure 4-1: Chapter overview.....	29
Figure 4-2: Examples of global and local thresholding (Nicolosi et al., 2012) .....	34
Figure 4-3: Comparison of Canny and Sobel edge detection techniques.....	36
Figure 4-4: DL in relation to AI (Sze, Chen, & Yang, 2017).....	37
Figure 4-5: Biological neuron vs artificial neuron .....	38
Figure 4-6: High-level NN structure (Engelbrecht, 2007) .....	39
Figure 4-7: Illustration of gradient descent (Engelbrecht, 2007).....	41

Figure 4-8: High-level general CNN architecture (Patterson & Gibson, 2017) .....	43
Figure 4-9: Convolution function (Patterson & Gibson, 2017) .....	43
Figure 4-10: Image classification framework (Shu, McIsaac, Osinski, & Francis, 2017) .....	46
Figure 4-11: Image classification techniques (Affonso, Rossi, Vieira, & de Carvalho, 2017).....	47
Figure 4-12: LeNet CNN architecture (LeCun, Haffner, Bottou, & Bengio, 1999) .....	48
Figure 4-13: Example of X-ray images used in skeletal bone age assessment (Spampinato et al., 2017) .....	51
Figure 4-14: Driver assist system architecture (Chen, Seff, Kornhauser, & Xiao, 2015).....	52
Figure 5-1: Chapter overview.....	56
Figure 5-2: Existing method vs. stages of the proposed solution .....	57
Figure 5-3: Mock-up CNN for the initial phase of experiments (Ker, Wang, Rao, & Lim, 2018) .....	59
Figure 5-4: LeNet training history – (a) model accuracy; (b) model loss .....	70
Figure 5-5: VGG 16 training history – (a) model accuracy; (b) model loss .....	71
Figure 5-6: MobileNet training history – (a) model accuracy; (b) model loss .....	71
Figure 5-7: Xception training history – (a) model accuracy; (b) model loss .....	72
Figure 5-8: LeNet multi-classification training history – (a) model accuracy; (b) model loss.....	73
Figure 5-9: MobileNet multi-classification training history – (a) model accuracy; (b) model loss..	73
Figure 5-10: Xception multi-classification training history – (a) model accuracy; (b) model loss...	74
Figure 5-11: Confusion matrix for multi-class classification (Deng et al., 2016) .....	75
Figure 6-1: Chapter overview.....	79
Figure 6-2: VGG performance history on Dataset B .....	80
Figure 6-3: LeNet confusion matrix.....	85
Figure 6-4: MobileNet confusion matrix.....	86
Figure 6-5: Xception confusion matrix.....	87

Figure 7-1: Dissertation structure .....	90
Figure B-1: LeNet – Dataset B vs. Dataset C.....	113
Figure B-2: MobileNet – Dataset B vs. Dataset C.....	113
Figure B-3: Xception – Dataset B vs. Dataset C.....	113
Figure B-4:TL Xception – Dataset C vs. Xception - Dataset C.....	114

## LIST OF TABLES

Table 2-1: Research approach stages and chapter mapping .....	8
Table 3-1: Factors that influence PV state .....	26
Table 4-1: Different image processing techniques .....	32
Table 5-1: Images used for the first phase of experiments .....	63
Table 5-2: Images used for the second phase of experiments .....	64
Table 5-3: Choice of DL CNN architectures .....	65
Table 5-4: Experiment hyperparameters .....	65
Table 5-5: Data augmentation techniques .....	65
Table 6-1: Performance results Dataset B (150 x 150 pixels) .....	81
Table 6-2: Performance results Dataset B (200 x 200 pixels) .....	81
Table 6-3: Performance results on Dataset C (150 x 150 pixels) .....	82
Table 6-4: Performance results on Dataset C (200 x 200 pixels) .....	83
Table 6-5: TL performance results on Dataset B (160 x 160 pixels) .....	83
Table 6-6: TL Performance results on Dataset C (160 x 160 pixels).....	84
Table 6-7: PV cell classification measurements .....	88
Table 7-1: Research Questions and Chapters .....	91

# 1 INTRODUCTION

This dissertation will document the research activities involved in using an image processing technique to determine solar cell defects from electroluminescence images of photovoltaic modules. The image processing technique will have to conform to the general rules used in the identification of solar cell defects.

## 1.1 Background

Increasing demand for energy across the globe has resulted in increased use of fossil fuels. The downside to the increased use of fossil fuels is the continuous depletion of the ozone layer, and the climate is changing, as well as rising environmental issues and possibilities of different health risks which living creatures might face (Hussain, Arif, & Aslam, 2017). The increased use of fossil fuels has resulted in the increased emission of carbon dioxide (CO<sub>2</sub>), a major greenhouse gas which also pollutes the environment. A call was made to keep the earth safe, which has given rise to pollutant free technologies of harnessing electricity from renewable energy sources, which comprise of hydropower, wind energy, solar energy, biofuels, biomass and geothermal energy (Hussain et al., 2017).

One of the devices that harness renewable energy uses photovoltaic (PV) technology, which converts the light radiated by the sun into electricity. Solar energy is a clean source of energy (Nogueira, Bedin, Niedzialkoski, De Souza, & Das Neves, 2015). A clean source of energy causes zero or very minimal ecological damage (Nowotny et al., 2018). It is believed that the solar energy received on the earth's surface in three days is equivalent to all the energy stored in all fossil energy sources (Askari, Abadi, & Mirhabibi, 2015). The oil crisis in the 1970s resulted in an increased interest in PV cells as alternative power generating technology. A collection of PV cells connected in either a series or parallel circuit makes up a PV module, which is commonly known as a solar module (Askari et al., 2015).

Different types of PV cells exist due to different semiconductor materials used in manufacturing the PV cells as well as the method used in making the PV cell. The two main classes use either crystalline or thin-film PV technology. Silicon is still the material that is used in most PV devices and is either single-crystalline, multi-crystalline (polycrystalline) or amorphous silicon (thin-film technology) (Goetzberger, Hebling, & Schock, 2003; Crozier, 2012). Each type of PV cell performs differently under similar natural conditions, which affects the electricity output of the PV cell module (Guenounou, Malek, & Aillerie, 2016).

Cell defects affect the performance of all types of PV cells. The underperformance of cells emerges from cells being shaded or from defects such as cracked or corroded contacts thus preventing PV cells from generating an equal output current similar to other cells in the same series string. In addition, shading and defects result in lower power output of an entire PV module (Alonso-García, Ruiz, & Chenlo, 2006; Crozier, 2012). There are several ways of identifying the presence of cell defects within a PV cell, which include infrared imaging, electroluminescence (EL), large-area laser beam induced current, and current-voltage (I-V) characteristics (Crozier, 2012). One method involves manually analysing EL images of solar modules. However, hundreds of thousands of images may need to be inspected since the analysis methods are tedious and time-consuming. Therefore a faster more efficient way of flagging EL images are needed. EL images primarily show the presence of cracks on cells as well as dark areas where the cell is either electrically disconnected from the rest of the cell or low electroluminescence occurs. The analysis of the EL images determines the state of the solar cell based on the percentage of the solar cell affected by the defect.

This study aims to use images to identify cell defects in solar modules. EL images of solar modules will be used for this research. The images will either be provided or will be taken in a laboratory to increase the variety of defects where necessary.

## **1.2 Problem Statement**

Currently, no automated way to effectively identify defective polycrystalline PV cells, according to known PV cell defect standards from EL images, could be found. However, there are conventional ways that exist in photovoltaics that are used to identify defective polycrystalline PV cells.

## **1.3 Thesis statement**

Image processing can be used to identify patterns that may indicate PV cell defects in polycrystalline solar modules from EL images. The identified defects can be used to determine the state of the PV cell.

## **1.4 Research Questions**

The main research question (MRQ) of this study is:

**How can an image processing technique be used to effectively identify defective polycrystalline PV cells from EL images of such cells?**

The following sub research questions (RQs) will be used to answer the main research question:

RQ<sub>1</sub>: What are the existing methods for examining PV cell defects?

RQ<sub>2</sub>: What are the constraints on existing methods of identifying PV cell defects in polycrystalline solar modules using EL images?

RQ<sub>3</sub>: How can an image processing technique be used to assist in identifying defects in polycrystalline PV cells using EL images of the PV cells?

RQ<sub>4</sub>: How can an image processing technique be used appropriately to identify defective PV cells?

RQ<sub>5</sub>: How effectively can the chosen image processing technique identify defective PV cells?

## 1.5 Project Goal

The goal of this project is to identify defective polycrystalline PV cells from EL images effectively. This is to be achieved by determining the how precisely the derived solution can classify EL images of defective PV cells.

In addition, the identified defects will be based on standards defined by Kajari-Schröder et al., (2010) and are used in the Physics Department at Nelson Mandela University (NMU). The PV cell EL image classification is based on the following factors:

- Very critical: 20% or more of the cell area is affected;
- Critical: more than or equal to 8% but less than 20% of the cell area is affected;
- Uncritical: less than 8% of the cell area is affected; and
- Normal: the cell is not affected.

## 1.6 Project Scope and Risks

The focus of this study is to identify an image processing technique that can be used to identify cell defects in polycrystalline solar modules. In addition, the known standards of identifying PV cell defects (Sections 1.5 and 3.6) will have to be incorporated to classify the defects appropriately.

One possible constraint may be that the initial images available for this study may be of poor quality, thus making it difficult to distinguish between defective PV modules and normal PV modules. Since the data is historical data, there might be a discrepancy in the voltage throughput at which the EL images were taken.

## 1.7 Research Methodology

This research will use the experimental research methodology. The experimental research methodology pursues to determine factors and causal links that influence different research outcomes (Creswell, 2010). The experimental research methodology will be discussed as part of the research design in the following chapter.

## 1.8 Dissertation Structure

The current chapter provides an introduction to the research. The following chapters will discuss the different aspects of this research, which will include the research design, literature review, experimental design and implementation, experimental results and a conclusion chapter (Figure 1-1). The chapters depicted in Figure 1-1 will document the following aspects:

- **Chapter 1 – Introduction:** Chapter one introduced the problem at hand and gave a brief background on different aspects of this research.
- **Chapter 2 – Research Design:** Chapter two discusses the research design and provides support on why the experimental research methodology is the most appropriate research methodology for this research.
- **Chapter 3 – Literature Review:** Chapter three comprises literature reviewed regarding different aspects of photovoltaics.
- **Chapter 4 – Literature Review:** Chapter four comprises literature reviewed regarding different aspects of computer vision.
- **Chapter 5 – Experimental Design:** Chapter five documents the design of the different experiments based on the literature reviewed in chapters three and four. This chapter discusses the different requirements needed to conduct the designed experiments and the two phases of experiments that were conducted for this research.
- **Chapter 6 – Experimental Results:** Chapter six discusses the experiment results from the experiments designed in Chapter five. The experimental results chapter provides evidence on whether or not the MRQ has been answered.
- **Chapter 7 – Conclusion:** The final chapter documents the achievements and conclusion from this research, problems encountered throughout the research, and limitations identified and provides recommendations for future research.



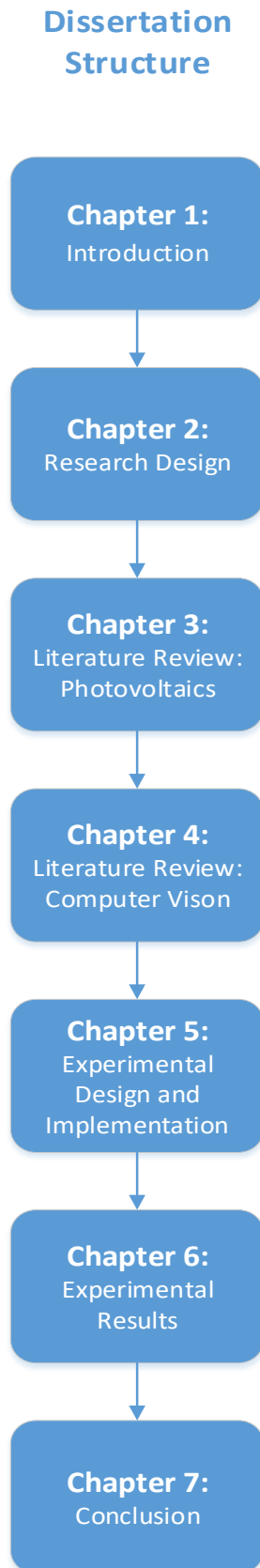


**Figure 1-1: Dissertation structure**

## **2 RESEARCH DESIGN**

### **2.1 Introduction**

This chapter provides a high-level overview of the research methodology selected for this project. The research questions (Section 1.4) and the goal of this research (Section 1.5) were identified in the preceding chapter. The research design provides a plan for how the research questions will be addressed throughout the research.

The research onion (Saunders, Lewis, & Thornhill, 2008) is briefly discussed in this chapter (Section 2.2) to provide a foundation for identifying the different research methods that will be appropriate to this research. This is vital since research methods are influenced by the research methodology (Section 2.3) and the RQs identified in the previous chapter (Section 1.4).

### **2.2 Research Onion**

The research onion (Figure 2-1) provides an effective process of determining which research methodology to apply to a particular research study. The research onion is used in conjunction with the research questions identified in the preceding chapter to determine the research methods appropriate for this research. The research methods are used to answer the research questions, which are greatly influenced by the research plan and methodology. The research methods chosen for this research are defined in the following sections by critically considering several factors. The research methods are chosen with the aid of the research onion (Figure 2-1) (Saunders et al., 2008), which describes the stages to follow based on the most appropriate research methodology. The philosophy (Section 2.2.1), approach (Section 2.2.2), strategy (Section 2.2.3) and techniques (Section 2.2.4) of this study are discussed in the subsequent sections, which will motivate the chosen research methodology.

#### **2.2.1 Research Philosophy**

The first layer of the research onion (Figure 2-1) comprises different research philosophies. A research philosophy adopted in research relates to how the researcher views the world (Gray, 2004). In addition, different approaches and strategies through which research is conducted are dependent on the research philosophy. Furthermore, the research philosophy determines how data vital to the research is gathered, analysed and used.

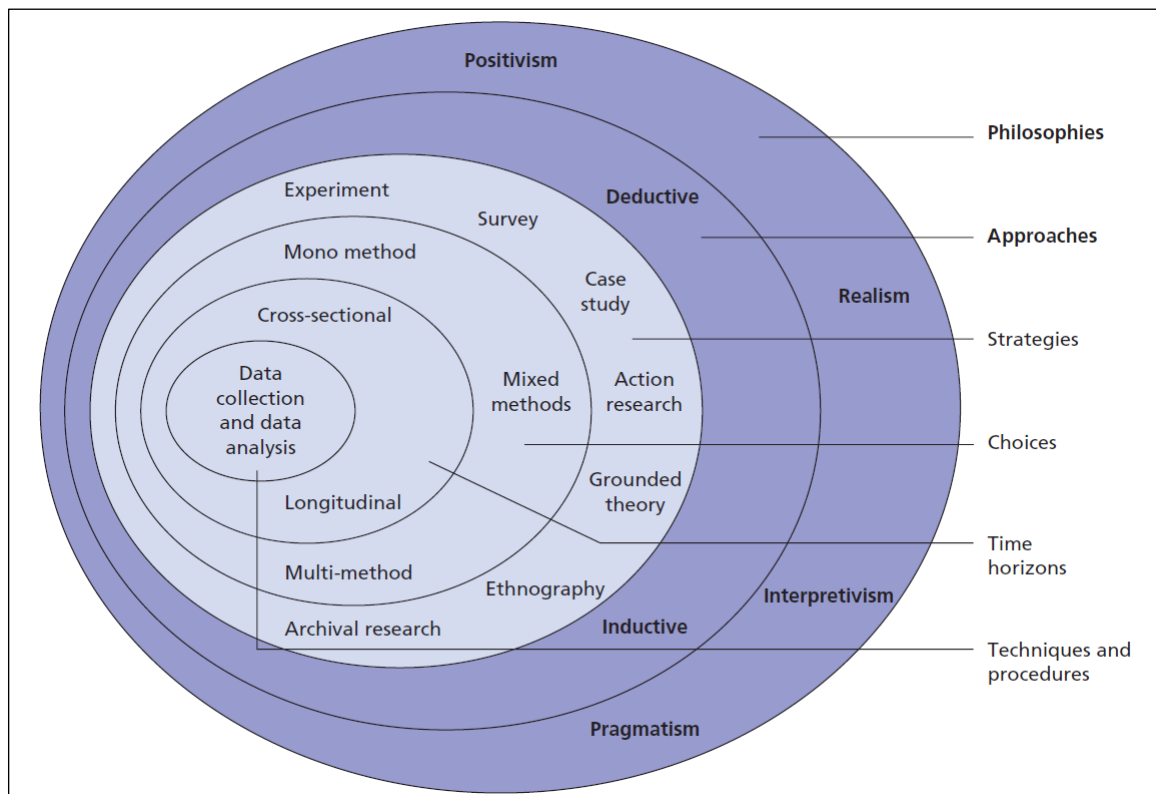


**Figure 2-1: The research onion** (Saunders et al., 2008)

This research will utilise the positivist paradigm or philosophy. The positivist paradigm holds that knowledge is absolute and objective and that a single objective reality exists external to human beings (De Villiers, 2005). In other words, meaningful data is obtained from experiments and observations (McGregor & Murnane, 2010). The data to be collected should be according to developed research questions. The main research question is therefore tested throughout the research processes to further develop existing theories (Saunders, Lewis, & Thornhill, 2009).

The positivist approach will be used to address the main research question through experiments and the use of quantitative data. This research revolves around an observable reality, which is supported by the selected research philosophy. The following section discusses the research approach.

### 2.2.2 Approach

The second layer of the research onion (Figure 2-1) depicts different approaches that can be taken when conducting research. A research approach may not always be clear in the early stages of research, but the conclusion of the research usually sums up the research approach. An important question to ask at this stage is whether to develop the main research question and design a research strategy based on existing theories (*deduction*), or develop the main research question based on collected and analysed data (*induction*) (Saunders et al., 2009).

This study will make use of the deductive approach, which complements the positivist research philosophy (Section 2.2.1). The deductive approach allows for the main research question to be deduced based on existing theories. The main research question will undergo rigorous tests throughout the research. In addition, the deductive research approach is commonly used in scientific research. The deductive approach consists of five stages (Saunders et al., 2008):

1. Deducing the main research question;
2. Expressing the research question in operation terms (secondary research questions);
3. Testing said operational research questions;
4. Examining the specific outcome of the inquiry; and
5. Examining the main research question.

These five stages revolve around the main MRQ which is expressed into secondary RQs. The five stages of the research approach allow the research approach to be mapped onto the different chapters of the dissertation as depicted in Figure 2-2.

The main research question will be explicitly examined in Chapter 6 (Figure 2-2). The main research question is expressed in secondary research questions in Section 1.4. The secondary research questions are tested in Chapters 3 to 6. The research questions are tested to answer the main research question and provide different deliverables for the different chapters. Table 2-1 tabulate the research approach stage and the chapter in which the stage is handled. The following section discusses the research strategy.

**Table 2-1: Research approach stages and chapter mapping**

<b>Research Approach Stage</b>	<b>Chapter</b>
<b>Deducing the MRQ</b>	1
<b>Expressing research question in operation terms</b>	1
<b>Testing operational research questions</b>	3, 4, 5, 6
<b>Examining specific outcomes of inquiry</b>	6
<b>Examining the MRQ</b>	6

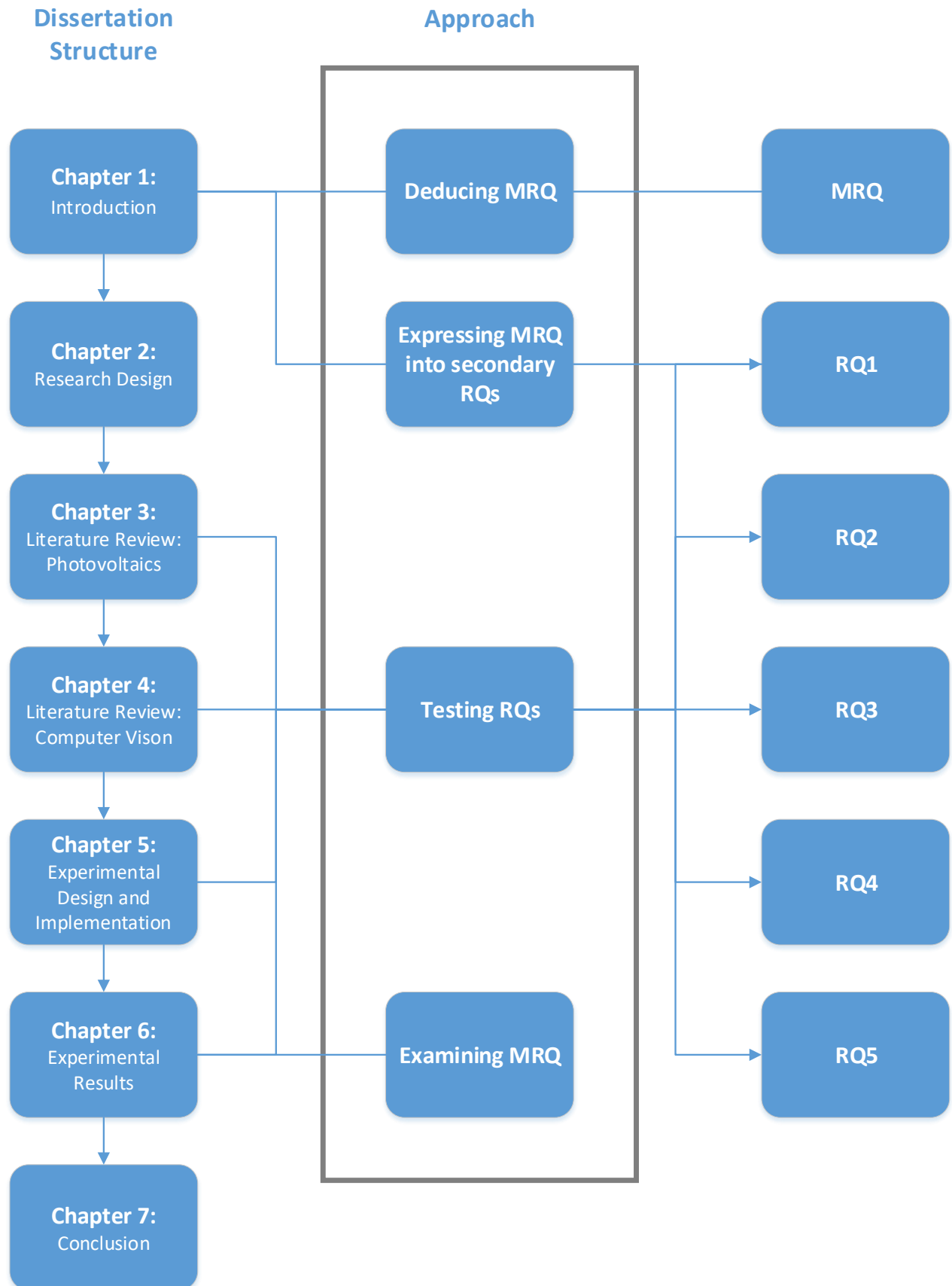


Figure 2-2: Research approach

### 2.2.3 Strategy

Research strategies can be used to either explain, explore or describe the research being carried out. The research strategy selected for this research is important in answering the identified research questions. To an extent, the research strategy is influenced by the research questions and the objective of the research. In addition, the research philosophy and approach guide the selection of the research strategy. Possible research strategies include survey, case study, experiment, and ethnography (Figure 2-1). Furthermore, the research strategy is influenced by the nature of the research. The deductive nature of this research identified in Section 2.2.2 requires that the main research be testing, which further influences the research methodology of choice.

Upon considering all the factors that influence the research strategy, it was decided to employ the experimental strategy to this research. Most experiments aim to study causal links between variables. An experimental strategy typically involves the following aspects (Saunders et al., 2008):

- The definition of research questions;
- Selection of samples;
- Random allocation of samples;
- Introduction of planned intervention or manipulation;
- Testing of a small number of dependent variables; and
- Control of all other variables.

The aspects of the experimental strategy will aid in addressing the research questions defined in Section 1.4. Figure 2-3 depicts how the research questions will be addressed throughout the dissertation. Furthermore, the main research question will help achieve the objective of the research and provides a foundation for the research questions listed in Section 1.4.

The selection of the samples that were used for this research were briefly mentioned in Chapter 1, but further support for this choice will be discussed in Chapter 3. The sampled data was allocated based on the EL image classification (Sections 1.5 and 3.6). In support of the classes identified in Section 1.5, different image classification techniques will be discussed in Section 4.3.3.

The experimental strategy requires an outlined plan of data manipulation. Literature will be reviewed in Chapter 3 to identify ways of manipulating the samples. In addition, a way in which data was manipulated for this research is discussed in Chapter 5. Furthermore, testing a small number of dependent variables and the control of all other variables is carried out in Chapter 5. Figure 2-3 depicts how the experimental strategy is mapped onto the dissertation structure.

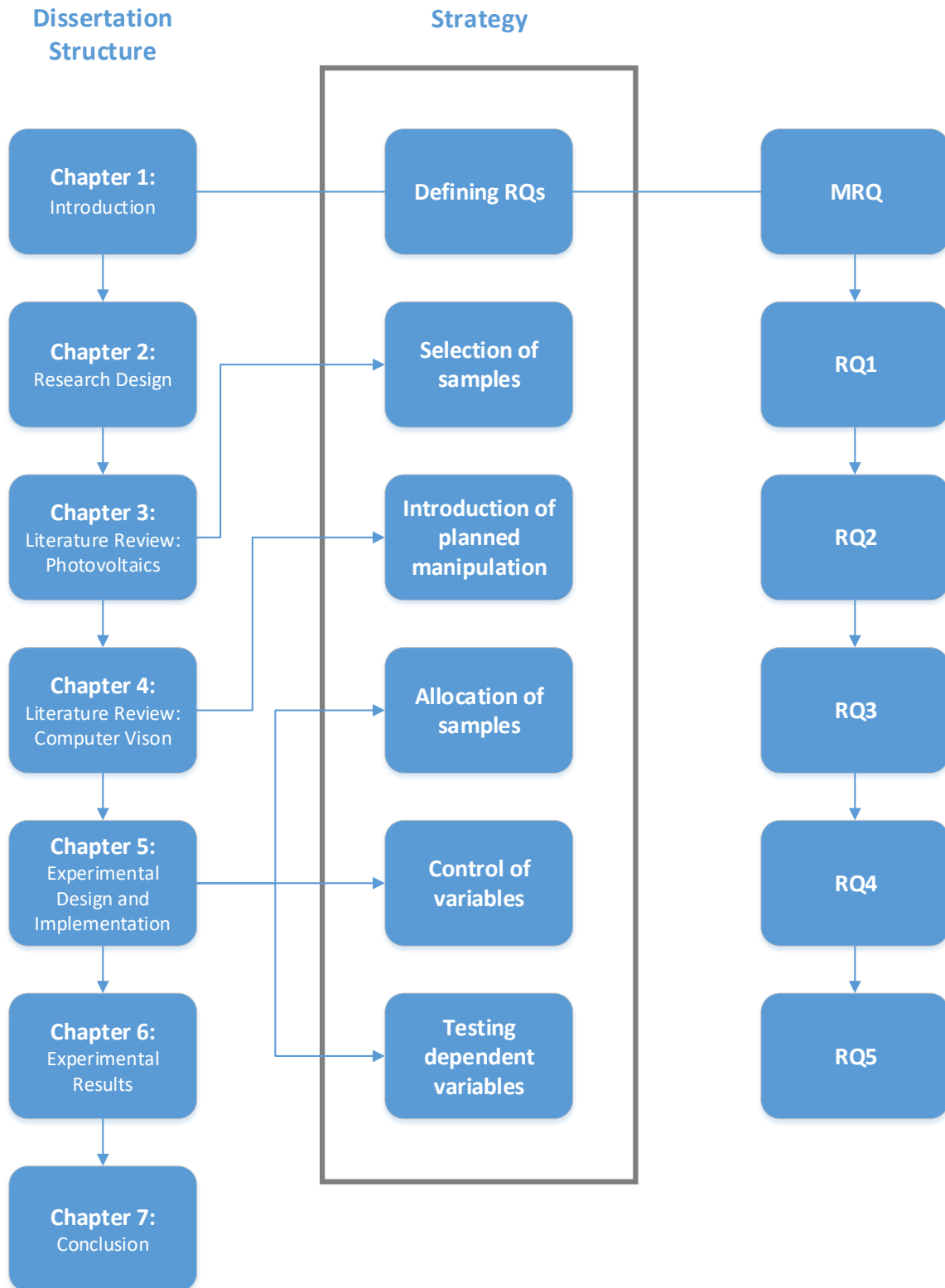


**Figure 2-3: Research strategy**

Data collecting methods and data sampling methods that drive this research are discussed under techniques (Section 2.2.4). Techniques form the core of the research onion (Figure 2-1). Data are

used to determining the causal links between different variables, therefore, making the next section important to this research.

## **2.2.4 Techniques**

Research techniques include data collection and sampling methods. Data collection and sampling methods are important aspects of research design and these methods influence ways in which research should be conducted. Data collection and sampling methods outline how the necessary data will be obtained and analysed for this research.

### **2.2.4.1 Data Collection**

Data collection is the process of gathering information on variables of interest. The purpose of this process is to answer research questions, as well as to evaluate the outcomes of the research (Creswell, 2010). The necessary data for this research will include EL images of PV modules collected from industry by the Physics Department at Nelson Mandela University (NMU) and data collected from tests within the Physics Department. As a result, secondary data collection will be the initial data collection method. Secondary data analysis is the use of data that was collected for a different primary purpose (Johnston, 2014). This research aims at analysing PV modules at a cell level because PV cell mismatch is the leading cause of PV module outputting less power than intended (Section 3.3). This will result in the manipulation of the original data received from the Physics Department at NMU, by segmenting EL images of PV cells from the module data. The segmentation of the EL images will ensure that the original PV modules are not in any way identifiable.

Furthermore, the data collected needs to represent different problem cases. Within the context of this research, the data needs to represent PV cells with different types of defects. The variation of the data representing the different types of defects will ensure that different cases (including those defined in Section 1.5) are tested in order to reduce bias and chances of error. In the event that the secondary data does not provide the necessary variety to represent the different types of defects, primary data collection might be required to ensure that the variation of data is present. Primary data collection allows data collected to be for a specific research problem (Hox & Boeijs, 2005).

### **2.2.4.2 Data Sampling**

Data sampling is a process of selecting a representative portion of data from data obtained during data collection (Latham, 2007). The data collected for this research has an equal probability of being selected. Therefore, simple random sampling will be used for this research. Data sampling



also includes the manipulation discussed in Section 2.2.4.1 and analysis of a subset of data that represents a larger dataset (Section 5.3.2.2) to identify trends and patterns within data.

This research relies on images classified based on the defect classification defined by Kajari-Schröder et al., (2010), (Section 1.5) before any analysis can be done. The classification of images will be discussed in depth in Chapter 4 (Section 4.3.3).

## **2.3 Research Methodology**

The experimental research methodology was preliminarily identified as the most appropriate research methodology for this research in the previous chapter (Section 1.7). In support of the experimental strategy which was discussed in Section 2.2.3, the experimental methodology will be used to study causal links between variables. The experimental research methodology was developed to reduce biases of all kinds as much as possible (Hulbert, 2008). Sections 2.2.1 to 2.2.4 provide a summary of why the experimental methodology was the most appropriate methodology for this research.

According to Gray (2009), the experimental research methodology comprises two main steps: the planning and operational stage. The planning stage gives perspective on what will be investigated which is achieved in Chapter 1. The main research question defined in Section 1.4 is used to deduce secondary RQs as identified by the deductive research approach. RQs are a crucial part of the planning stage of research. All research questions have to be answered throughout this research. This is achieved with the aid of the operational stage of the experimental research methodology. The operational stage also allows for experiments designed based on the planning stage to be conducted. Figure 2-4 shows the mapping between the dissertation and the research methodology.

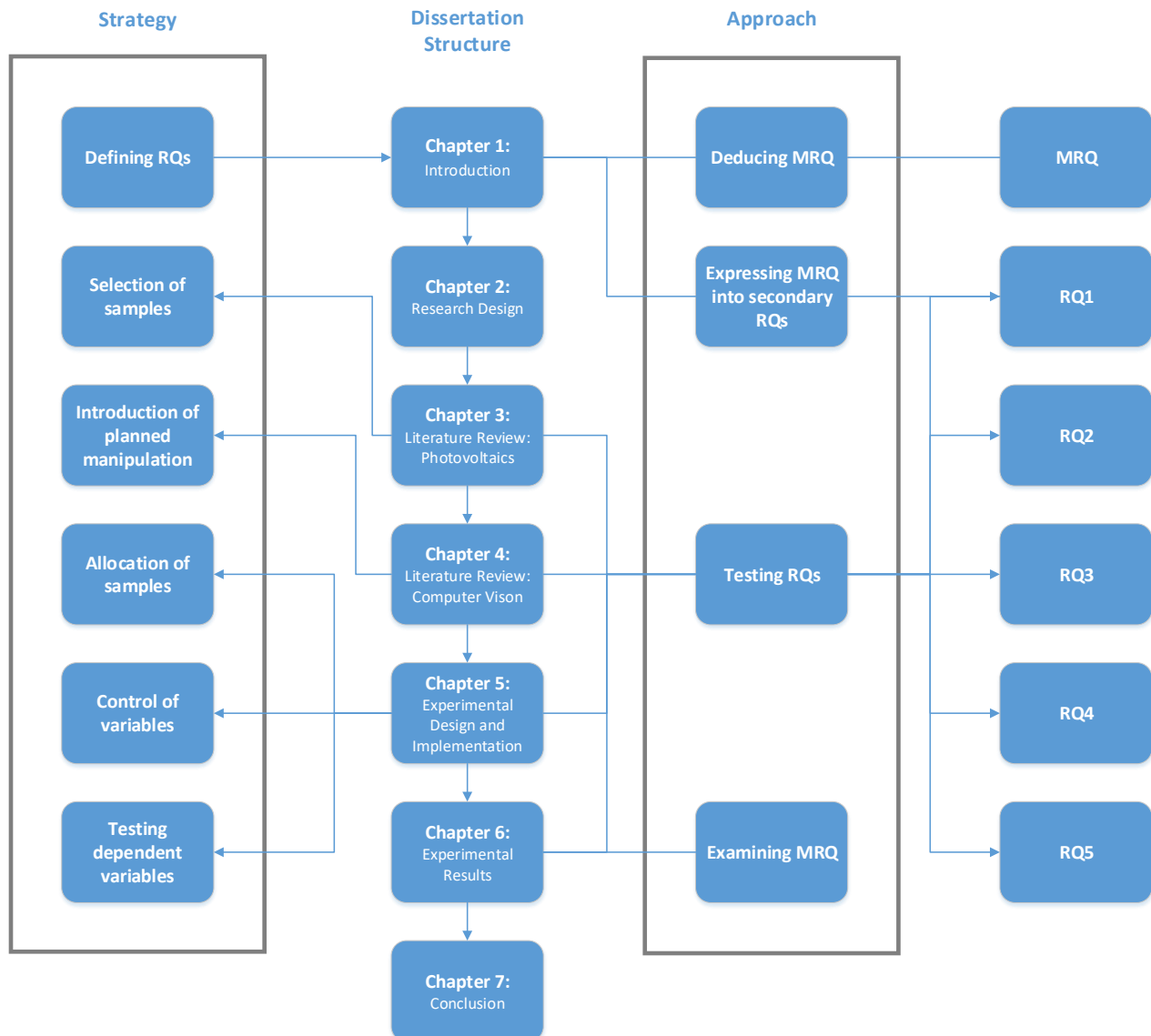


Figure 2-4: Research methodology

## 2.4 Summary

This chapter aimed to present the research design and to discuss the factors that influenced the selection of the most appropriate research methodology for this research. It was highlighted in this chapter that each section of this research had to conform to the chosen research methodology. Different methods were identified to ensure that the relevant research methodology is strictly followed. The methods included a positivist research philosophy (Section 2.2.1), a deductive research approach (Section 2.2.2), an experimental research strategy (Section 2.2.3) and research techniques (Section 2.2.4) which encompassed data collection and sampling methods. The research approach and strategy provided different aspects to ensure that the research methodology is applied relevantly to this research (Figure 2-2 and Figure 2-3).

Data collection and data sampling were discussed in Sections 2.2.4.1 and 2.2.4.2 respectively. These aspects are necessary to identify the different processes and analysis techniques that will be used on the data collected. Existing methods of analysing PV cell defects and the constraints with these existing methods are discussed in the following chapter.

In addition, the different methods (Sections 2.2.1 to 2.2.4) were discussed to confirm whether the choice made to use the experimental research methodology was appropriate for this research. A summary of the different factors posed by each method in support of the experimental research methodology were discussed in Section 2.3. Furthermore, Figure 2-4 depicts how the dissertation structure utilises the selected approach and strategy.

The following chapter provides support to why EL images are the data sampled for this research and will begin to test the RQs as part of the research methodology as depicted in Figure 2-2.

## 3 LITERATURE REVIEW: PHOTOVOLTAICS

### 3.1 Introduction

The focus of this chapter revolves around a brief overview of the primary photovoltaic (PV) technologies and the materials that are used to manufacture PV devices (Section 3.2), PV module design (Section 3.3), the type of defects that occur in polycrystalline silicon (Si) material (Section 3.4) and how the defects are identified (Section 3.5). Furthermore, ways in which characterisation techniques currently used to identify polycrystalline PV cell defects can be used in conjunction with computer vision techniques are introduced (Section 3.6).

This chapter aims to address the first two research question as depicted in Figure 3-1:

*RQ<sub>1</sub>: What are the existing methods for examining PV cell defects?*

*RQ<sub>2</sub>: What are the constraints on existing methods of identifying PV cell defects in polycrystalline PV modules using EL images?*

Answering RQ<sub>1</sub> will help provide evidence of the data sampled (EL images) for this research is used to analyse PV cell defects. Furthermore, the constraints that currently exist from identifying PV cell defects from EL images are identified.

### 3.2 Photovoltaic (PV) Technologies

Different PV (solar) technologies exist due to the different semiconductor materials used in the manufacturing process of the PV device. PV technologies can be broadly divided into crystalline silicon (Si) and thin film devices (Honsberg & Bowden, 2013). Crystalline Si PV cells are made by thinly slicing crystalline Si material to form wafers that are then processed further. Thin film devices are made by monolithically depositing layers of PV materials on a transparent substrate to form semiconductor junctions. Long strips of interconnected cells are formed by isolating the deposited material using a laser scribing process.

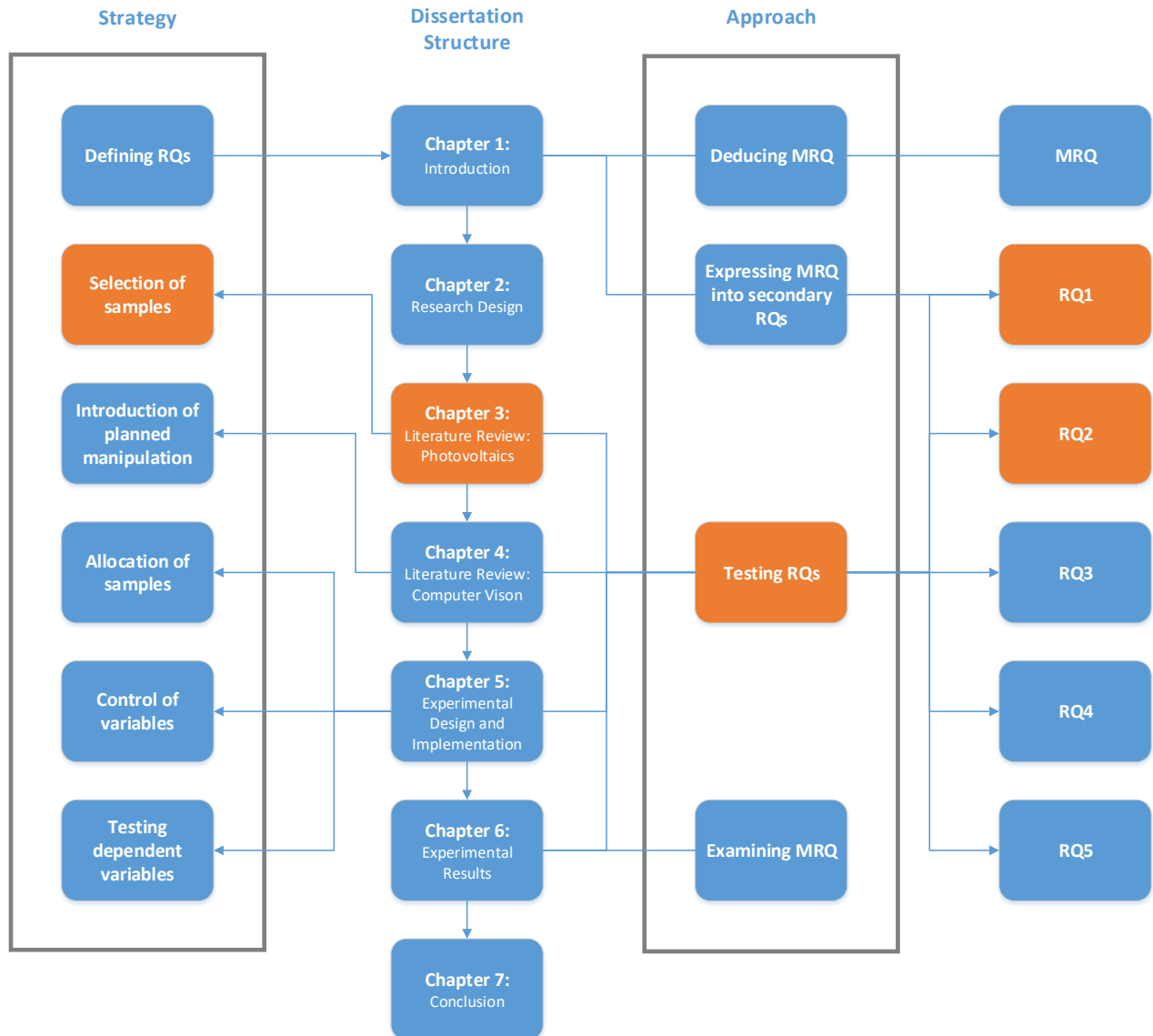


**Figure 3-1: Chapter overview**

For this discussion crystalline Si can be further grouped into either single-crystalline silicon (c-Si) or polycrystalline (multi-crystalline) silicon (p-Si) PV devices. Thin-film PV devices are made from a very wide variety of semiconductor materials. The most common materials are; amorphous silicon (a-Si), copper indium selenide (CIS), copper indium gallium selenide (CIGS) and cadmium telluride (CdTe) (Goetzberger et al., 2003; Crozier, 2012).

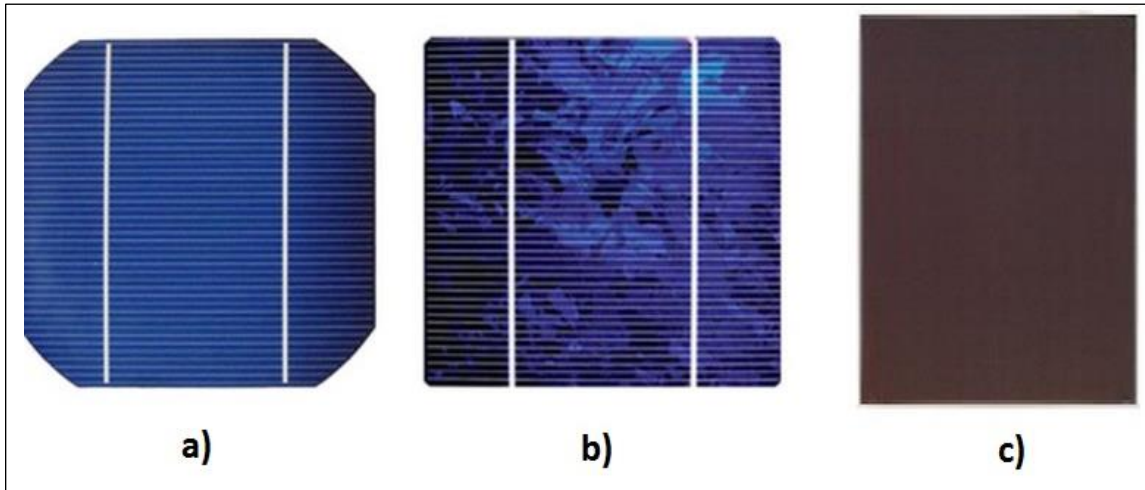


**Figure 3-2: Images showing examples of PV devices a) Single-crystalline Si PV cell, b) multi-crystalline/polycrystalline Si PV cell, c) thin film PV device**

Figure 3-2 shows examples of single-crystalline, multi-crystalline, and amorphous silicon PV materials respectively. The following sections will discuss the differences between the three different types of PV devices.

### 3.2.1 Single-crystalline Si

Single-crystalline or monocrystalline PV cells are manufactured from a slightly lower grade silicon that is used to make silicon chips in electronic equipment. The Czochralski (Cz) process is the most commonly used method to grow single crystalline ingots (Bothe, Sinton, & Schmidt, 2005; Glunz, Rein, Warta, Knobloch, & Wettling, 2001). The PV cells are sawed from a round single crystalline silicon ingot that consists of a continuous crystal lattice. A visible feature is the absence of a multi-crystalline structure with grain boundaries shown in Figure 3-2 (b) (Bagher, 2015). Figure 3-2 (a) is an example of a single-crystalline PV cell (Askari et al., 2015).

### 3.2.2 Multi-crystalline/Polycrystalline Si

Multi-crystalline or polycrystalline PV devices are made from a high purity form of metallurgical grade silicon through a chemical purification process. The silicon is cast directly into multi-crystalline ingot slabs or bricks, which are then recrystallised. The multi-crystalline bricks are then sliced into thin wafers and used to manufacture polycrystalline PV cells. Polycrystalline PV cells are the most common PV cells (Askari et al., 2015). Figure 3-2 (b) is an example of a polycrystalline PV cell.

### 3.2.3 Thin Film PV materials

A wide variety of PV materials are used to manufacture thin film PV devices. The most common materials are; amorphous Si, copper indium selenide (CIS), copper indium gallium selenide (CIGS),

and cadmium telluride (CdTe) compounds. Thin film PV devices are made by depositing a thin layer of Si, CIS, CIGS or CdTe vapour onto a smooth surface (Bergmann, Berge, Rinke, Schmidt, & Werner, 2002). Thin film PV devices products are usually about one micrometre thick. Thin film PV devices are much cheaper to manufacture than the other types of PV devices since a small amount of material is needed to manufacture the device. One major drawback of thin film PV devices is that they are not as efficient as the other types of PV cells (Askari et al., 2015). Figure 3-2 (c) is an example of a thin film PV device.

### 3.3 Photovoltaic (PV) module design

A PV module consists of interconnected PV cells, typically made from one of three PV materials (Section 3.2). This research aims to analyse polycrystalline PV cells to identify defective polycrystalline PV cells automatically (Section 1.5).

PV cells in PV modules are connected in series (Figure 3-3) to increase the available voltage, and this connection is commonly referred to as a string. In an ideal operational state of a PV module, the current through each PV cell in the PV module is equal. If a discrepancy between the current through each PV cells in a module arise, PV cell current mismatch is said to be present within the PV module. A current mismatch may lead to affected cells to become reverse biased causing power loss in the string. Figure 3-3 shows PV cells that have an equal current passing through them and are of equal voltage.

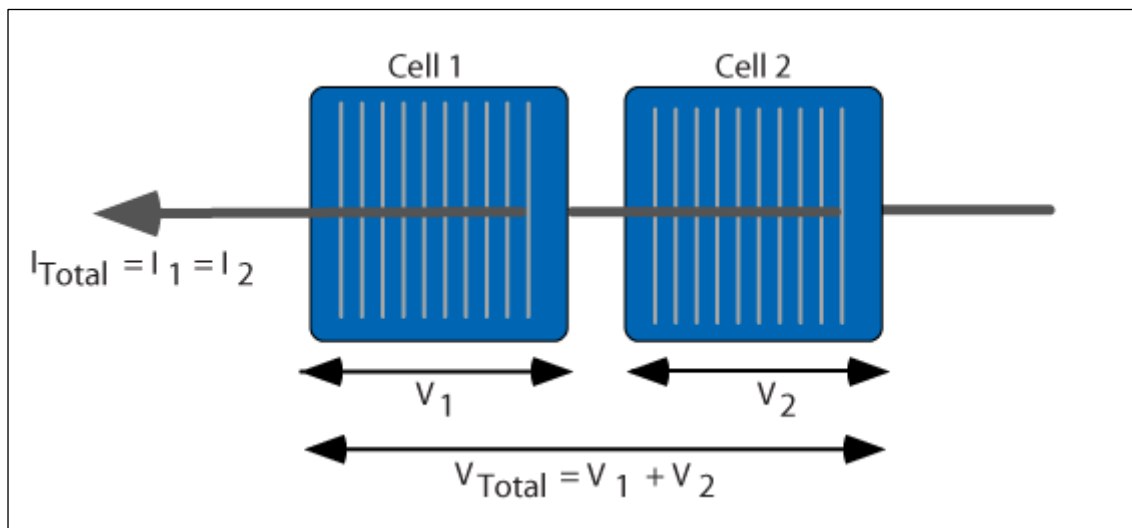


Figure 3-3: Two PV cells connected in series<sup>1</sup>

<sup>1</sup> <https://www.pveducation.org>

PV cell mismatch is a serious problem in PV modules. PV cell mismatches are induced by defects (Section 3.4) and lead to thermal heating of PV cells (Alonso-García et al., 2006). The defects prevent the PV cells from generating current equal to other PV cells in a string. PV cell mismatch is the degradation of a PV module and results in a PV module having a lower power output than expected.

### 3.4 Photovoltaic (PV) cell defects

It was mentioned in Section 1.1 that PV defects affect the performance of PV cells. A variety of PV cell defects that are inherent in the material exists ranging from point defects to dislocations and grain boundaries (Budhraj, 2012). Other defects such as fine cracks in crystalline Si material may not always result in reduced power outputs and it may not always indicate a defective cell. However, the PV defects that affect the efficiency of PV cells (Mari, Ullah, & Sanchez Ruiz, 2016) are of interest in this study. This section provides an overview of the currently known types of defects.

The cell defects listed below do not affect the performance or efficiency of PV cell and consequently a PV module (Köntges et al., 2014):

- Crystal dislocation: irregularities within a crystal structure;
- Edge wafer: a result of the materials used to make the PV cell falling off the edges of a PV cell; and
- Striation rings: caused by convective instabilities during crystal growth.

On the other hand, the defects listed below are some of the identified defects that cause PV cell failures and affect the performance of PV modules (Köntges et al., 2014):

- Cell cracks: PV cells are made from silicon, which is very brittle. Cell cracks are of different lengths and orientation. Only cracks that electrically disconnect active parts of cells cause current mismatch and will lead to power loss and possible failure. Unfortunately, these cracks may not always be visible to the naked eye. Apart from cracks that are formed due to mechanical impact to the PV module, wafer slicing and the embedding of strings during production may cause cells to crack.
- Finger failure: Cracks beyond the cell interconnection ribbons are called finger failures. Finger failures usually indicate high strain at solder joints. Thermochemical stress usually induces finger failure and lead to high power loss.
- Humidity corrosion: the humidity condenses between the glass over the PV cell material and the PV material itself. The resulting water residue causes the radiant light to reflect, refract or diffract before hitting the cell.



- Contact forming failure: temperature inhomogeneities during the firing process of manufacturing the PV cell causes contact degradation.
- Shunt fault: the linkage of positive and negative terminals of PV modules due to the degradation conductor insulators, resulting in shunt paths.

### 3.5 Identifying Photovoltaic (PV) cell defects

As discussed in Section 3.4, a variety of defects exist and not all defects affect the efficiency of PV cells. The most common defects include corrosion and cracks within the PV cell and these common defects will impact the performance of PV cells.

Even though there is a variety of defects, their existence within PV modules can be identified using appropriate techniques. These techniques include EL, large-area laser beam induced current (LA-LBIC), I-V measurements, and infrared (IR) imaging. All these methods provide PV module data that can be used for PV module defect analysis. It was identified in Chapter 1 that EL images will be used in this research to identify defective PV cells automatically, and the data collection and sampling techniques were introduced in Sections 2.2.4.1 and 2.2.4.2 respectively.

#### 3.5.1 Electroluminescence (EL)

Luminescence in semiconductor materials occurs when charge carriers (holes and electrons) recombine radiatively by emitting electromagnetic radiation in the visible to near infrared (NIR) part of the spectrum (Dexter, 1953). Charge carrier separation can be generated (excited) either optically or electrically. Radiative recombination from charge carriers that were optically generated emits photoluminescence (PL) while electrically generated charge carriers emit electroluminescence (EL). EL in the visible part of the spectrum is important for the functioning of light emitting diodes (LED) and are now also extensively used in the lighting industry. EL from Si derived PV devices only occurs in the NIR part of the spectrum. A very sensitive NIR camera is required to create EL images of PV cells.

The intensity variation showing up as features in EL images of PV cells, therefore, indicates the magnitude of radiative carrier recombination that occurred. Carrier recombination is by implication an indicator of the presence of charge carriers and electrical activity. The bright parts of the EL image, therefore, correlates to the presence of charge carriers and electrical activity. And the dark parts correlates to the absence of charge carriers and electrical activity (Fuyuki, Kondo, Yamazaki, Takahashi, & Uraoka, 2005).

EL can be used in photovoltaics to identify defective PV cells. EL is used to measure the current density in a PV cell, which is carried out by inducing photons allowing a flow of current through the

PV cell. Light sensitive sensors are then used to capture images of the PV module. Figure 3-4 shows three examples of EL images.

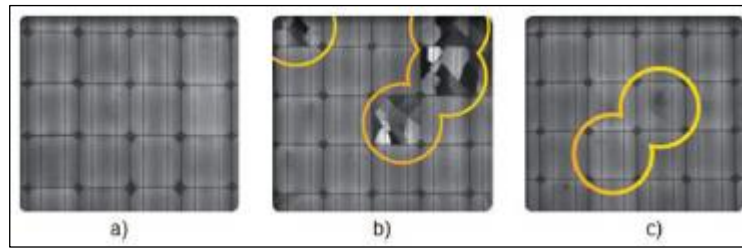


**Figure 3-4: Scanned EL images of part of a PV modules a) The PV module without defects, b) non-functional PV module, c) PV module with cracked cells (Friedrischková & Horák, 2013)**

Figure 3-4 (a) shows a PV module with no defects. In theory, this PV module should be functioning optimally. On the other hand, Figure 3-4 (b) contains cracked cells that have parts of cells electrically disconnected. The circled regions indicate defective areas. Lastly, Figure 3-4 (c) shows PV cells with cracks that do not disconnect parts of the cell, which is a known type of PV defect. Unlike the non-functional PV cells, the PV cells in Figure 3-4 (b and c) still work, although at a much lower performance than a PV module without defects.

EL images are usually taken of entire PV modules; therefore, a decision was made to analyse the EL images on a cell level (Section 2.2.4.1 and 2.2.4.2). Furthermore, EL images are possibly taken with a different voltage from different modules. The excitation current flowing through the PV module can therefore differ and affect the EL intensity of the cells that appear in the EL image. This can potentially be a source of error when running experiments. Normalisation must be considered before performing experiments. Normalisation is included in image pre-processing, discussed in Section 4.3.1. In this case, normalisation will ensure that all EL images are as similar as possible before the images are used in experiments.

Currently, EL images are examined manually to identify the defects marked in Figure 3-4 which affects the effectiveness of identifying defective PV cells which can be incurred by human error. The goal of this project (Section 1.5) is to automate this process of identifying defective PV cells from EL images using image processing (Section 4.3).

### **3.5.2 Large-area laser beam induction current (LA-LBIC)**

Large-area laser beam induced current (LA-LBIC) is another technique used to identify cell defects. Raster scanning a perpendicular beam of light across the surface of a sample induces a localised current in a PV cell. By plotting the current and corresponding position of the light beam a LBIC image is formed. The local photoresponse current of the cell is used to determine whether the cell is defective or not. LA-LBIC can be used to detect polycrystalline cells defects such as grain

boundaries (Crozier, 2012; Donolato, 1983; Phillips et al., 2016). Figure 3-5 shows the schematics of a LA-LBIC system. The camera captures the light beam generated by the laser device and is plotted against the current which is recorded by the PC.

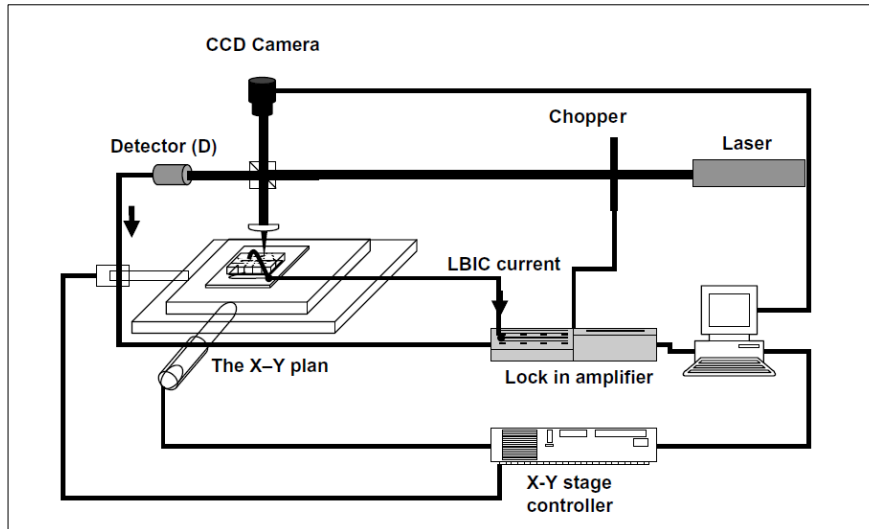


**Figure 3-5: Laser beam induction current system** (Rabha, Dimassi, Bouaïcha, Ezzaouia, & Bessais, 2009)

### 3.5.3 Current-Voltage (I-V) characteristics

PV cell I-V characteristics provide a detailed description of a PV cell energy conversion ability and its efficiency. I-V characteristic curves are a graphical representation of PV cell performance (Figure 3-6).

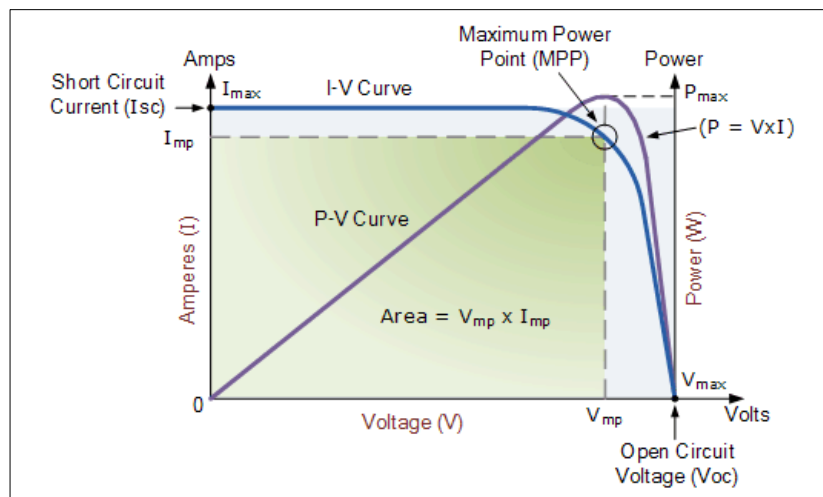


**Figure 3-6: I-V characteristic curve of a PV cell<sup>2</sup>**

<sup>2</sup> <http://www.alternative-energy-tutorials.com>

Certain cell defects affect the power output of a PV module (Budhreja, 2012). I-V characteristics of a PV module can be used to determine the presence of cell defects within a PV module since this indicates the possibility of a cell mismatch within a PV module. PV cells with a lower current output than the rest of the cells in the module are known as weak cells (Crozier & Van Dyk, 2015), and weak cells result in a current mismatch (Section 3.3) of cells in the same string. I-V curves are plotted which are compared to those of an optimally performing PV module. The differences in the curves are what suggest the presence of defects within the PV module, as this will be an indication of a decline in the power output of the PV module. Figure 3-7 shows how an I-V curve of a normal cell compares to an I-V curve when defects are present causing a current mismatch.

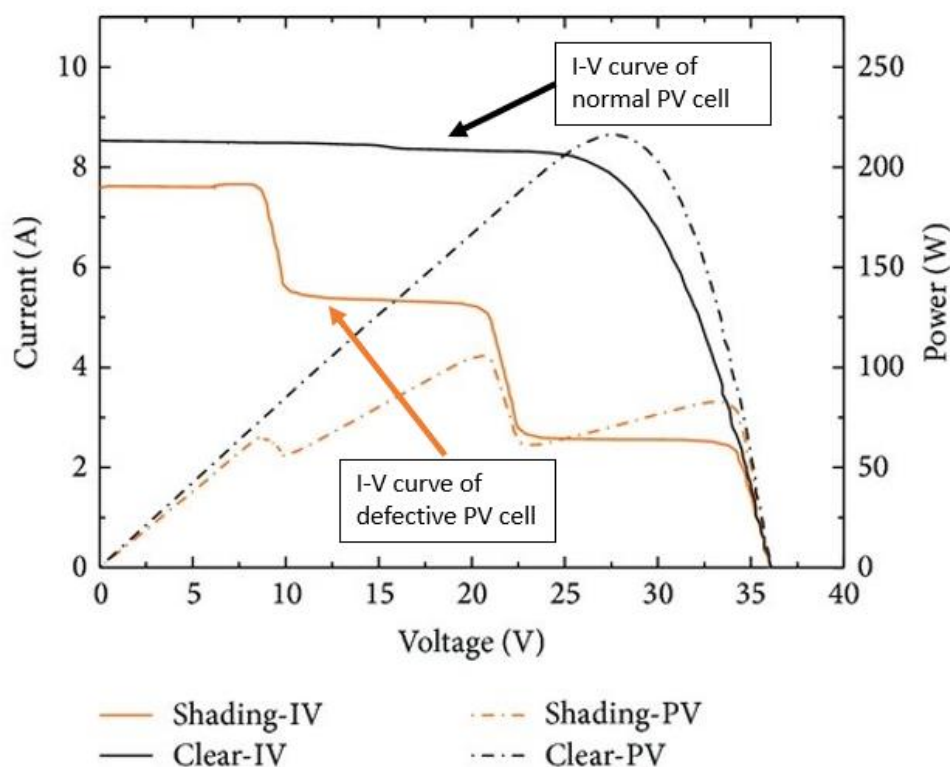
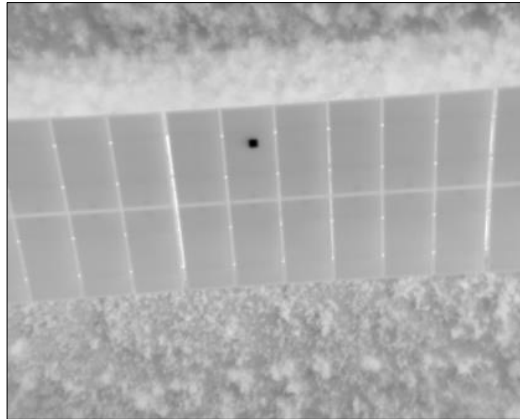


Figure 3-7: I-V curve of a normal PV cell from normal PV module vs an I-V curve of a defective PV cell in defective PV module (Schill, Brachmann, & Koehl, 2015)

### 3.5.4 Light Infrared Imaging

Infrared images can be used to determine whether cell defects are present in a PV module. This is done by analysing the heat distribution captured in a thermal image of the surface of a PV module. PV cells with slightly higher temperatures correspond to energy loss and indicate the presence of a defect. If this is not attended to, the heat generated affects the performance of neighbouring PV cells (Mayekar, Kotmire, Wagh, & Shinde, 2016).



**Figure 3-8: A greyscale thermal image of a string of PV modules with a single defective cell**

Figure 3-8 shows a greyscale thermal image of a PV module. Areas with a darker shade of grey represent higher temperatures, and lighter shades of grey indicate lower temperatures. In addition, the black spot indicates a possible current mismatch (Section 3.3), which indicate the presence of a PV cell defect. One downside of thermal images is that the type of defect cannot be identified in the image.

In some cases, there is no correlation between thermal images and the defect properties of a PV cell. One way to mitigate this concern is by comparing thermal images with optical images. However, the sensor differences between the optical and thermal cameras raise another concern. The difference in sensors can result in thermal and optical images of a different resolution which can pose a challenge during automatic analysis. In addition, the images are likely captured at different flight times which introduce other discrepancies which include; images taken from different angles and at different altitudes. The one defect characteristic known to be identified from optical images is whether the PV module is covered in dirt or has areas that are being shielded from the sun's radiation. Lastly, the weather might introduce other irregularities, as cloud cover might make it seem to appear as if PV cells are shaded, which might incorrectly indicate the presence of a defect.

### **3.6 Proposed integration**

This section discusses the preliminary integration between photovoltaics and computer vision proposed in this research. This research aims at using EL images (used in photovoltaics) to identify defects through image processing (computer vision). Currently, no automated ways of identifying defective PV cells from EL images were found. The existing methods of identifying defects only indicate the presence of a defect but cannot be used to identify the nature of the defect.

Initially, thermal images and optical images were identified as the possible sources of data to be used to automatically identify defective PV cells (Section 1.2). Upon further refinement of the

problem and concerns identified in Section 3.5.4, it was decided to use EL image. The primary reason was due to the fact that no defect properties are exhibited in thermal images besides the average temperature of the PV cell. The average temperature of the PV cell only indicates the presence of a defect, but this temperature cannot be used to identify the actual defect present in the PV cell. The inability of the average temperature to identify the defect present is one of the constraints of existing methods of identifying PV cell defects.

The EL images have been identified as the data source to be used to identify defective PV cells using image processing automatically. Different image processing techniques that can be used will be investigated in Chapter 4 to deduce the most appropriate image processing technique that can be used for this research. Furthermore, this research will discuss different image processing tasks that can be used to automate the process of identifying defective PV cells. The automated process of identifying defective PV cells will have to be able to distinguish between normal and defective PV cells. The standards used to distinguish the PV cells were defined by Kajari-Schröder et al. (2010) and were highlighted in Section 1.5. Table 3-1 tabulates the factors that influence how to distinguish the PV cells.

**Table 3-1: Factors that influence PV state**

PV cell state	Area affected by defect
<b>Normal</b>	0%
<b>Uncritical</b>	<8%
<b>Critical</b>	>=8% but <20%
<b>Very Critical</b>	>=20%

### 3.7 Summary

The aim of this chapter was to discuss the, different PV technologies (Section 3.2), PV module design (Section 3.3), different types of PV cell defects (Section 3.4), different ways of identifying PV cell defects (Section 3.5) and the proposed integration (Section 3.6) between PV and computer vision.

Different types of PV cell technologies were discussed in Section 3.2. However, this research will only investigate defects found in polycrystalline PV cells. In addition, module designs of the identified PV cell technologies were discussed in Section 3.3, which lead to the introduction of PV cell current mismatch which is the phenomenon that arises when defective PV cells are present in a PV module. In addition, different types of PV cells defects were discussed in Section 3.4, as they result in PV cell current mismatch.

The discussion on different types of PV cells defects leads to the investigation of existing methods of examining PV cells (RQ<sub>1</sub>) which were discussed when addressing different techniques of

identifying PV cell defects in Section 3.5. One of these techniques includes EL (Electroluminescence), of which EL images is a by-product. Furthermore, the constraints on existing methods of identifying PV cell defects (RQ<sub>2</sub>) were highlighted in Section 3.6.

EL images were identified as the images that will be used to solve the problem identified; currently, no automated way to effectively identify defective polycrystalline PV cells, according to known PV cell defect standards from EL images could be found (Section 1.2). Therefore, evidence was provided that EL images are indeed used in photovoltaics supporting their use in automating the process of identifying defective PV cells from EL images. The use of EL images in photovoltaics confirmed that the right data was sampled for this project.

The integration of PV and computer vision were briefly discussed in Section 3.6. The following chapter discusses different techniques that may be employed within computer vision to effectively identify defective polycrystalline PV cells from EL images of such defective PV cells.

## 4 LITERATURE REVIEW: COMPUTER VISION

### 4.1 Introduction

This chapter aims to introduce computer vision (Section 4.2) and discuss how image processing (Section 4.3), a technique within computer vision may be employed to effectively identify defective polycrystalline PV cells (Section 3.2.2 and 3.5) from EL images of such defective cells. In addition, different aspects of image processing will be discussed such as deep learning (DL) (Section 4.3.2), image classification (Section 4.3.3), and pattern recognition (Section 4.3.4). Related work (Section 4.4) to this research will also be discussed in this chapter. Furthermore, this chapter documents ways in which computer vision can be used in conjunction with techniques of identifying defective PV cells (Section 3.5) as proposed in Section 3.6.

The literature review (Chapter 3 and Section 4.2 to 4.3) and the related work (Section 4.4) reviewed in this chapter aims to provide insight into how to design experiments to extract patterns within PV cell EL images and classify them accordingly to address the MRQ. In addition, this chapter aims at explicitly addressing the 3<sup>rd</sup> and 4<sup>th</sup> research questions. These RQs are as follows:

*RQ<sub>3</sub>: How can an image processing technique be used to assist in identifying defects in polycrystalline PV cells using EL images of the PV cell?*

*RQ<sub>4</sub>: How can an image processing technique be used appropriately to identify defective PV cells?*

Figure 4-1 shows how this chapter aims to address the RQs using the research approach and research strategy. Figure 4-1 depicts how this chapter introduces how the data sampled for this research will be manipulated (Section 4.3). The introduction to data manipulation is required to answer RQ<sub>3</sub> and RQ<sub>4</sub>. All this is achieved in this chapter through an in-depth discussion of computer vision (Section 4.2), image processing (Section 4.3), and work related to this research (Section 4.4).



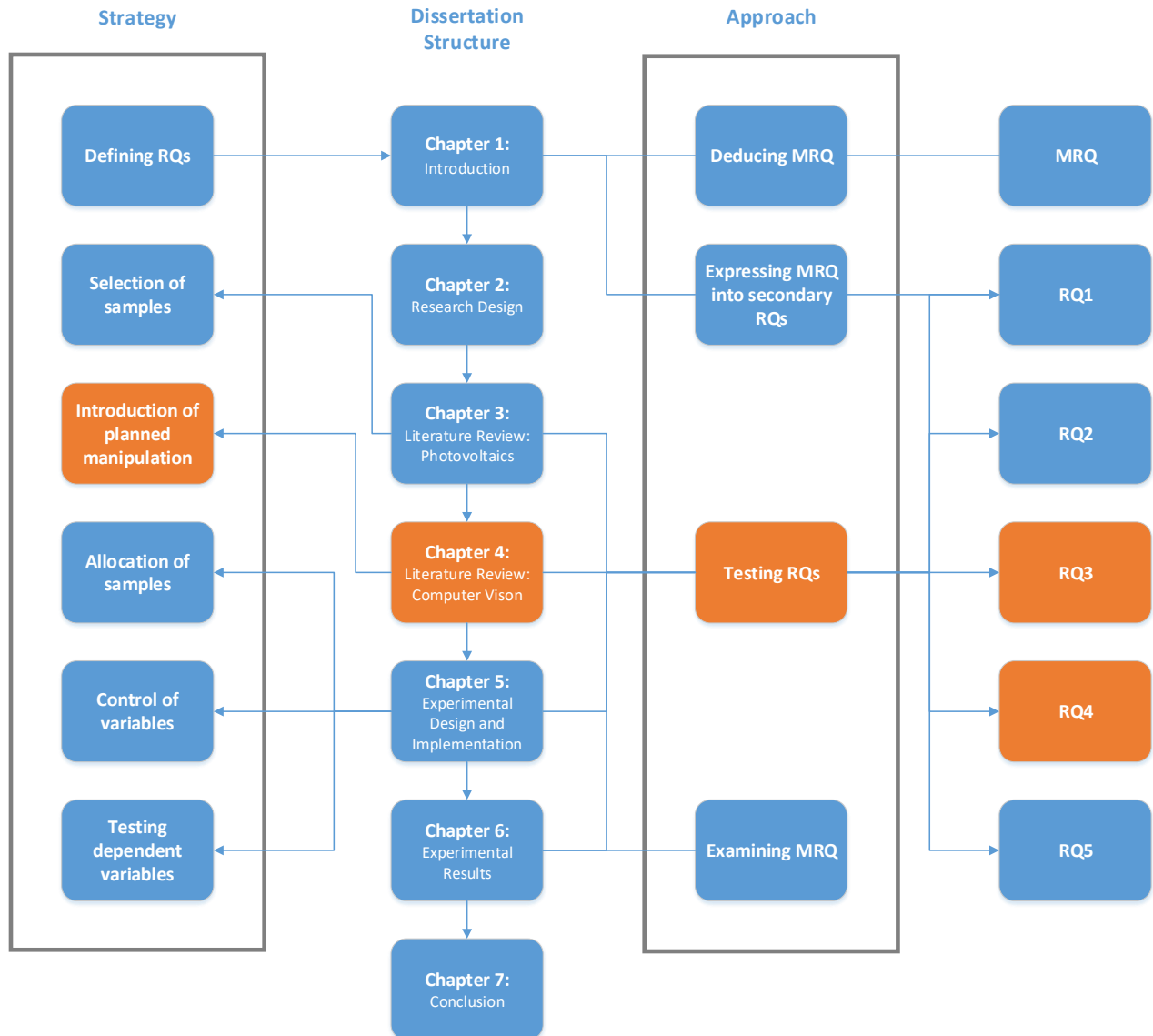


**Figure 4-1: Chapter overview**

The following section discusses different aspects of Computer vision.

## 4.2 Computer Vision

Computer vision is a useful field that uses human vision principles to help computers gain a high-level understanding of digital images and videos. In most cases, computer vision is used in the implementation of assistive technologies, which help individuals overcome limitations when executing tasks (Leo, Medioni, Trivedi, Kanade, & Farinella, 2017). Assistive technologies are used in different fields, including the medical field. Certain aspects regarding the use of computer vision in the medical field are discussed in Section 4.4.1.

Computer vision systems are usually used to characterise objects or patterns within digital images and videos. In most cases, computer vision systems can characterise textures, shapes, colours, and sizes (Bhargava & Bansal, 2018). More sophisticated systems go as far as grading and detecting defects through automated inspections.

Computer vision systems execute four main tasks. These tasks are acquiring, processing, analysing and the understanding of digital images (García-Pulido, Pajares, Dormido, & de la Cruz, 2017).

1. **Acquiring:** images are acquired using different sensors or devices. Some of these devices include cameras, magnetic resonance imaging (MRI) devices or computed tomography (CT) devices. Image acquisition is required as data collection process for a computer vision system.
2. **Processing:** images are processed to gain an understanding of the information concealed within an image. Image processing allows for the implementation of computer vision tools that can recognise objects or patterns within an image.
3. **Analysis:** the analysis task in computer vision permits computer vision systems to describe information embedded within an image.
4. **Understanding:** this task permits computer vision systems to be able to classify images. The understanding task in computer systems allows more sophisticated implementations can automatically caption images.

The three main tasks of computer vision systems are required to address the third research question identified in Section 1.4:

*RQ<sub>3</sub>: How can an image processing technique be used to assist in identifying defects in polycrystalline PV cells using EL images of the PV cell?*

Acquiring, the first task in computer vision links to data collection (Section 2.2.4.1). The data acquired for this research are EL images that will be used to perform image classification experiments.

Image processing (Section 4.3) is a core component of this research as there is a need to understand features concealed in EL images relating to the defects present in PV cells.

Besides image acquiring and processing, there is a need to analyse and understand the images. These are the last two tasks of computer vision systems. The analysis task in the proposed solution will, therefore, have to discern features that describe defects. Lastly, the understanding task of the proposed solution will have to correctly classify EL images exhibiting an understanding of different features within EL images. The next sections further identify and discuss image processing techniques used in this research.

### 4.3 Image Processing

Image processing was briefly introduced in Section 4.2 and was identified as a task within computer vision. Image processing is an approach used to enhance raw images for various applications. Different techniques within image processing have been developed since the 1970s to enhance and interpret images (Rao, 2006). Image processing can further be used to transform, manipulate or analyse digital images (Fu & Rosenfeld, 1976).

In most cases, image data must be improved before image processing in order to complete a task (Krig, 1993). The initial stage before image processing is known as image pre-processing, which allows for distortions present within images to be suppressed. Image pre-processing is required because distortions result in the misrepresentation of data within images. Image pre-processing is discussed in Section 4.3.1.

A variety of tasks can be achieved using image processing. The tasks within image processing include image classification (Section 4.3.3), pattern recognition (Section 4.3.4) and image feature extraction. Image classification and image recognition can be carried out using different image processing techniques (Table 4-1). Table 4-1 lists different image processing techniques, the details of the image processing techniques, whether the different image processing techniques apply to this research and motivation to why the techniques were applicable or not. These image processing techniques include image restoration, image edition and neural networks (NNs). These are just some of the image processing techniques that can be used to carry out image processing tasks to help identify defective PV cells from EL images. Table 4-1 provides details of the different image processing techniques, which provides evidence on whether the listed image processing technique can be used for this project. The two image processing techniques that can be utilised in this project based on the list tabulated in Table 4-1 are linear filtering and NNs. Linear filtering and NNs allow for feature enhancement within images and feature extraction. The extracted features are used to train generative models. The resulting models can be used to classify images; in the context of this project EL images of PV cells. The other image processing techniques, even though useful, were not suitable to solve the identified problem; automatically identifying defective PV cells from EL images of PV cells. Brief motivations of whether or not each image processing technique is applicable to this project is tabulated in Table 4-1.

This research will take the NN approach as the image processing technique to automatically identify defective PV cells from EL images based on the image processing techniques reviewed in Table 4-1. NNs have been identified over the years as a technique that can be used to accomplish different image processing tasks (Ferreira & Giraldi, 2017; Litjens et al., 2017). Furthermore, NNs are a fundamental basis of DL which has successfully revolutionised computer vision (LeCun, Bengio, & Hinton, 2015). DL will be discussed in depth in Section 4.3.2. In addition, linear filtering

is vital to this research as it makes up part of pre-processing (Section 4.3.1) and can be in the convolutional layer of convolutional neural networks (CNNs) (Section 4.3.2.3).

**Table 4-1: Different image processing techniques**

Image Processing Technique	Details	Applicable to Research	Motivation
Image Edition	Altering digital images using graphics software tools.	No	There was no need to alter the PV cell images with graphical software in order to identify whether the PV cell was defective or not.
Image Restoration	Estimating a clean, original image from a corrupt or noisy image.	No	The images provided were in a good state and did not require estimating a clean image from the provided dataset.
Independent Component Analysis	Decomposing multi-variant signals	No	The dataset provided was not multivariate.
Anisotropic Diffusion	Reducing image noise without omitting important parts of the image.	No	The images did not require any noise reduction.
Pixellation	Converting printed images into digital ones	No	The dataset received was already in digital format.
Principal Components Analysis	Extraction of features from images	No	This technique extracts features from images to make it easier to visualise, which was not the goal of this project.
Self-organising Maps	Classifying images into different classes	No	This technique is not able to create a generative model that can be later used to classify a different dataset into different classes.
Linear Filtering	Enhances image features	Yes	Is used in CNNs to enhance features within images.
Neural Networks	Image feature extraction and image classification	Yes	NNs allow features to be extracted from images, used to train a classifier that produces a generative model that can be used to classify images.

Before discussing the different tasks of image processing (image classification and pattern recognition) and the image processing techniques (DL approach), image pre-processing, which is a subset of image processing and enhancement, needs to be discussed. Image pre-processing and how it can be applied to this study are explored in the next section.

### 4.3.1 Image Pre-processing

Image pre-processing is the normalisation of image data sets, which is important for different feature description methods. Image pre-processing usually has a positive effect on feature extraction and the results obtained after image analysis (Krig, 1993).

Image pre-processing is important in determining areas of interest within images. The areas of interest are important for the analysis at hand and the intended use of the images in this research. For this study, image pre-processing will be used to enhance defects, which are the areas of interest, within the images. Segmentation is one process that is used to identify areas of interest within images.

Segmentation is the partitioning of images into meaningful parts which have similar features and properties (Kaur & Kaur, 2014). Alternatively, segmentation is referred to as the process of partitioning areas of the image that are similar. The following sections will discuss some pre-processing techniques related to segmentation. These sections will highlight thresholding and edge detection.

#### 4.3.1.1 Thresholding

Thresholding is one of the first segmentation techniques. Thresholding is used on greyscale images, and the distinction between objects and the background is made using black and white respectively. If there are different objects in the image, a threshold is determined for each object. Each sub-region that emerges is known as a local threshold. The characteristics of the objects (how light reflects off the images) help to determine the different threshold regions. When there is a single object in the image, thresholding is done using global information. This thresholding technique is known as global thresholding (Sahoo, Soltani, & Wong, 1988). Global thresholding is highly dependent on the level of distinction between the object and background pixels. Global allows for thresholding to be carried out on an entire image, resulting in a segmented output of the original image (Langote & Chaudhari, 2012). Figure 4-2 (2<sup>nd</sup> and 3<sup>rd</sup> column) shows an example of global thresholding.

Local thresholding works best over small regions. If the quality of the image is poor, it is best to use local thresholding. Since it is difficult to segment poor quality images properly, local thresholding can be used to isolate the image into smaller images, which are then segmented separately. The sub-images are then arranged to create a segmented output of the original image (Langote & Chaudhari, 2012). Figure 4-2 (4<sup>th</sup> column) shows an example of local thresholding.

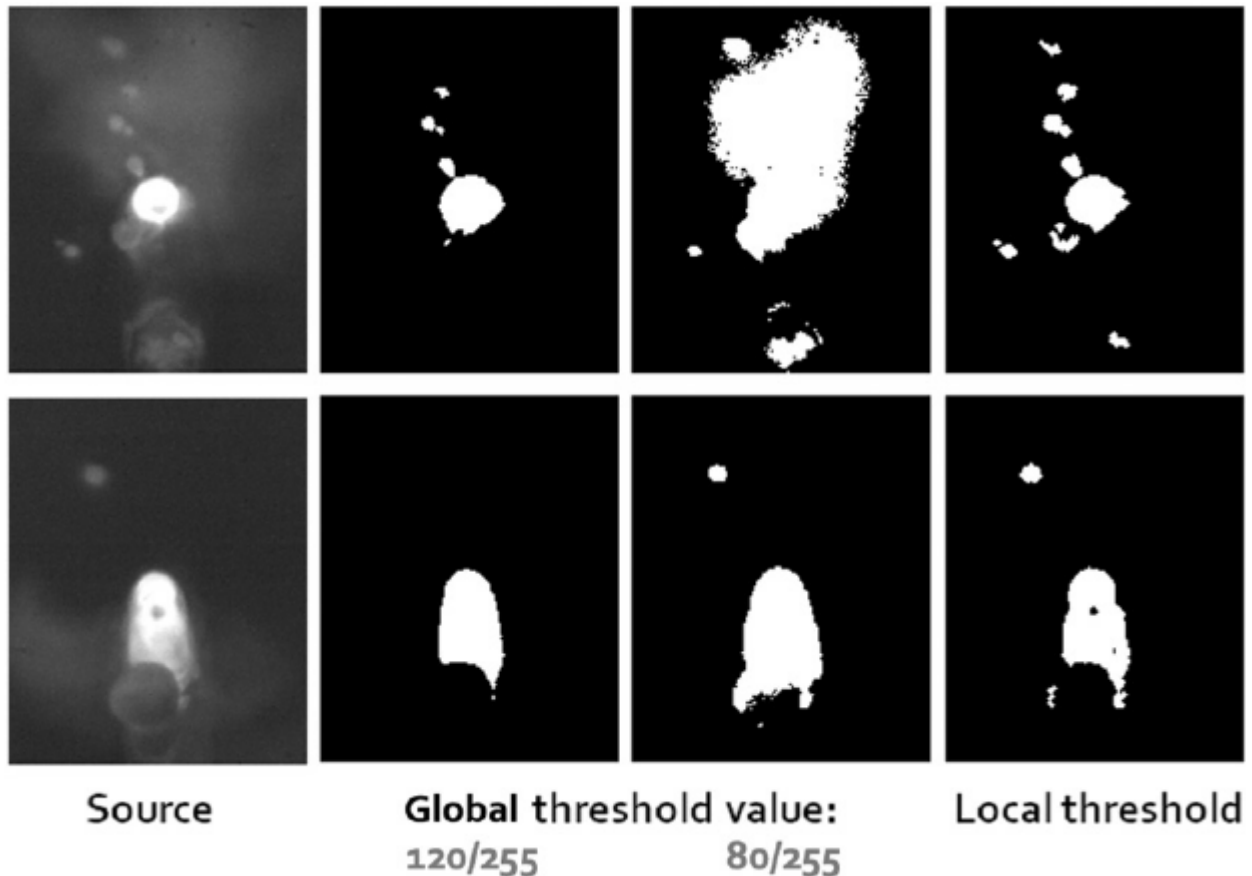


Figure 4-2: Examples of global and local thresholding (Nicolosi et al., 2012)

#### 4.3.1.2 Edge Detection

Edge detection is a fundamental step in computer vision and is a commonly used operation in image analysis (Bhardwaj & Mittal, 2012). Edge detection is a known segmentation method used to identify areas of interest within images, which may include interesting features or specific patterns (Zheng, Rao, & Wu, 2010). Edge detection techniques consider edges as points of abrupt change in greyscale images. Image processing techniques are said to reduce the amount of data processed while preserving important structural information of objects (Canny, 1986). Edge detection techniques can be classified into five different categories (Sharifi, Fathy, & Mahmoudi, 2002):

1. Gradient Edge Detectors contain classical operators and use first directional derivative operations. Sobel edge detection is an example of gradient edge detection;
2. Zero Crossing uses second derivatives and includes Laplacian operators and second directional derivatives;
3. Laplacian of Gaussian is a combination of Gaussian filtering and Laplacian;

4. Gaussian Edge Detectors is symmetric along the edge and reduces noise by smoothing the image. The main operators involve derivatives of Gaussian. Canny edge detection is an example of Gaussian edge detection; and
5. Coloured Edge Detectors are divided into three categories, which include output fusion methods, multi-dimensional gradient methods, and vector methods.

According to Ansari, Kurchaniya, and Dixit (2017), Bhardwaj and Mittal (2012), Chandwadkar, Dhole, Gadewar, Raut, and Tiwaskar (2013) and Shrivakshan and Chandrasekar (2012), the use of the Sobel edge detection technique is recommended since Sobel edge detection is sensitive to horizontal and vertical edges, and the Canny edge detection is recommended because it is not very prone to noise within image data.

### **Sobel Edge Detection**

Sobel is a gradient edge detection method. Sobel edge detection makes use of the differentiation operator, by computing the gradient of the image's intensity function. Sobel edge detection is based on convolving images with integer values filtered into vertical and horizontal directions (Zhang Jin-Yu, 2009).

### **Canny Edge Detection**

The Canny edge detection technique falls under Gaussian edge detectors. This edge detection technique aims to maximise the possibility of detecting real edge points while minimising the chances of falsely detecting a non-edge point. The detected edges have to be as close as possible to the actual edges. Furthermore, the real edges should not be detected more than once (Canny, 1986).

Figure 4-3 shows a comparison of the Canny and the Sobel edge detection techniques applied to an EL image of a PV cell. This was to show whether edge detection techniques can indeed enhance cracks in EL images of PV cells. Figure 4-3 shows an original EL image of PV cells, and how cracks are enhanced once the Sobel and Canny detection techniques have been applied to the original EL image of a PV cell.

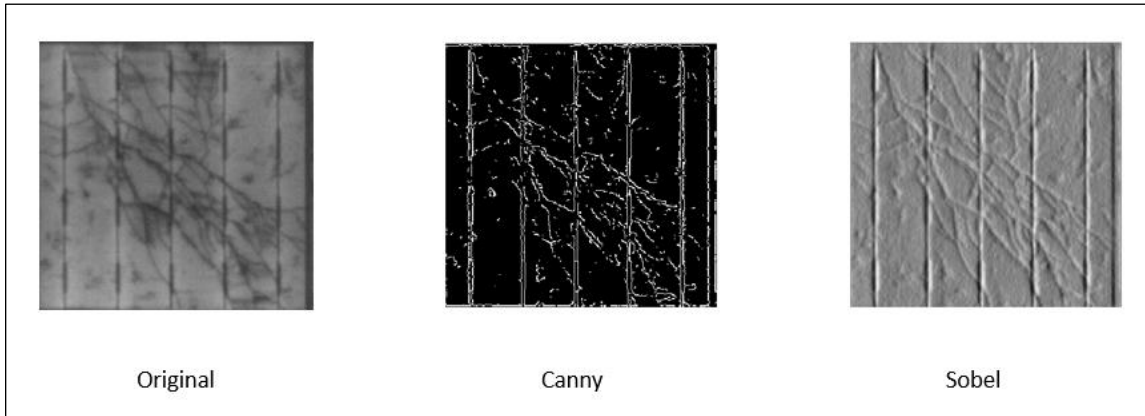


**Figure 4-3: Comparison of Canny and Sobel edge detection techniques**

Edge detection can be vital to this research to identify cracks effectively. Cracks are abrupt changes in the crystal lattice of semiconductors (Section 3.2 and 3.4) used to manufacture PV cells. Alternatively, edges in computer vision are considered as points of abrupt change. Therefore, these principles can be used to identify cracks in PV cells. Furthermore, the edge detectors can enhance only the crack and not the grain boundaries with the PV cells.

Linear filters utilise most of the principles of image pre-processing in the convolutional layer of CNNs (Section 4.3). CNNs are the foundation of DL which is considered an image processing technique under NNs. A discussion of DL is documented in the following section.

### **4.3.2 Deep Learning (DL)**

DL was identified in Section 4.3 as an approach that will be used for this research. DL was of interest to this research after identifying NNs as an image processing technique that can be used for this research. CNNs are vital to DL (Goodfellow, Bengio, & Courville, 2016) and will be discussed in this section. CNNs are a result of successfully applying machine learning (ML) to visual imagery applications such as image classification (Section 4.3.3) and image recognition (Section 4.3.4) systems. The following sections will provide an overview of DL, by providing brief details of ML, NNs, and CNNs.

#### **4.3.2.1 Machine Learning (ML)**

DL is a class within ML that provides systems with the ability to automatically learn and improve their experience without being explicitly programmed (Mitchell, 1994). In addition, DL exploits many layers of non-linear information processing (Deng & Yu, 2013). ML systems are an application of artificial intelligence (AI). Figure 4-4 shows different branches of AI. Furthermore, ML systems are used to identify objects in images, transcribe speech into text or select relevant results for searches. DL makes it possible to solve problems that the best attempts of AI have failed to solve to date (LeCun et al., 2015).



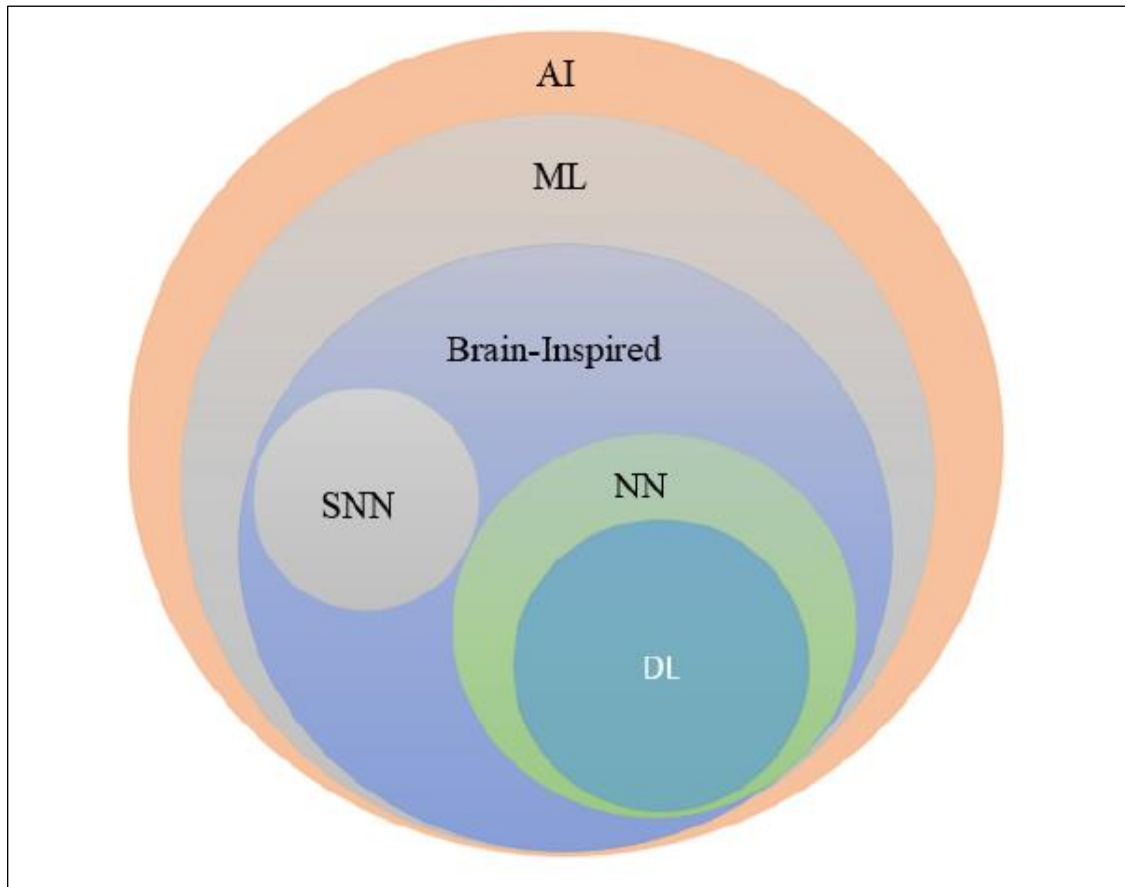


**Figure 4-4: DL in relation to AI** (Sze, Chen, & Yang, 2017)

DL adopts different ML techniques and architectures that use many layers of non-linear information processing stages which are hierarchical (Deng, 2014). One notable technique which DL adopts from ML is the learning algorithms.

ML algorithms are usually divided into two classes: supervised and unsupervised learning. DL, on the other hand, has three broad classes. In addition to supervised and unsupervised learning, DL also has a hybrid learning aspect. (Alom et al., 2018; Deng, 2014; Sze et al., 2017).

1. Supervised Learning: target labels are provided from which patterns necessary for classification are obtained.
2. Unsupervised Learning: it is referred to as generative learning in some cases. Unsupervised learning is expected to capture a high-order correlation of data patterns when no information about class labels is provided.
3. Hybrid Learning: hybrid learning is achieved through optimisation of supervised learning networks, that are then used to estimate parameters in a generative network.

Even though DL is a class within ML, it exists as a subfield of NNs (Figure 4-4), which is a class within ML (Schmidhuber, 2015). NNs will be discussed further in the following section.

### 4.3.2.2 Neural Networks (NNs)

NNs typically model biological neurons of a brain which construct a computational model of artificial neurons. This results in NNs consisting of many connected processes called neurons (Schmidhuber, 2015). Figure 4-5 shows a biological neuron (on the left) and how it is artificially represented (perceptron, on the right).

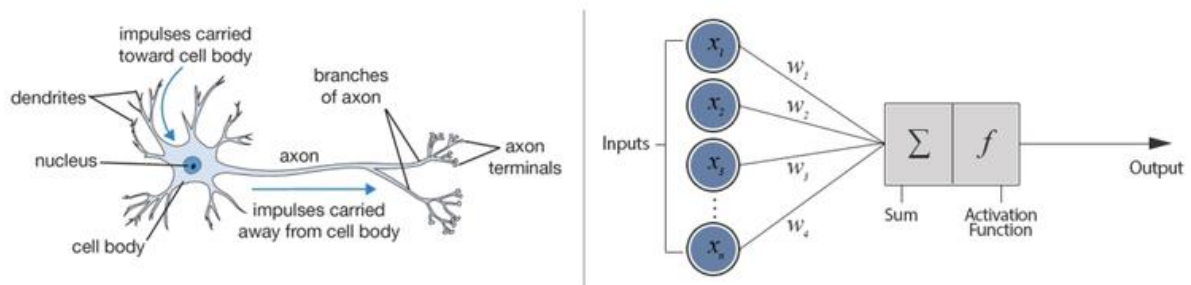


Figure 4-5: Biological neuron vs artificial neuron<sup>3</sup>

The basic component of an artificial neuron is a node. The node receives input signals which are then used to compute the output signal. Input signals either come from the ‘environment’ or other artificial neurons. The output signals of a neuron are a weighted sum of all input signals of a neuron, due to some internal parameters of the neuron (weights and bias) that are learned during training.

$$output = f \left( \sum_{i=1}^N x_i w_i + b_i \right) \quad (1)$$

Equation 1 is a mathematical representation of the artificial neuron depicted in Figure 4-5. The equation also comprises of an activation function. An activation function in artificial neurons is used to compute an output signal from input signals. Activation functions are important in NNs as they enable NNs to learn and allow mappings between inputs and response variables. Equation (2) and (3) are some of the commonly used activation functions (Engelbrecht, 2007):

#### Linear function

$$f(x) = mx \quad (2)$$

<sup>3</sup> <https://www.datacamp.com/community/tutorials/deep-learning-python>

## Sigmoid function

$$f(x) = \frac{1}{1 + e^{-\lambda(x)}}$$

(3)

The sigmoid function (Equation 3) is the activation function used in the experiments designed in Section 5.3. The non-linearity of the function allows it to saturate when it is subjected to very negative or very positive arguments from the input signals, which makes the function insensitive to very small changes (Goodfellow et al., 2016). The linear function (Equation 2) is simple to solve but is volatile when subjected to very positive and very negative arguments from the input signals. The following section will discuss NN architectures.

## Neural Network (NN) Architecture

Artificial neurons are vital to NNs and are used to compose NNs. A NN can be defined as a layered network of artificial neurons, which consist of an input, hidden and an output layer (Figure 4-6). Artificial neurons in one layer are fully or partially connected to artificial neurons in the next layer (Engelbrecht, 2007) and compute output signals using any of the available activation functions. Figure 4-6 is an example of a NN structure.

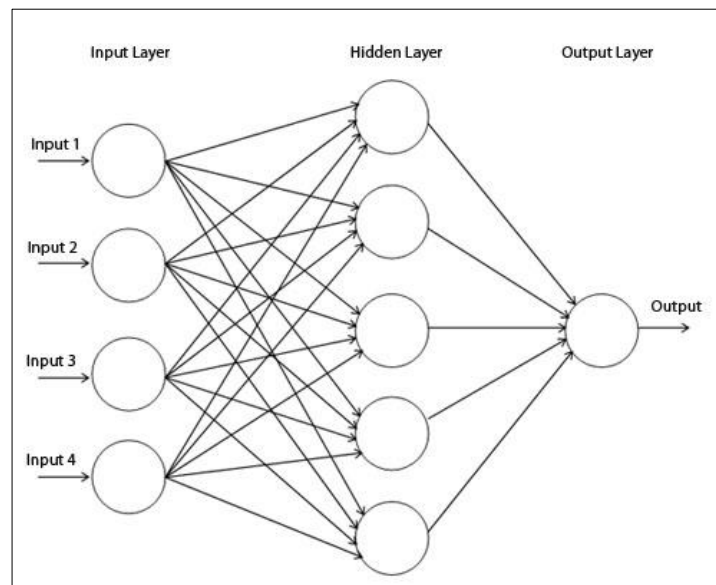


Figure 4-6: High-level NN structure (Engelbrecht, 2007)

The list below describes the different layers that make up a NN (Figure 4-6):

- Input layer: the input layer of a NN receives the initial data, which is then further processed by the other layers of the NN. The input layer comprises of several neurons.

- **Hidden layer:** the hidden layer in a NN is the layer between the input and output layer. The neurons in the hidden layer take in weighted inputs, which are passed through an activation function to produce outputs.
- **Output layer:** the output layer is the last layer of neurons in a NN. The neurons in the output layer produce the final output of the entire NN.

Different NN architectures are used to retain information from the data the NN receives. The following section discusses the different types of NN learning and the different learning rules that exist within NNs.

### **Types of NN learning and Learning Rules**

The three types of learning in NNs are listed below and are similar to how DL classes are defined (Engelbrecht, 2007; Kriesel, 2005):

1. **Supervised learning:** a NN is provided with a labelled dataset (training set). The labels are associated with the target output of the input set. Supervised learning aims to minimise the error between the real output of the neuron and the target output.
2. **Unsupervised learning:** the aim of unsupervised learning is for the NN to discover patterns within input data. The aim is to achieve this without any interference with labelled data. The NN has to create pattern classes.
3. **Reinforced learning:** the principle of reinforced learning is to incentivise a NN for good performance or castigate the NN for poor performance. The training set consists of input patterns and allows the NN to return results based on the input patterns. The network is then incentivised if the returned result is correct.

The different learning types have resulted in the development of different learning rules. The different learning rules are as follows (Engelbrecht, 2007):

1. **Augmented Vectors:** this learning rule allows the input vector to be augmented which allows an additional input unit to be added. The additional input unit is called the bias unit.
2. **Gradient descent:** Gradient descent involves defining an error function which is used to measure the error while approximating the target. This learning rule works towards finding the weight values that minimise the error. The error is minimised by calculating the gradient of the error in the weight space, while moving the weight vector along the negative gradient. An illustration of the Gradient descent is depicted in Figure 4-7.

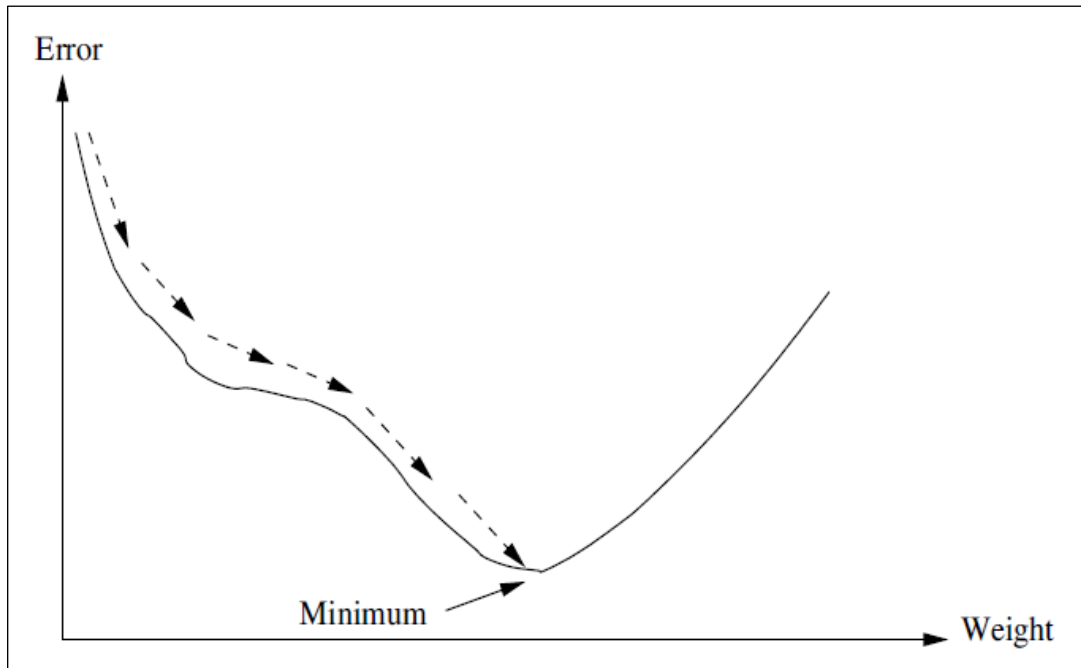


Figure 4-7: Illustration of gradient descent (Engelbrecht, 2007)

3. Widrow-Hoff: the Widrow-Hoff learning rule is referred to as the least-mean-square (LMS) algorithm in some cases. This learning rule was one of the first algorithms to train layered NNs with multi-adaptive linear neurons.
4. Generalised Delta: the generalised delta learning rule is the generalisation of the Widrow-Hoff learning rule.
5. Error correction: this learning rule is used in supervised learning, and this method compares the NN output and the intended output. The obtained error is therefore used to direct the training process.

Up until this point, the focus has been on single-layer NNs. However, single-layer networks have a limitation of the perceptron, which only permits the implementation of binary classifiers. The limitation of single-layer NNs is overcome by the implementation of a multilayer perceptron (MLP). MLP introduces the following factors to NNs:

- The model of each neuron includes a non-linear activation function that is differentiable;
- The network contains one or more hidden layers from both input and output nodes; and
- Multilayer perceptron networks have a high degree of connectivity.

A special class of multilayer perceptron is known as convolutional networks or convolutional neural networks (CNNs) and are well suited for pattern recognition. CNNs have been commonly used in signal and image processing, making CNNs vital to this research (Haykin, 2008). CNNs will be discussed in the following section.

### 4.3.2.3 Convolutional Neural Networks (CNNs)

According to Goodfellow, Bengio, & Courville (2016), CNNs are a specialised kind of NNs that processes data with a grid-like topology. Furthermore, CNNs are NNs that employ a mathematical operation called convolution. CNNs are designed to recognise two-dimensional shapes with a high tolerance for scaling, skewing, translation and other different forms of distortion (Haykin, 2008). This case of recognition is achieved through supervised learning and such networks exhibit the following factors:

1. Feature extraction: neurons take synaptic input from the previous layer from a local receptive field, allowing the neuron to extract local features. After the features have been extracted, the location of the features is no longer important, as long as the position relative to other features is preserved.
2. Feature mapping: each computational layer of the network comprises of multiple feature maps, each of which are in the form of a plane. Within the planes, individual neurons are constrained to share the same set of synaptic weights. The neuron constrain allows for shift invariance and reduction in the number of free parameters.
3. Subsampling: local averaging and subsampling are performed by computational layers that follow each convolutional layer. Subsampling results in the reduction of the feature map's resolution. Subsampling reduces the shift sensitivity of output feature maps and other forms of distortion.

CNNs have over the years become popular in image and sound classification tasks. In addition, CNNs have gained considerable attention in computer vision research (Ferreira & Giraldi, 2017). CNNs similarly to NNs are an important part of DL. CNNs are regarded as a DL application. CNNs have been applied in several computer vision research and have provided effective results in different image classification tasks. Figure 4-8 shows a high-level general CNN architecture used for image recognition (Patterson & Gibson, 2017). CNNs are similar to NNs (Section 4.3.2.2) and comprise of layers of neurons similar to those depicted in Figure 4-6. The layers in CNNs can be grouped as the input layer, feature-extraction layers and classification layers.

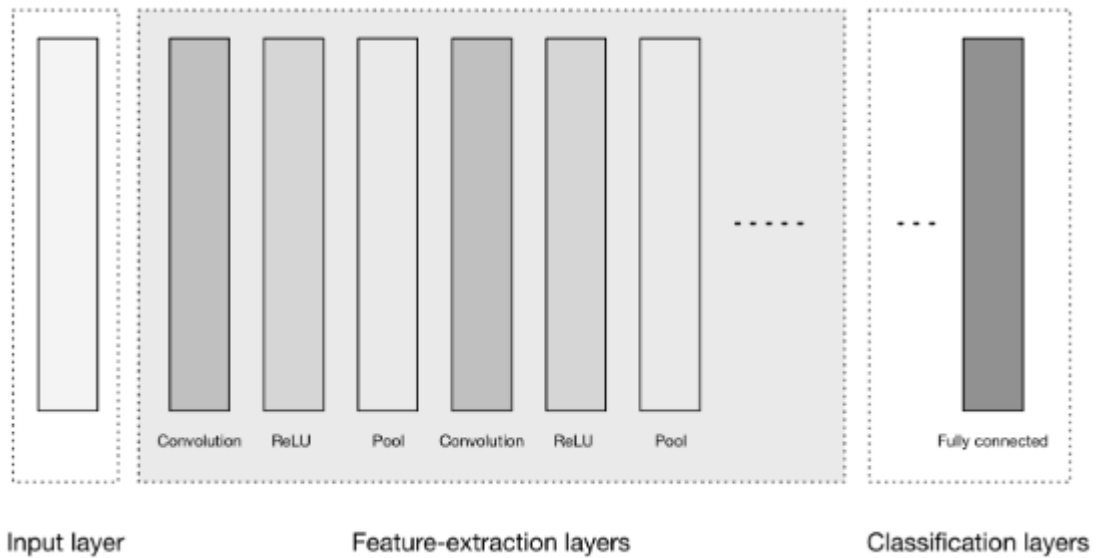


**Figure 4-8: High-level general CNN architecture** (Patterson & Gibson, 2017)

The different layers that make up a CNN architecture are listed below and are depicted in Figure 4-8:

1. **Input layer:** data is fed into the network through the input layer. Raw image pixels can form part of this input data.
2. **Convolution layer:** a convolution is an operation on two functions. The convolution layer consists of a function of image's input values and filter (or kernel) function which is an array of numbers. Kernels are responsible for extracting high-level features that are fed to proceeding layers. The input image values are in the form of 2D matrices as depicted in Figure 4-9, which are used to generate the output matrices.

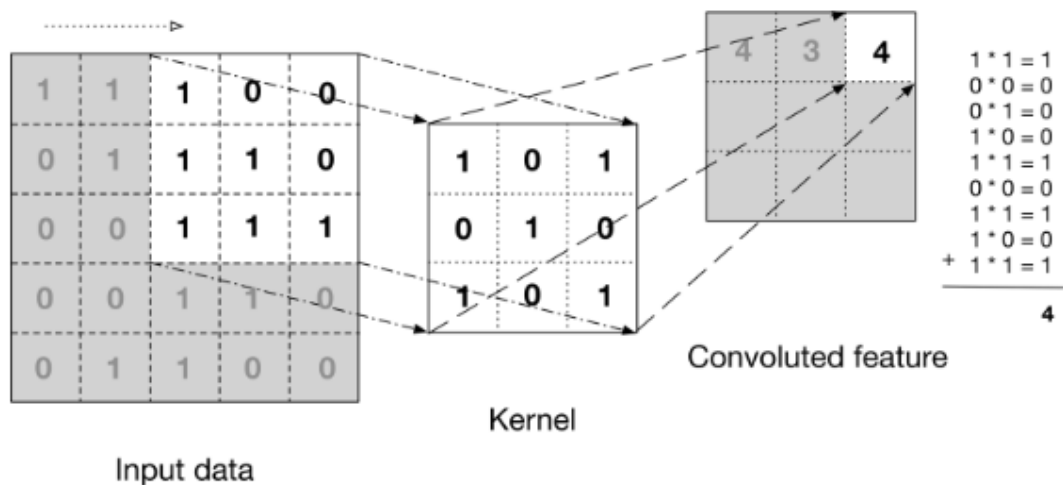


**Figure 4-9: Convolution function** (Patterson & Gibson, 2017)

The filter highlights patterns that can be used in characterising input images. These filters may incorporate edge detectors similar to those discussed in Section 4.3.1.2. The dot product of the input and kernel function gives an output.

$$O_j = f\left(\sum_{i=1}^N I_i * K_{i,j} + B_j\right) \quad (4)$$

In Function 4,  $I_i$  is the input matrix which is convoluted with a corresponding kernel matrix  $K_{i,j}$ .  $B_j$  is a bias matrix which is added to the resulting convoluted matrix.  $O_j$  is the output matrix which is produced by the non-linear function  $f$  which is applied to each element.

3. **Rectified Linear Unit (ReLU):** ReLU layers are used to apply non-linear functions to outputs of previous functions. Non-linear functions are used as the neuron activation function (Section 4.3.2.2). The activation function is defined as:

$$f(x) = \max(0, x) \quad (5)$$

where  $x$  is the input to the neuron. The ReLU improves learning and classification performance in CNN applications.

4. **Pooling layer:** the pooling layer is found between the convolution and ReLU layers. The pooling results in CNNs using fewer parameters in the learning process. As a result, the network only focuses on the most important patterns.
5. **Fully-connected layer:** every neuron from all the other layers is connected in this layer. This is done to get an understanding of all the patterns generated in the preceding layers. This layer computes the possible score for the different classes used to train the network.
6. **Loss layer:** this is usually the last layer of a network. The aim of this layer is to evaluate how much the predictions from the trained model deviate from the true labels assigned to data during supervised training.

The following section discusses the learning techniques that exist in CNNs. CNN learning techniques conform to NN learning types; supervised, unsupervised and reinforced learning.

### CNN learning

CNNs are a DL application. CNNs allow DL systems to identify useful patterns from images automatically. CNNs are similar to normal NNs, but CNNs tend to use fewer parameters in their



learning algorithms (Ferreira & Giraldi, 2017). The ability of CNNs to achieve shift/translation invariance makes it suitable to be used on images (Wahab, Khan, & Lee, 2017). There are a number of ways in which CNNs can learn parameters from image data, which includes the following (Spampinato, Palazzo, Giordano, Aldinucci, & Leonardi, 2017):

- Training CNNs from scratch;
- Off-the-shelf features extracted from CNNs trained on general imagery;
- Fine-tuning pre-trained CNN models; and
- Transfer learning (TL).

CNNs trained from scratch extract all features needed to complete a computer vision task from data that has been provided to the network as input data. However, the resulting adaptive model from training a CNN can be used in off-the-shelf feature extraction, fine-tuning and TL.

One approach of the off-the-shelf feature extraction uses a pre-trained CNN that have been trained from scratch as a feature extractor. The output vector of the fully-connected layer is based on input images used to train a much simpler classifier. This approach works best if the images used to train the dataset are similar to the input dataset (Spampinato et al., 2017). However, the off-the-shelf approach would not be useful for this research because no systems were trained on a dataset similar to the dataset used for this research could be found.

On the other hand, fine-tuning pre-trained CNN models is an alternative DL approach. An existing model is analysed and is fine-tuned to the target dataset. This technique helps speed up the training process of the CNN and helps prevent overfitting (Section 5.5) (Spampinato et al., 2017).

Lastly, TL is achieved by transferring knowledge gained from one task to help solve a different task (Oquab, Bottou, Laptev, & Sivic, 2014). The knowledge is essentially transferred when weights (Section 4.3.2.2) from one CNN model are used in a different CNN model provided that the CNN architecture is the same. TL allows for the transfer of knowledge between different CNNs that are intended to solve completely different tasks (Pan & Yang, 2010). Although TL is similar to fine-tuning, it is not the same.

The following section discusses image classification and briefly discusses how DL CNNs can be used to complete image classification tasks.

### **4.3.3 Image Classification**

Image classification is an important aspect of this research as there is a need to distinguish between normal and defective polycrystalline PV cells and different types of polycrystalline PV cell defects. The PV cell data (EL images) collected for this research need to be classified according to similarities

in features. Image classification is, therefore, the process of categorising all pixels in an image to obtain a given set of labels (Al-doski, Mansor, Zulhaidi, & Shafri, 2013). Image classification is an image processing task (Section 4.3) thus making it a subset of computer vision.

Image classification frameworks include feature extraction before images are fed into a classifier. Figure 4-10 depicts a basic image classification framework. Currently, feature extraction to identify defective PV cells from EL images is done manually, and this research aims to automate the feature extraction and classification processes.

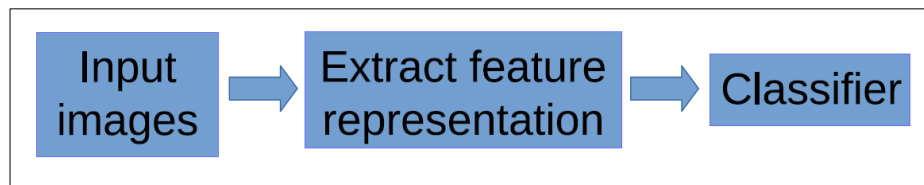


**Figure 4-10: Image classification framework** (Shu, Mclsaac, Osinski, & Francis, 2017)

Feature extraction is the elimination of inconsistencies from image data by the reduction of variables within the data to end up with a more manageable group of image data (pixels) for processing (Sahu, Saxenaa, & Manoria, 2015). The goal for feature extraction is to map data to labelled classes. The features obtained from the feature extraction process are usually used for image selection or classification tasks (Choras, 2007). The descriptive and discriminative power of a feature extractor are crucial in attaining good classification performance (Li et al., 2014).

Classifiers perform the role of a discriminant. Image pixels are grouped before the classification process, through feature extraction processes. The pixel grouping process is known as training in other systems. The classifier, therefore, identifies which class new images belong to from the features within the image (Gaur & Chouhan, 2017).

The feature extraction process for this research will be supervised. The pre-processed images will have to be labelled correctly. The images will be labelled according to features describing the defects present in the images. The labelled images will, therefore, be used to produce a trained classifier that will be used to predict to which classes the images belong. Figure 4-11 shows different image classification techniques that produce classifiers as a by-product.

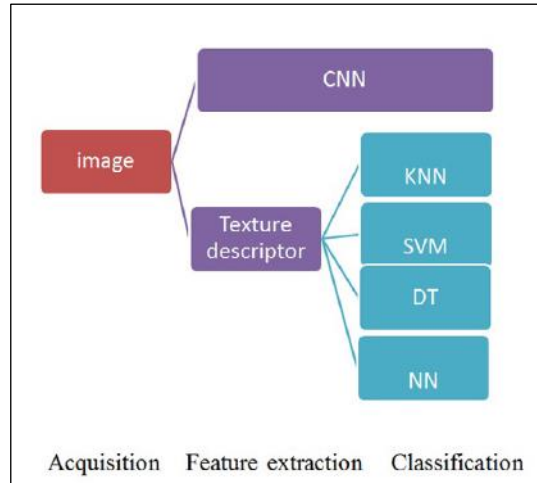


**Figure 4-11: Image classification techniques** (Affonso, Rossi, Vieira, & de Carvalho, 2017)

The different image classification techniques are listed below (Affonso et al., 2017):

- NN: NNs are a computer system modelled on a human's brain and the nervous system. NNs were discussed in Section 4.3.2.2.
- CNN: CNNs are a specialised kind of NNs that process data with a grid-like topology (Goodfellow et al., 2016). CNNs were discussed in Section 4.3.2.3.
- Support Vector Machine (SVM): SVM is a learning technique, using statistical learning theories as to its foundation. SVM is robust to high-dimensional data and has high generalisation ability in different domains.
- K-Nearest Neighbours (KNN): KNN is one of the simplest ML algorithms.
- Decision Tree (DT): A DT requires splitting a complex decision into a combination of simpler decisions in the hopes that the final solution is similar to the intended solution.

There are two broad categories of image classification techniques, namely supervised and unsupervised classification (Al-doski et al., 2013). Furthermore, supervised and unsupervised classification are commonly used to distinguish the different learning techniques within machine learning. DL (Section 4.3.2) was identified as the image processing technique that can be used to solve the classification of EL images of defective PV cells in this research. In addition, DL shares similar learning techniques as image classification as stated by Al-doski et al., (2013). The following section discusses some of the DL CNN architectures that can be trained to create adaptive models that can be used in image classification.

### Image Classification Architectures

DL CNN architectures are suited for tasks ranging from general image classification to multi-stream data processing (Patterson & Gibson, 2017). The effectiveness of CNNs in image classification tasks

has in some cases outperformed humans (He, Zhang, Ren, & Sun, 2015). CNNs were identified in Figure 4-11 as an image classification technique. Some of the DL CNN architectures include LeNet, AlexNet, MobileNet and GoogLeNet, Xception.

**LeNet:** LeNet is a CNN architecture proposed by LeCun in the 1990s. At the time it proved difficult to implement the algorithm due to limited computation capability and memory capacity. Figure 4-12 shows a LeNet CNN architecture.

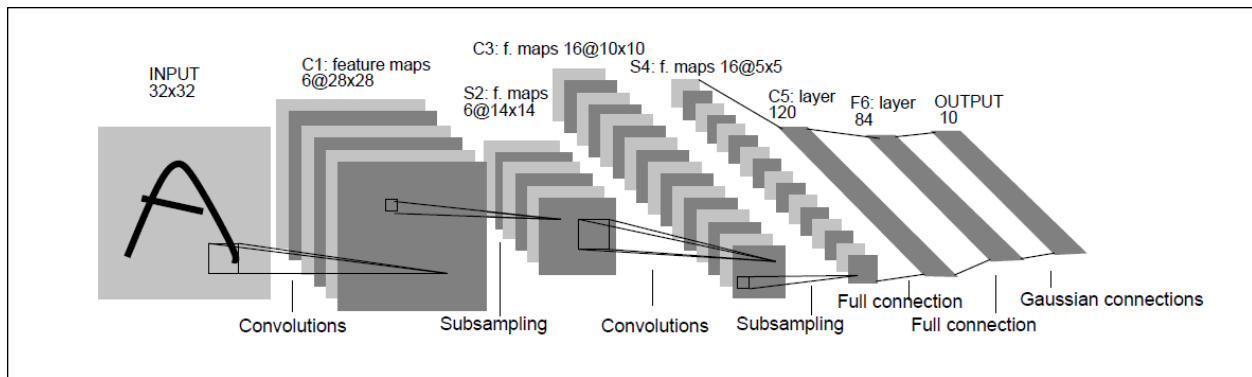


**Figure 4-12: LeNet CNN architecture** (LeCun, Haffner, Bottou, & Bengio, 1999)

**AlexNet:** This network architecture comprises of eight layers. Five of the layers are convolutional layers and the remaining three are fully connected layers (Krizhevsky, Sutskever, & Hinton, 2012). AlexNet was proposed by Krizhevsky et al. (2012) and at the time it was the deepest layer hierarchy.

**VGGNet:** VGGNet was a result of investigating how the depth of a network affects recognition or classification accuracy of a CNN (Simonyan & Zisserman, 2015). The VGG architecture is comprised of two convolutional layers. Both convolutional layers use the ReLU activation function. The following layers consist of a single max pooling layer and a few fully connected layers which use the ReLU activation function. The final layer of the VGG model is a softmax layer responsible for classification (Alom et al., 2018).

**GoogLeNet:** The GoogLeNet architecture was developed to reduce computational complexity in comparison to traditional CNN architectures. This was achieved by increasing the depth and width of the base network while maintaining the computation budget (Szegedy et al., 2014).

**Xception:** The Xception architecture is a linear stack of depthwise separable convolutional layers with a residual connection. This makes the architecture very easy to modify and define (Chollet, 2017). Xception was developed from the GoogLeNet architecture.

**MobileNet:** MobileNet architectures are primarily built from separable convolutional layers. MobileNets were proposed with the aim of reducing latency while yielding a small network (Howard et al., 2017; Sze et al., 2017).

The following section discusses pattern recognition, an image processing task that uses similar principles to image classification.

#### **4.3.4 Pattern Recognition**

Pattern recognition is an important part of computer vision and image processing and is a useful principle in automatic image recognition systems (Do, 2007). Patterns within images are key in the classification and the interpretation of images (Acharya & Ray, 2005). Pattern recognition is the process of classifying images based on similar descriptors or objects within an image (Dutt, Chaudhry & Khan, 2012; Fu & Rosenfeld, 1976). This research aims to identify defective PV cells automatically; therefore, making pattern recognition essential for this project.

Classification is an integral part of pattern recognition. Image classification was discussed in the previous section (Section 4.3.3). Aspects of the classification framework are also used in pattern recognition systems. Primarily, image classification involves feature detection within images and thus grouping images based on labels describing the detected features.

In addition, matching and feature detection (extraction) are important techniques that form a pattern recognition system. In order to detect patterns within images, the image being processed are matched to a standardised version of the pattern (Fu & Rosenfeld, 1976). Patterns are detected using techniques similar to edge detection and segmentation, which have been discussed throughout Section 4.3.1.

Pattern recognition systems require the image and image scene to be analysed in conjunction with all of the techniques within image recognition. Image and image scene analysis is useful in identifying image descriptors, which are deduced from the relationships and the properties of parts of images (Fu & Rosenfeld, 1976).

Different approaches exist for developing pattern recognition system. These approaches are (Dutt et al., 2012):

- Statistical pattern recognition;
- Data clustering;
- Fuzzy sets;
- NN;
- Structural pattern recognition;
- Syntactic pattern recognition; and
- SVM.

Pattern recognition systems are developed based on the approaches mentioned above. Pattern recognition systems can be broken into three parts, which include; acquiring the data, analysis and classification. This can serve as confirmation that pattern recognition is a computer vision task (Section 4.2). Pattern recognition can be used to identify patterns within EL images that indicate the presence of defects within PV cells. Therefore, pattern recognition can be considered as a computer vision task that can be applied to this research. Furthermore, it can be noted that both pattern recognition and image classification systems can be implemented using NNs.

The following section reviews different areas in which computer vision tasks such as image classification and pattern recognition have been applied. The following section will also provide insight into how this research project can utilise the different aspects discussed in this chapter.

## **4.4 Related Work**

Existing systems related to the field of image recognition, processing, and classification will be discussed in this section. A review of these systems will examine different ways in which images are analysed to identify different patterns within the images. The findings of this review will be used to identify possible ways in which a solution can be implemented to use image processing to identify patterns that may indicate PV cell defects in polycrystalline solar modules.

### **4.4.1 Medical Image Analysis**

Image-based diagnosis, disease prognosis and risk assessment are some of the ways in which images are used in the medical field. X-rays, CT scans, MRI, positron emission tomography and retinal photography are some of the common images used in different areas of medical image analysis (Litjens et al., 2017; Spampinato et al., 2017).

Since the 1970s, AI paradigms have been adopted in different areas of medicine (Shen, Wu, & Suk, 2017). However, the increase in the use of hand-crafted feature extraction techniques paved the way for the use of machine learning in medical image analysis. In addition, pattern classification is another technique that has been used for medical image analysis for decades (de Bruijne, 2016). Furthermore, image segmentation and image recognition are other techniques that have been introduced in medical images analysis and have shown great promise with regards to the use of computer vision in medicine (Li et al., 2014).

X-ray images were listed as one of the common images used in image-based diagnosis. One way in which x-rays are used is to perform automated skeletal bone age assessment. Skeletal bone age assessment is a procedure used in pediatric radiology for diagnostic and therapeutic investigation of children growth and genetic disorder (Spampinato et al., 2017). Figure 4-13 shows examples of x-rays used in CNN-based skeletal bone age assessment system. A CNN is used to asses a dataset

of x-ray images and predicts the right diagnosis or the right genetic disorder of the patient. Regions of interests are identified (joints), and the features extracted from the regions of interest are used predict a diagnosis (Spampinato et al., 2017).

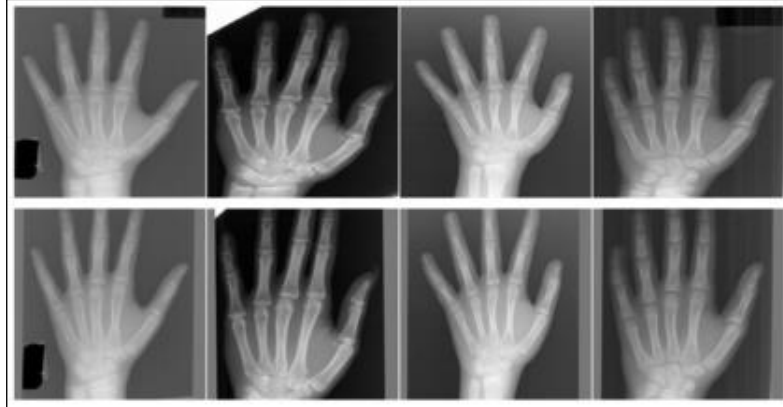


Figure 4-13: Example of X-ray images used in skeletal bone age assessment (Spampinato et al., 2017)

#### 4.4.2 Feature Learning and Image Classification

Feature learning and feature extraction are used for text recognition, especially from handwritten extracts (Balci, Saadati, & Shiferaw, 2017). Text recognition tends to cause problems because of different writing styles that exist. CNNs have the capability of learning different handwriting styles used to represent the same character.

Secondly, feature learning and image classification can be used in remote sensing. Remote sensing is a process of obtaining information about objects or areas of the earth's surface without being in direct contact with the object and area (Aggarwal, 2004). In this case, satellite images have to be classified for a variety of reasons, some of which include landscape planning and resource management (Al-doski et al., 2013). The images are classified based on pre-existing images from which the feature have been extracted. After that, new images are matched to the most appropriate class based on extracted features.

Feature learning and image classification have been adopted in the automotive industry, which is made possible using DL. DL makes traffic sign recognition in vehicles systems possible, which is helpful in driver assist systems (Cireşan, Meier, & Schmidhuber, 2012). Figure 4-14 depicts how DL is used in vehicles. An image is read into the system, which is then subjected to a CNN. The output from the CNN is used to adjust different controls of the vehicle.

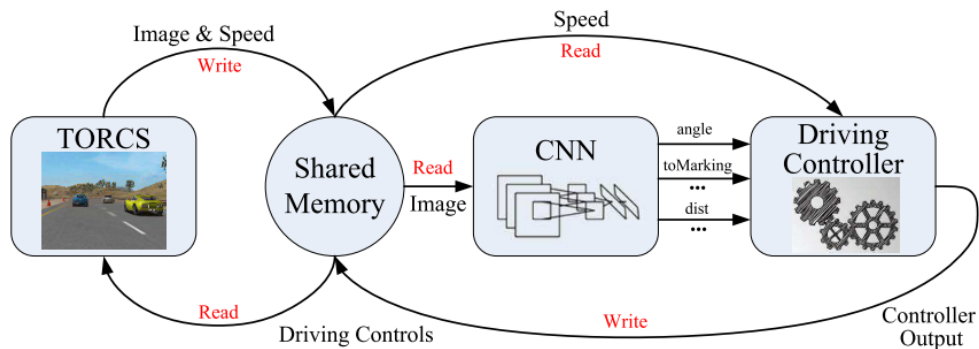


**Figure 4-14: Driver assist system architecture** (Chen, Seff, Kornhauser, & Xiao, 2015)

Feature learning and image classification are further used in defect detection systems. These systems include surface damage detection, metallic surface defect detection and crack damage detection (Cha, Choi, & Büyükoztürk, 2017; Huang, Xie, Yao, Li, & Chen, 2018; Tao, Xu, Ma, Zhang, & Liu, 2018). CNNs are used to learn features of surfaces, and the resulting adaptive models are used to recognise damaged surfaces, cracks and defective metallic surfaces. This provides further evidence that DL can be used to attempt to automatically identify defective PV cells from EL images.

Furthermore, feature learning and image classification are used to determine defective PV cells from thermal images (Pierdicca et al., 2018). However, there is no physical properties that can be determined by analysing thermal images of solar panels (Section 3.5.4). This project aims to use EL images to PV cells that are either normal, uncritical, critical and very critical.

The following section discusses a preliminary investigation of tools that can be used to implement experiments for this research.

#### 4.5 Preliminary Investigation of Implementation Tools

A variety of development environments are available to implement DL experiments, but Python appears to be the most popular programming language used when implementing AI systems and consequently deep neural networks (Goodfellow et al., 2016; LeCun et al., 2015; Srivastava, Hinton, Krizhevsky, Sutskever, & Salakhutdinov, 2014; Sze et al., 2017). DL was one approach that was discussed in this chapter that can be used to identify defective PV cells from EL images automatically.

TensorFlow is an open source software library that was developed by Google's Machine Intelligence research organisation for conducting machine learning and deep neural network



research (TensorFlow, 2017). Keras is a high-level API, written in Python. Keras was developed to enable fast experimentation, and it can run on top of TensorFlow (Keras Documentation, 2017).

Open Source Computer Vision Library (OpenCV) is an open source computer vision and machine learning software library. The library comprises of more than 2500 classes and state of the art computer vision and machine learning algorithms. OpenCV interfaces with C++, Python, Java and MATLAB. OpenCV supports Windows, Linux Android and MAC operating systems (OS) (OpenCV library, 2017).

## 4.6 Summary

This chapter aimed to discuss computer vision (Section 4.2), image processing (Section 4.3) and to review work related (Section 4.4) to this research. Section 4.2 provided a foundation into image processing, and different computer vision tasks within image processing were identified.

In addition, different image processing techniques were identified (Section 4.3), and the most appropriate image processing technique to apply to this research was identified. DL was identified as the suitable image processing techniques as it was a subclass of NNs and it was discovered that DL has successfully revolutionised computer vision. Furthermore, image pre-processing (Section 4.3.1) was discussed, which highlighted, that different edge detection techniques which are in some cases used in DL for feature extraction.

DL was discussed in Section 4.3.2, and it was discovered that DL is developed from existing fields such as ML, NNs and CNNs. Moreover, ways in which DL can be used to assist in identifying defects in polycrystalline PV cells using EL image of PV cells (RQ<sub>3</sub>) were motivated by the discussion in Section 4.3.2.

Image processing tasks, specifically image classification (Section 4.3.3) and pattern recognition (Section 4.3.4) were discussed. It was identified that these tasks were vital to this research. In addition, it was identified that image classification and image recognition systems could be developed using NNs which further motivated the use of DL in this research. DL CNNs that can be used to accomplish image classification tasks were also discussed in Section 4.3.3. This provided evidence on how an image processing techniques (DL) can be used appropriately to identify defective PV cells from EL images (RQ<sub>4</sub>).

Related work (Section 4.4) that used DL as an image processing technique were reviewed. These included the application of DL in medical image analysis and feature learning and image classification. This was a preliminary investigation on how the identified image processing could be used appropriately to identify defective PV cells from EL images (RQ<sub>4</sub>). Furthermore, this provided

insight on how to design DL CNN that can be used to extract patterns within PV cell EL images to classify them accordingly.

Lastly, a preliminary investigation of the different tools that could be used to implement DL were discussed in Section 4.5. The following chapter will discuss the experiments designed to demonstrate whether image processing can be used to identify defective PV cells from EL images effectively.

# 5 EXPERIMENTAL DESIGN AND IMPLEMENTATION

## 5.1 Introduction

This chapter discusses the experiments designed to test aspects of the main research question. In addition, the proposed solution (Section 5.2), the experimental design (Section 5.3), the implementation of the experiments (Section 5.4), the experimental procedure (Section 5.5) and the evaluation plan (Section 5.6) are discussed in this chapter.

Section 2.3 presented the motivation for selecting the experimental research methodology for this research. Therefore, this chapter is the core component of the work presented in Section 2.3. In addition, literature was reviewed in Chapters 3 and 4 to confirm the data to be sampled for this research. Plans were introduced on how the data (EL images) should be manipulated (Section 2.2.4.1) for the experiments designed and implemented in this chapter.

This chapter will aim to address the fourth research question (Figure 5-1). The research question reads:

*RQ<sub>4</sub>: How can an image processing technique be used appropriately to identify defective PV cells?*

Figure 5-1 depicts the activities that are carried out in this chapter. In addition to testing RQ<sub>4</sub>, samples are categorised into different classes (Section 5.3.2.2) for experiments, and variables are controlled (Section 5.5) to produce the most effective model to identify defective PV cells from EL images. A small sample from the allocated samples is used to test the dependent variables in order to evaluate the model. The results of the evaluation are reported in Chapter 6.

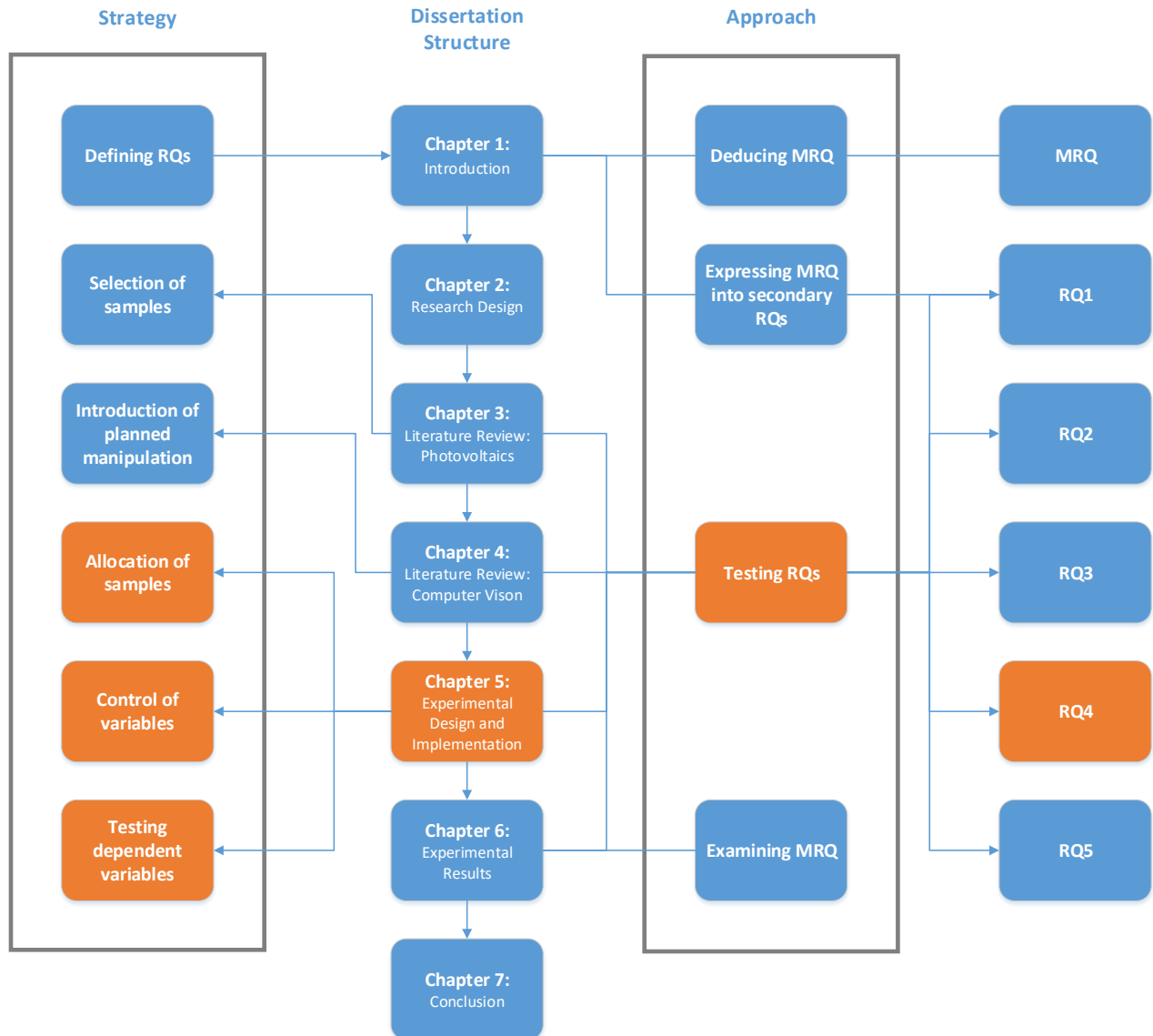


Figure 5-1: Chapter overview

The next section discusses the solution that was proposed to identify defective PV cells from EL images automatically.

## 5.2 A proposed solution for automatic identification of defective photovoltaic (PV) cells

Based on literature and the related work reviewed in Chapter 4, it was decided that DL (Section 4.3.2) in some cases referred to as deep CNNs (Rawat & Wang, 2017) will be used for the purpose of this research in an attempt to automatically identify defective PV cells from EL images. Specifically, CNNs with a deep layer hierarchy will be applied to this research (Section 4.3.2.3).

EL images will be used to automate the process of identifying defective PV cells as an image classification task; therefore it was appropriate to include image processing in the proposed solution. Figure 5-2 shows the different stages of the proposed solution. The proposed solution will take in an input image, and this input image is then segmented into individual PV cells (Section 2.2.4.1). Features from PV cell EL images are then extracted to train a classifier.

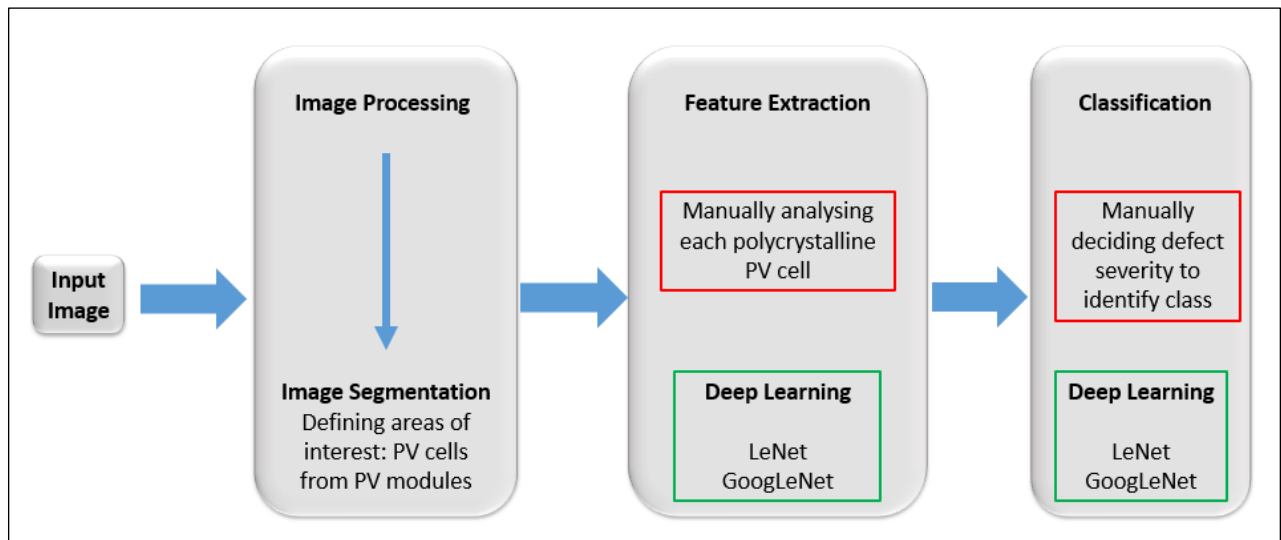


Figure 5-2: Existing method vs. stages of the proposed solution

The proposed solution maps onto different aspects of the main research question identified in Section 1.4. The main research question reads:

***MRQ) How can an image processing technique be used to efficiently identify PV cell defects of polycrystalline PV cells from EL images?***

**Image processing technique** – image processing was identified in the research question as a way to automatically identify defective PV cells from EL images (Section 1.5). Section 4.3 provides an overview of image processing and the different image processing techniques were also identified. DL was determined to be the most appropriate image processing technique.

**Efficiently identifying polycrystalline PV cell defects from EL image** – currently, the process of identifying defective PV cell from EL images is done through a tedious manual process. Chapter 3 discussed constraints in existing methods of identifying PV cell defects using EL images. A DL CNN can extract features automatically from EL images, and the extracted features can be used to classify new EL images into the appropriate defect category correctly.

The image processing stage of the proposed solution in Figure 5-2 deals with how data is handled. The data collection process (Section 2.2.4.1) resulted in EL images of PV modules being provided. The proposed solution suggests segmenting (Section 4.3.1.1) EL images of PV modules into

separate PV cells making up a PV module. The area of the PV cell image was considered as the area of interest for this research, especially if the area was affected by defects. The proposed solution will extract features from the segmented (pre-processed) images. Therefore, all the adaptive models used in this research were trained in EL images of PV cells. The original images that were provided for this research were each split into individual cells before any training process was carried out. The provided PV module images were normally oriented; therefore, a simple region splitting algorithm was applied to the PV module images (Kamdi & Krishna, 2012) with the OpenCV library used for this project. Each EL image of a PV module comprised on 72 PV cells. Below are the details of the algorithm:

---

```

load image;
  for row in range (0, image, 12) do // 12 rows
    for column in range (0, image, 6) do // 6 columns
      writeNewImage(img{row}_{column}.png)
    end
  end
end

```

---

The second stage of the proposed solution in Figure 5-2 deals with feature extraction. This stage required features to be extracted and learned from different labels (classes) of PV cells; two classes for the first phase of experiments (binary classification) and four classes for the second phase of experiments (multi-class classification) (Section 5.3.2.2).

The features extracted in the second stage of the proposed solution in Figure 5-2 are used to train a classifier which is used in the last stage; classification (Section 4.3.3). The classification allows trained DL models to identify to which class a PV cell belongs automatically. The following section discusses the experiments designed as a result of the proposed solution.

### 5.3 Experimental Design

This section documents how the experiments needed for this research were designed and outlined a plan on how to conduct the experiments. The proposed solution aims to identify a process to effectively and automatically identify defective polycrystalline PV cells from EL images. The experimental design discussed in this section includes all the necessary steps taken in all the experiments that were designed and carried out. The experiments are required to answer the MRQ.

The experiments were designed in two phases, namely a binary classification experiment and multi-class classification experiment. The initial phase of experiments was the binary classification

experiments and these experiments were necessary to confirm whether a DL approach (Section 4.3.2) was an appropriate image processing technique. The literature reviewed highlighted similar problems that were solved using DL. The initial phase required scaling down the problem, by assuming that PV cells belong to two classes. The two classes for this phase of experiments were said to be normal and defective. Figure 5-3 depicts a high-level architecture describing the CNN used in the first phase of experiments. The CNN takes EL images of a PV cell as input images, and then the features are extracted and learned in the different layers of the CNN to produce an adaptive model that can classify EL images PV cells. The experiments in the initial phase were used to determine how feasible the proposed solution was to the identified problem. The four identified classes could be represented by two simple classes. This was done to observe whether the resulting classifiers were able to model the data representing two classes. This was done before the data was allocated into four different classes. Based on the training history of the models using this data, the solution was extended to incorporate the four classes identified in Chapter 1.

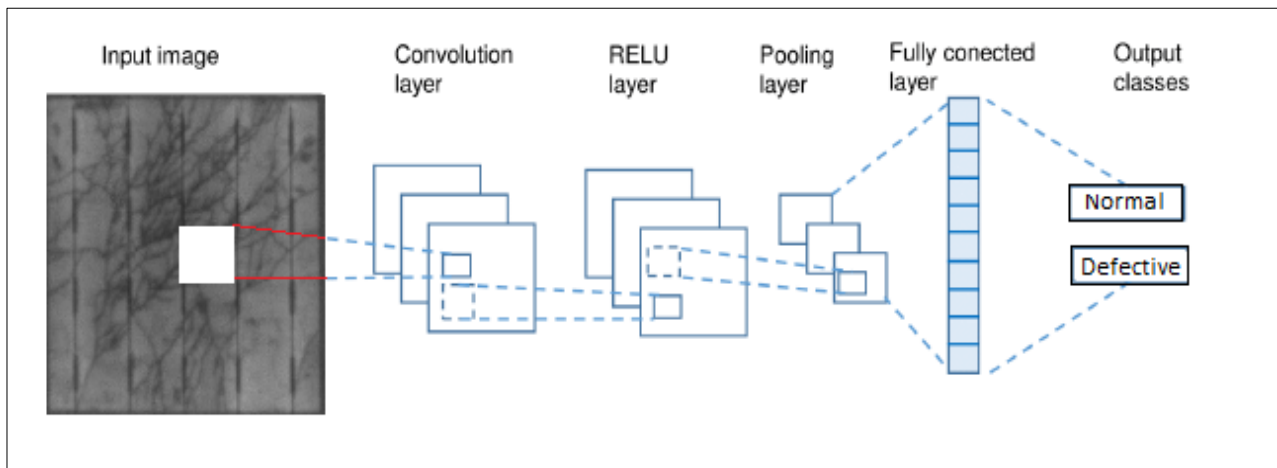


**Figure 5-3: Mock-up CNN for the initial phase of experiments** (Ker, Wang, Rao, & Lim, 2018)

The second phase of experiments, the multi-class classification experiments, on the other hand, were reliant on results from the first phase of experiments. Failure to obtain a positive result from the initial phase of experiments would indicate that the proposed solution would not be a viable option. In addition, the classes in which PV cells would be classified into for the second phase of experiments were based on standards defined in Sections 1.5 and 3.6. The standard classifies PV cells into four classes based on the presence or absence of defects, namely: normal, uncritical, critical and very critical. In addition, the same CNN architecture as the one used in the initial phase of experiments (Figure 5-3) can be used to describe the second phase of experiments; the only difference being the number of output classes. The performance history of these experiments are discussed in Section 5.5.3. The results of the second phase of experiments based on the evaluation plan (Section 5.6) are discussed in the next chapter, and the results of the second phase of

experiments are used to determine the effectiveness of image processing using DL in identifying defective PV cells from EL images.

Before any of the experiments could be carried out, the data (EL images) had to be pre-processed (Section 4.3.1). The different ways in which the EL images were processed for this research are discussed in Section 5.3.1.

Besides data processing, the experimental setup had to be defined. The experimental setup included the platform on which experiments were conducted and the PC configuration that was used for the experiments. Details regarding the experimental setup are discussed in Section 5.3.2.

### **5.3.1 Data processing**

Image processing is one of the main foci of this research (Section 4.3). EL images of polycrystalline PV cells were used for this research, and this section discusses some pre-processing that was performed on the data.

The EL images were obtained from the Physics Department at NMU (Section 2.2.4.1). The EL images provided for this research all represented entire polycrystalline PV modules. For this research, PV cells were the main focus (Section 2.2.4.1). Therefore, PV cell images had to be segmented from the PV module images. According to the literature reviewed in Chapter 4, segmentation is a process within image pre-processing (Section 4.3.1).

The resulting images from image pre-processing were used in both the phases of experiments planned for this research. The details of the experiments conducted using the processed data are discussed in Section 5.5.

### **5.3.2 Experimental Setup**

This section defines the different apparatus that were required in order to conduct the experiments designed in this chapter. The plan was to conduct two phases of experiments of which the main difference was the number of classes in which PV cell images could be classified.

The initial phase of experiments was to deduce whether DL, the selected image processing technique, could distinguish between a normal and a defective PV cell. The second phase of experiments was to obtain models that were then used to deduce how effectively DL could identify defective polycrystalline PV cell into the appropriate class.

The following sections discuss the software and hardware requirements for the experiments (Section 5.3.2.1). In addition, the data requirements for both phases of experiments are discussed in Section 5.3.2.2.



### 5.3.2.1 Hardware and Software

A preliminary investigation of the implementation technique and tools was discussed in the previous chapter (Section 4.5). This section includes the software and hardware requirements of the experiments as well as the data requirements. These requirements in some way influence the implementation of the different experiments.

Both phases of experiments were implemented using Python<sup>4</sup>, coupled with Keras<sup>5</sup> and TensorFlow<sup>6</sup> libraries. More details regarding the implementation of the different experiments are discussed throughout Section 5.3. The experiments were performed on a Mecer Proficient computer, with an i7 - 4790 central processing unit (CPU), 3.60 GHz, 16 GB of ram, a Nvidia GeForce GTX 1080 graphics processing unit (GPU) with 8 GB dedicated memory and running on Windows 10 OS.

A GPU was used because it provides a highly parallel computation, therefore providing an exception magnitude of executing threads in comparison to CPUs. GPUs help reduce the time it takes to perform experiments (Litjens et al., 2017). One of the libraries used to implement experiments provided the capability of executing DL experiments on GPUs. The different implementation tools used in this research are discussed in the following section.

#### Implementation tools

Several tools were used to implement the experiments required for this research, which included IntelliJ<sup>7</sup>. IntelliJ is an integrated development environment (IDE) used to implement the designed experiments. This was more of a researcher's preference. IntelliJ can run python directly as long as the necessary plugins are installed and permits the configuration of NNs in a few steps<sup>8</sup>.

NVIDIA develops CUDA toolkit and it provides a development environment for creating high-performance GPU-accelerated solutions. This allows utilisation of the GPU that was in the PC configuration that was used to perform the experiments. In addition, cuDNN, a library which is part

---

<sup>4</sup> <https://www.python.org/>

<sup>5</sup> <https://keras.io/>

<sup>6</sup> <https://www.tensorflow.org/>

<sup>7</sup> <https://www.jetbrains.com/idea/>

<sup>8</sup> <https://deeplearning4j.org/docs/latest/deeplearning4j-quickstart>

of the NVIDIA DL software development kit (SDK) had to be installed. cuDNN is responsible for accelerating DL frameworks.

The DL framework that was used to implement the experiments was TensorFlow. The framework was coupled with Keras, which is a high-level application programming interface (API). Other libraries that were used in the implementation of the experiments were:

- Pillow – imaging library.
- Matplotlib – plotting library.
- Pydot – python interface to GraphViz dot language.
- OpenCV – open source computer vision library.

The following section discusses the data requirements of the experiments that were performed as part of this research.

### 5.3.2.2 Data

The images received from the Physics Department at NMU were of modules that had to be pre-processed (Section 5.3.1) to obtain useful EL images of individual PV cells of each module provided. The individual PV cell images were approximately 150 by 150 pixels each, and a total of 5136 images were used for the different experiments.

For the initial phase of experiments, the images were manually divided into two classes. It was ensured that each class had an equal number of images. The second phase of experiments, however, required the images to be divided into four classes. In both cases, each class was comprised of images with defects that have been defined to be similar. The classes used in the two phases of experiments are defined below:

The first phase (binary classification) of experiments:

- i. Normal – normal and uncritical PV cells
- ii. Defective – critical and very critical PV cells

The second phase (multi-classification) of experiments as per classes defined in Section 3.6:

- i. Normal cells
- ii. Uncritical cells
- iii. Critical cells
- iv. Very Critical cells

Each class of images was split into three additional groups, namely training, validation and test (Bishop, 2013; Haykin, 2008; Kriesel, 2005). This served as the allocation of data as per the experimental strategy (Section 2.2.3):

- Training data: training data is used to tune the parameters of an adaptive model;
- Validation data: validation data is used to provide an unbiased evaluation of the model during training while tuning the hyperparameters (Section 5.4) of the model. In addition, validation data is needed to avoid overfitting; overfitting happens when the model learns details and noise in the training data in such a way that it impacts the performance of the model; and
- Testing data: test data is used to perform an unbiased evaluation of the resulting model that is completely tuned using the training data.

The first phase of experiments used 600 images to train the different models. Both the normal and the defective classes contained 300 images. An additional 48 images were used to validate the model during training. Table 5-1 contains a summary of the images used for the first phase of experiments. The outcome of the first phase of experiments is discussed in Section 5.5.2.

**Table 5-1: Images used for the first phase of experiments**

Dataset	Classes	Number of Training Data	Number of Validation Data
<b><math>\alpha</math> (n = 648)</b>	Normal	300	24
	Defective	300	24
	Total	600	48

The second phase of experiments were carried out in three groups which were determined by the datasets that were salvaged from the provided data. The first dataset (Dataset A) used a total of 736 images to train the different models. Each of the four classes, normal, uncritical, critical and very critical, contained 184 images. An additional 128 images were used for validation in the second phase of experiments. The training histories of the second phase of experiments are discussed in Section 5.5.3.

The last two Datasets B and C were used to produce the most optimum model to identify defective PV cells effectively. This required requesting an additional set of data from the Physics department at NMU. Experiments using an unbalanced dataset were performed to test how different the models performed when subjected to an unbalanced dataset. The unbalanced dataset represents a dataset which had classes with a different number of training data. Table 5-2 contains a summary of how the data was split in all the experiments conducted in the second phase. The classification results obtained from the second phase of experiments are discussed in the following chapter.

**Table 5-2: Images used for the second phase of experiments**

Dataset	Classes	Number of Training Data	Number of Validation Data
<b>A (n = 864)</b>	Normal	184	32
	Uncritical	184	32
	Critical	184	32
	Very Critical	184	32
	<b>Total</b>	<b>736</b>	<b>128</b>
<b>B (n = 1248)</b>	Normal	200	112
	Uncritical	200	112
	Critical	200	112
	Very Critical	200	112
	<b>Total</b>	<b>800</b>	<b>448</b>
<b>C (n = 5136)</b>	Normal	3424	112
	Uncritical	373	112
	Critical	415	112
	Very Critical	476	112
	<b>Total</b>	<b>4688</b>	<b>448</b>

The data represented different cases of defects that may occur in each of the classes. It should be noted that defects in the same class are similar, based on the area on the area the defect covers but the defects may appear differently. Furthermore, data augmentation was introduced during training to increase the defects that may be represented by the data provided as well as to reduce the chances of overfitting by generating more data for the models to train on (Section 5.4). Dataset C was used to increase the representation of the data provided and to ensure that all the data that was provided for this research, was utilised.

The adaptive models (Section 4.3.2.3) from the second phase of experiments (Multi-class classification) are evaluated to determine whether DL as an image processing technique could effectively identify defective PV cells from EL images. The evaluation plan is discussed in Section 5.6 and the results from the evaluation are discussed in Chapter 6. The next section outlines the implementation of the experiments based on the experimental design discussed in this section.

## 5.4 Experiment Implementation

The experimental design discussed in Section 5.3 allowed for the implementation of the experiments. The implementation of the experiments required the incorporation of different DL CNN architecture (Section 4.3.2.3). Some DL CNNs used to accomplish image classification tasks were discussed in Section 4.3.3, however, not all of the architectures mentioned in Section 4.3.3 were used in this research. Table 5-3 lists the DL CNN architectures that were incorporated in the implementation of experiments and a reason indicating why it was implemented was provided

(Alom et al., 2018; Chollet, 2017; Howard et al., 2017; LeCun et al., 1999; Simonyan & Zisserman, 2015).

**Table 5-3: Choice of DL CNN architectures**

Model	Reason for choice
LeNet	Simple to implement
VGGNet	To investigate how depth affects performance
MobileNet	Efficient and the resulting CNN is small
Xception	Easy to modify and define

Hyperparameters had to be set accordingly when implementing experiments. A hyperparameter is a parameter where values are set before the learning begins (Goodfellow et al., 2016; LeCun et al., 2015). The hyperparameters that were set for the different experiments performed in this research are tabulated in Table 5-4.

**Table 5-4: Experiment hyperparameters**

Hyperparameter	Value
Optimiser	Adam
Activation Function	Sigmoid
Batch Size	25
Epochs	500
Dropout	0.5

Data augmentation was included in the implementation of all the experiments performed for this research. Data augmentation was included to increase the number of parameters. A high number of parameters is advantageous to the training process of a DL CNN. This increases the amount of relevant data since data augmentation allows for the creation of synthetic data which is then added to the training set (Wu, Yan, Shan, Dang, & Sun, 2015; Wu, Zhong, & Liu, 2017). Data augmentation is used to help prevent overfitting (Section 5.5). Table 5-5 contains the data augmentation techniques that were employed during training on all datasets that were used for experiments in this research.

**Table 5-5: Data augmentation techniques**

Data Augmentation Technique	How was it applied?
Flip	Images were flipped along the horizontal axis
Zoom	Images enlarged by 20%
Rescale	Images were scaled up by a factor of 4
Shear	Images were displaced horizontally by 20%

The following section discusses the experimental procedure of the different experiments conducted in this research.

## 5.5 Experimental Procedure

Experiments were performed to determine causal links between variables (Sections 2.2.3 and 2.3). The experiments performed were essentially image classification experiments, to investigate whether EL images of PV cells could be classified in four different classes; normal uncritical, critical and very critical. This required the implementation of the proposed solution discussed in Section 5.2 which incorporates the image classification architectures discussed in Section 4.3.3. Furthermore, the classification architectures used in the implementation of the solution were trained from scratch (Section 4.3.2.3) in both phases of experiments. Section 5.3 outlined the different phases of experiments performed. The experiments in each phase covered the following aspects:

- Choose-feature experiment;
- Tune-model experiment; and
- Compare-model experiments.

One concern before the second phase experiments were performed was underfitting. Underfitting usually arises when there is little training data (Wu et al., 2015). Another phenomenon that was of concern due to the small size of the training data was overfitting. Overfitting occurs when the models extract features from data so well that noise within the data tends to have a negative impact on the performance of the model. The number of epochs used in training models can be used as a preventative measure of overfitting.

An epoch is the number of times iterations are made through data when training a model and is one of the hyperparameters (Section 5.4) used in this research. The number of epochs for the different model architectures was deduced by checkpointing and early stopping (Brownlee, 2016). As a result, the number of epochs for the different architectures are different. However, the number of epochs were set to 500 to ensure that checkpointing was effective. In addition, checkpointing and early stopping were used to ensure that overfitting did not occur while training the different models.

Checkpointing is a fault tolerance technique which saves optimal states of a system during training in cases of failure (Brownlee, 2016). The validation dataset is used for checkpointing. The validation accuracy is monitored and weights that result in the best accuracy are saved. Each time the accuracy improves, a model with updated weights is saved. A check known as the 'patience' is put in place in order for early stopping. 'Patience' is the number of permitted epochs allowed after the best validation accuracy has been recorded before the training process is terminated.

As stated earlier, early stopping is a preventative measure for overfitting. Two ways can be used to avoid overfitting: reducing the number of dimensions of the parameter space or reducing the effective size of each dimension (Prechelt, 2012). Early stopping is one technique of reducing the size of each parameter dimension. Early stopping was widely recommended in a number of studies (Mahsereci, Balles, Lassner, & Hennig, 2017; Prechelt, 2012; Zhang & Yu, 2005).

In addition, a dropout of 0.5 (Table 5-4) was incorporated in the training process. Dropout is one of the regularisation methods that can be used to prevent overfitting.

The experiments were carried out by training different deep CNN architectures from scratch using the provided EL images, after checkpointing and early stopping had been incorporated to the designed experiments. The performance history of the different experiments in each phase are discussed in Sections 5.5.2 and 5.5.3. However, the results from the evaluation of the adaptive models obtained from the second phase of experiments (multi-class classification) will be discussed in the following chapter.

The next section discusses the experimental procedure of the two learning techniques used in this experiment; training from scratch and TL. Furthermore, the groups in which experiments are conducted is discussed.

### 5.5.1 Learning Techniques and Experiment Groups

This section will discuss the two different learning technique used for experiments in this research and how the experiments were grouped based on the datasets.

#### 5.5.1.1 Training from Scratch

As stated earlier in this section this learning technique was utilised by experiments in phase one and phase two. The experimental procedure of this learning technique is described in pseudo code below:

---

**Parameters:**

optimisers – adam  
 set seed variable – dimension  
 initialise model – LeNet; VGGNet; MobileNet; Xception.

**train from scratch:**

**foreach** model **do**  
     train (optimiser)  
     reset model  
     clear memory  
**end**

---

### 5.5.1.2 Transfer learning (TL)

TL experiments were performed to examine how TL affects the performance and the results of the experiments. TL experiments were only performed in the second phase of experiments (multi-class classification). Inductive TL was suitable to be applied to this research. Inductive TL is defined as:

Given a source domain and a learning task (T1), a target domain and a learning task (T2), inductive TL aims to help improve the learning of the target predictive function in the target domain using the knowledge in source domain and learning task, where two learning tasks are not the same ( $T1 \neq T2$ ) (Pan & Yang, 2010).

The adaptive models evaluated in this section were trained having had preloaded ImageNet<sup>9</sup> weights. ImageNet is an image database that is organised according to the nouns within WordNet<sup>10</sup> hierarchy. WordNet is a lexical data of English nouns, verbs, adjectives and adverbs which are grouped in cognitive synonyms that express distinct concepts. ImageNet is a very large image dataset, comprising of many classes. TL can be considered when presented with a new but small dataset that has to be classified. This is achieved by introducing weights from a different classifier that was trained on a large dataset. This made it suitable for ImageNet weights to be used for experiments that were carried out for this project to achieve inductive TL. TL experiments were performed to observe how TL affects the performance of the adaptive models when classifying EL images of PV cells.

The experimental procedure of the TL experiments is described in pseudo code below:

---

<sup>9</sup> <http://www.image-net.org/>

<sup>10</sup> <https://wordnet.princeton.edu/>



**Parameters:**

optimisers – adam  
 set seed variable – dimension  
 initialise model – MobileNet; Xception.  
 load ImageNet weights

**TL:**

**foreach** model **do**  
     train (optimiser, learning rate)  
     reset model  
     clear memory  
**end**

---

### 5.5.1.3 Experiment Groups

Table 5-1 and Table 5-2 shows how the data was split across the different experiments which consequently determined the different experiments performed for this research. The list below is a breakdown of how the experiments were grouped based on the datasets and what was being examined at each stage:

- Dataset  $\alpha$ : this dataset was used to get an initial indication of whether DL could be used to identify defective PV cells from EL images (Banda & Barnard, 2018)(Appendix A – Article). In addition, different models that could be used to identify defective PV cells were identified. The performance of the different experiments are discussed in Section 5.5.2. The experiments performed using Dataset  $\alpha$  were strictly binary classification.
- Dataset A: this dataset was then used to determine whether a multi-class classification was possible on the dataset. The performance history of these experiments are discussed in Section 5.5.3.
- Dataset B: the experiment performed using this dataset permitted the evaluation of the adaptive models (LeNet, MobileNet and Xception) to determine how effectively defective PV cells defects could be identified from EL images of the PV cells.
- Dataset C: this dataset was used to examine how models cope when trained with an unbalanced dataset. This was to explore how differently the adaptive models (LeNet, MobileNet Xception) obtained in experiments performed on Dataset B compared to those obtained from experiments performed on Dataset C.

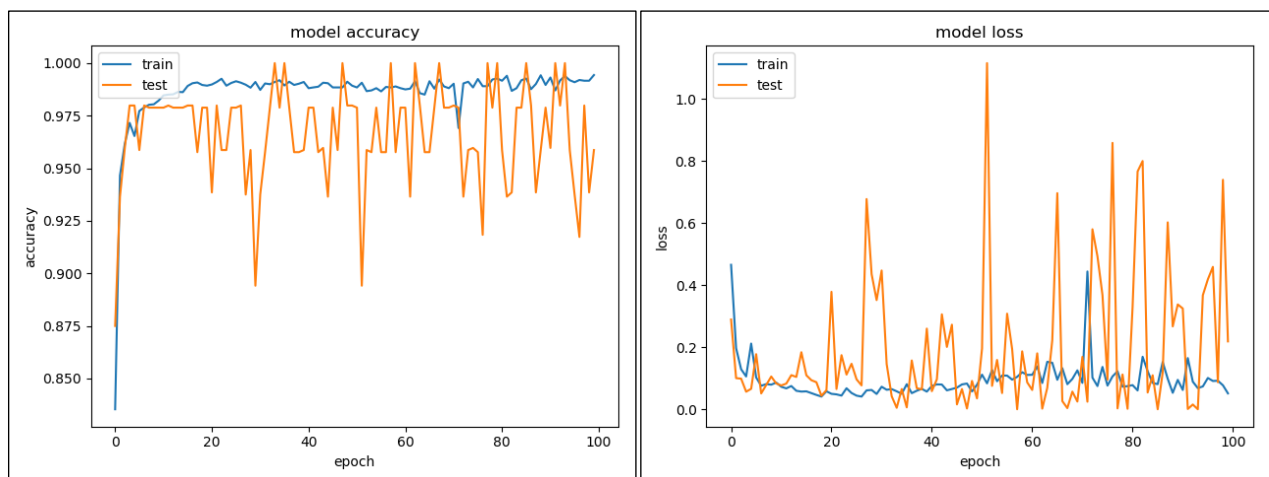
The results from the experiments performed on Dataset B and C in the second phase of experiments are discussed in the next chapter. One of the experimental strategies to be addressed in this chapter was controlling variables. One variable that was altered for different experiments

was the dimensions of the input images. The experiments were conducted with input image dimensions at 150 by 150 and 200 by 200. The following sections discuss the performance history obtained from the first and second phase of experiments.

### 5.5.2 Performance – Phase One (Binary Classification)

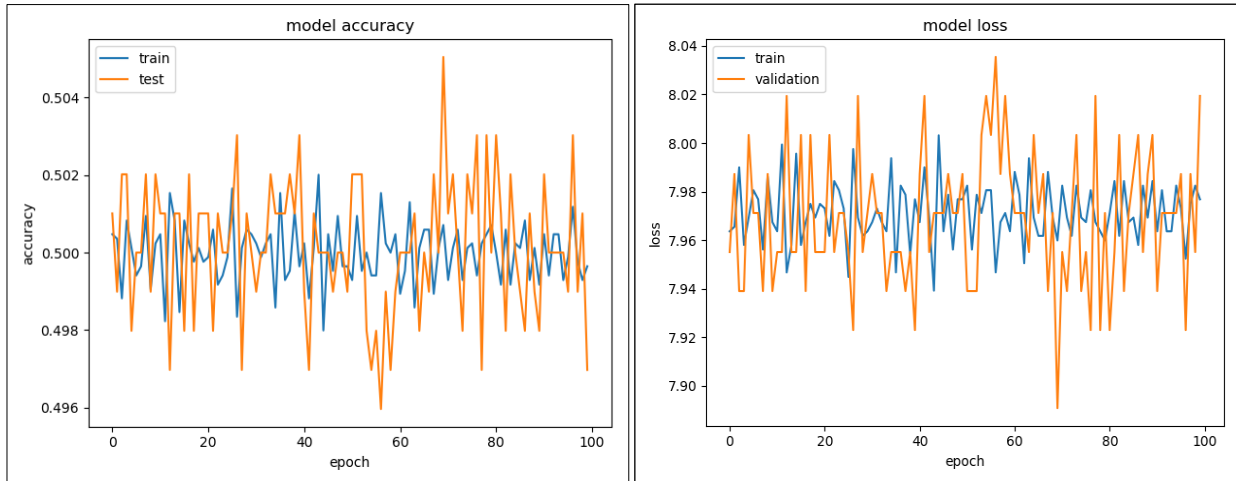
The training history of a model provides vital information on how well models performed during training. The training history was used to determine whether DL was an appropriate image processing technique to tackle the identified problem. Figure 5-4 to Figure 5-7 below show the performance of models from the initial phase of experiments. As discussed in Section 5.3, the first phase of experiments was to train a binary classifier. Furthermore, the initial phase of experiments was used to eliminate DL architectures that were not able to tune a model using the data that was provided for this research. In addition, the performance history depicted in Figure 5-4 to Figure 5-7 do not represent the performance of the adaptive models that were evaluated in the following chapter. The first phase of experiments merely served as an indication of whether DL could be used to solve the multi-class classification problem.

The first training history that was analysed was that of the LeNet (LeCun et al., 1999) model architecture. Figure 5-4 shows that the model did train from the provided data and there is an indication that the learning rate did improve. The model attained an accuracy of over 97.5 %. The model loss (Figure 5-4 (b)) did indicate a sign of overfitting. However, the LeNet model was later used in the second phase of experiments.



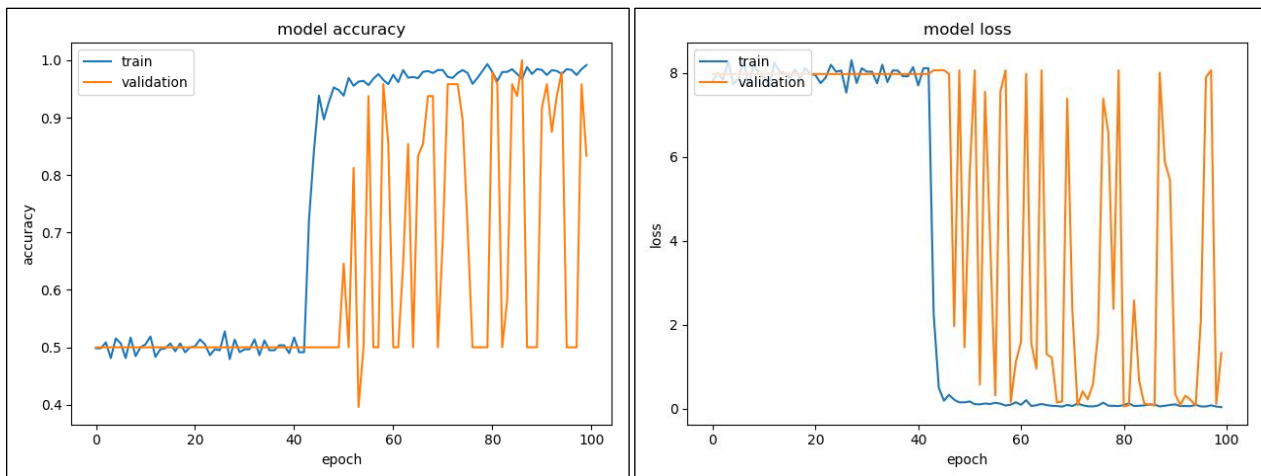
**Figure 5-4: LeNet training history – (a) model accuracy; (b) model loss**

The training history of the VGG (Simonyan & Zisserman, 2015) model architecture depicted in Figure 5-5 remained consistent over 100 epochs. This was an indication that the learning across the data provided did not improve. Furthermore, it was an indication that the VGG model was not ideal for the proposed solution.



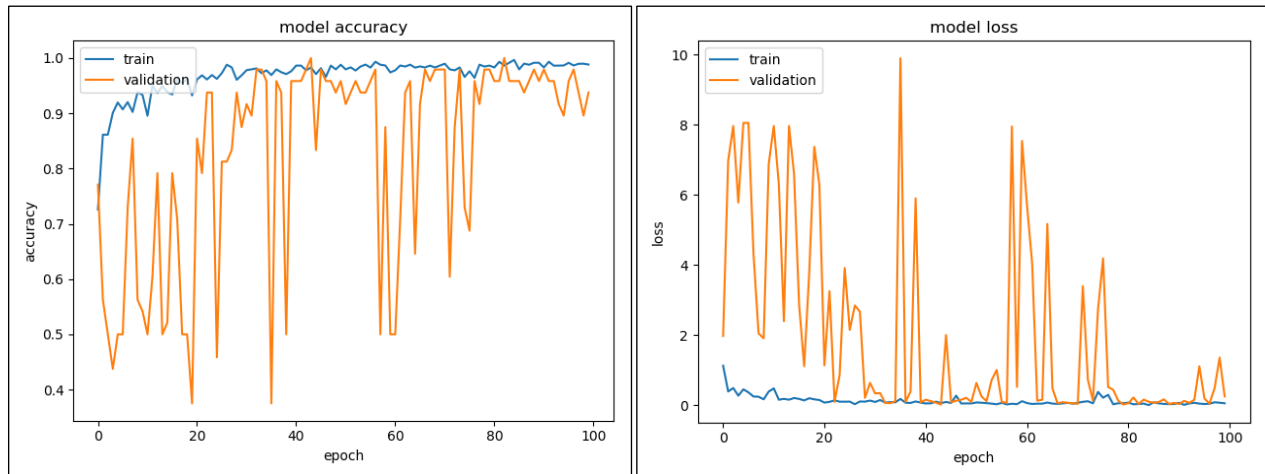
**Figure 5-5: VGG 16 training history – (a) model accuracy; (b) model loss**

Figure 5-6 depicts the performance of the MobileNet model (Howard et al., 2017), which indicate that the learning rate was consistent at 50% accuracy for the first 40 epochs. The model accuracy then improved to about 90% towards the end of the training process. The model loss (Figure 5-6 (b)) mirrored the accuracy of the model - as it dropped significantly after the 40<sup>th</sup> epoch. The MobileNet architecture performed well enough to be considered for the second phase of experiments.



**Figure 5-6: MobileNet training history – (a) model accuracy; (b) model loss**

Figure 5-7 depicts the performance of the Xception (Chollet, 2017) model. Figure 5-7 indicates that the Xception model performed as well as the LeNet model (Figure 5-4). The training accuracy of the Xception model was over 90%. In addition, the model loss did not indicate any sign of overfitting. This model was later used in the second phase of experiments.



**Figure 5-7: Xception training history – (a) model accuracy; (b) model loss**

The performance of the different models provides sufficient evidence that DL could be used to implement the proposed solution (Figure 5-2). The VGG model was the only model that did not support the attempt made to identify defective PV cells from EL images automatically using DL. It was concluded from the initial phase of experiments that DL can be used to automatically identify defective PV cells from EL images (

Appendix A – Article). The next section discusses the training history of models in the second phase of the experiments.

### 5.5.3 Performance – Phase Two (Multi-class classification)

The second phase of experiments were vital for the proposed research. Phase one of experiments was a mere confirmation whether DL could be used to solve the identified problem: eliminating the tedious nature of identifying defective PV cells from EL images. Figure 5-8 to Figure 5-10 show the performance while training different DL models which showed promising results in the first phase of experiments (Section 5.5.2). The three model architectures that performed well in the first phase of experiments were LeNet, MobileNet and the Xception model.

The training history of the LeNet model exhibited interesting characteristics. The model loss (Figure 5-8 (b)) of the validation set started decreasing initially, and then it escalated after the 20<sup>th</sup> epoch. This was an indication of overfitting despite having incorporated checkpointing and early stopping during training. This was an indication that the ‘patience’ had to be reduced. The evaluation results of the model will be discussed in the next chapter.

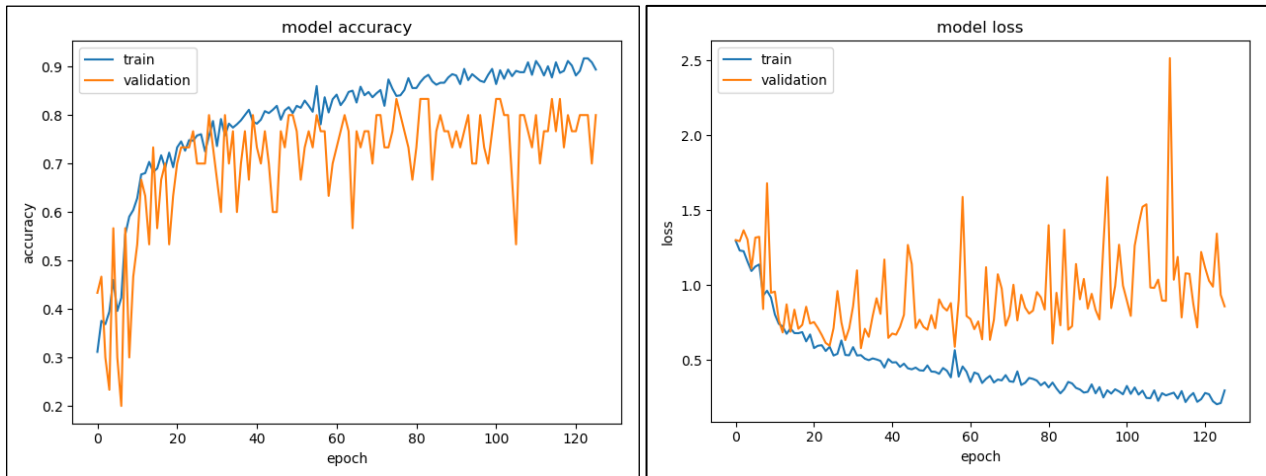


**Figure 5-8: LeNet multi-classification training history – (a) model accuracy; (b) model loss**

The MobileNet model performed better in the second phase of experiments than it did in the first phase of experiments. The learning rate gradually increased from the first epoch. The training accuracy reached the 90% mark. In addition, the model loss plot did not indicate any sign of overfitting. The evaluation of the different adaptive models obtained from training the MobileNet architecture will be discussed in the following chapter.

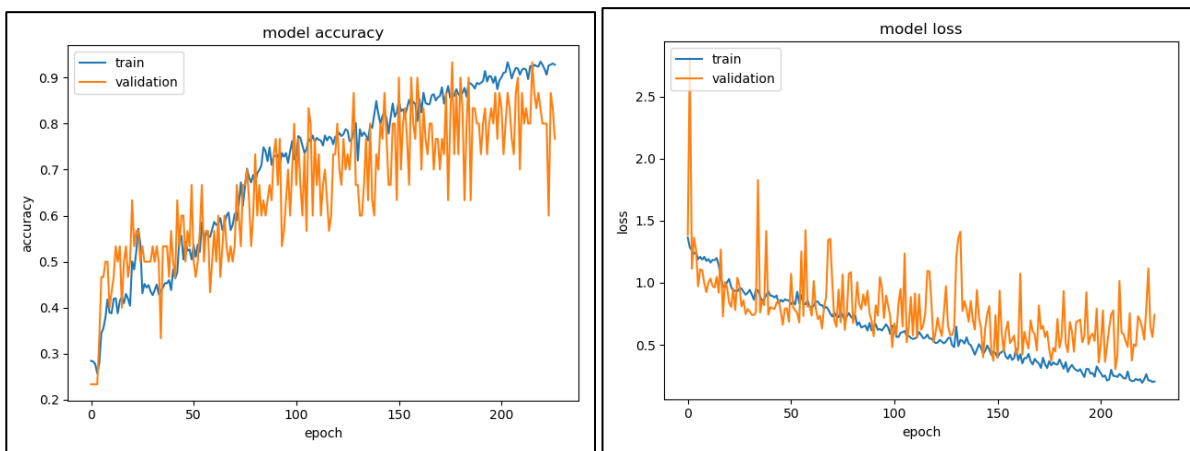


**Figure 5-9: MobileNet multi-classification training history – (a) model accuracy; (b) model loss**

The Xception model training history performed as expected. The learning rate did improve over time, confirming its ability to get tuned from the EL images provided. The model reached the training accuracy of about 90%. On the other hand, the model loss plotted in Figure 5-10 (b) did not indicate any sign of overfitting. The evaluation of the different adaptive models obtained from training the Xception architecture will be discussed in the following chapter.

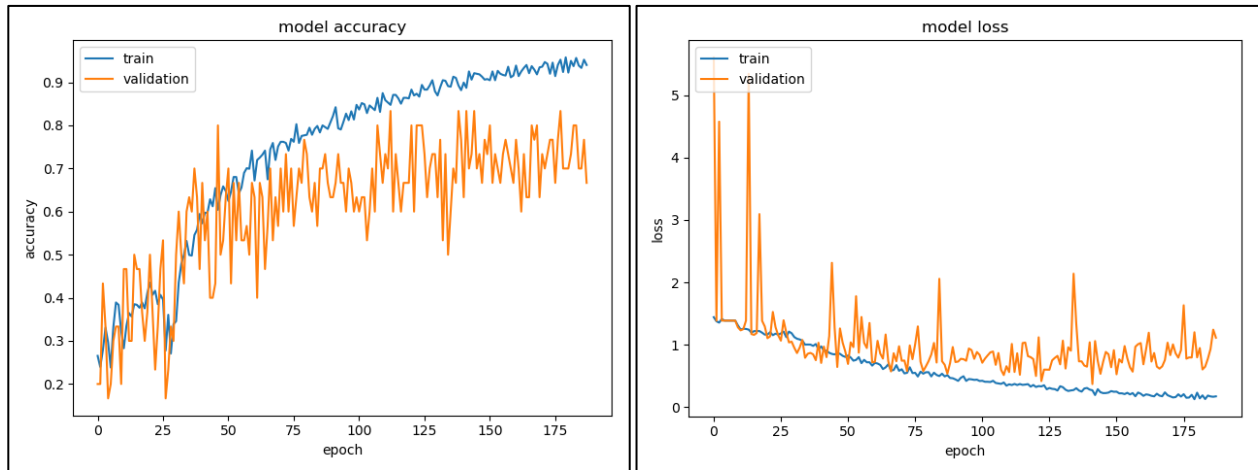


**Figure 5-10: Xception multi-classification training history – (a) model accuracy; (b) model loss**

This section discussed the training history of the models in order to confirm the assumption drawn from the first phase of experiments. The results obtained from the evaluating the adaptive models from these experiments will be discussed in the following chapter.

The next section discusses the evaluation plan intended to determine the effectiveness of the adaptive models (LeNet, MobileNet and Xception) obtained from the second phase of experiments (multi-class classification) performed in this research.

## 5.6 Evaluation Plan

This section will discuss a way in which the adaptive models will be evaluated in the next chapter. A confusion matrix is a concept in ML (Section 4.3.2.1) that is used to evaluate the classification ability of classification systems (Deng, Liu, Deng, & Mahadevan, 2016). A confusion matrix is two-dimensional which are indexed by the actual classes of objects and the classes the classifier predicted. Figure 5-11 depicts a confusion matrix of a multi-class classifier.  $A_i$  and  $A_j$  represent the actual and predicted classes respectively.  $N_{ij}$ , on the other hand, represents the number of samples that belong to class  $A_i$  but have been classified as belonging to  $A_j$ .

		Predicted			
		$A_1$	... $A_j$ ...	$A_n$	
Actual	$A_1$	$N_{11}$	$N_{1j}$	$N_{1n}$	
	$\vdots$		$\vdots$		
	$A_i$	$N_{i1}$	... $N_{ij}$ ...	$N_{in}$	
	$\vdots$		$\vdots$		
	$A_n$	$N_{n1}$	$N_{nj}$	$N_{nn}$	

Figure 5-11: Confusion matrix for multi-class classification (Deng et al., 2016)

Different measurements can be obtained from a confusion matrix. The measurements that are of interest for this research are the accuracy, precision, recall and the  $F_1$ -score (Deng et al., 2016; Han, Kamber, & Pei, 2012; Sokolova & Lapalme, 2009).

For this section of the evaluation of the models obtained after experiments, the accuracy is considered as the total number of correct prediction and is the average per-class effectiveness of a classifier. This is defined as:

$$Accuracy_i = \frac{\sum_{i=1}^n N_{ij}}{\sum_{i=1}^n \sum_{j=1}^n N_{ij}} \quad (6)$$

The precision is how accurate a specific class is predicted. Precision is the measure of exactness. Precision is defined as:

$$Precision_i = \frac{N_{ii}}{\sum_{k=1}^n N_{ki}} \quad (7)$$

Recall is the effectiveness of a classifier to identify classes correctly. Recall can be considered as the measure of completeness. This is defined as:

$$Recall_i = \frac{N_{ii}}{\sum_{k=1}^n N_{ik}} \quad (8)$$

F<sub>1</sub>-score is the relationship between the actual data labels and those given by a classifier. It is a combined measure of the classifier's precision and recall. F<sub>1</sub>-score is defined as:

$$F - score_i = 2 \times \frac{Precision_i \times Recall_i}{Precision_i + Recall_i} \quad (9)$$

For this research, the four measurements were calculated for the best performing models that were obtained after altering different variables. This was required to test dependent variables in this research as required by the research strategy (Section 2.2.3 and Figure 5-1). The measurements obtained from the experiments performed for this research are discussed in the next chapter (Section 6.2.3). The best results are expected to be obtained when the highest values are obtained along the diagonal of the of the confusion matrix, where N<sub>ij</sub> (i=j), which represent how accurately a specific class is predicted. The following section provides a summary of this chapter.

## 5.7 Summary

This chapter discusses the proposed solution to the problem identified in section 1.2. The proposed solution (Section 5.2) and the literature reviewed in Chapters 3 and 4 lead to the design of experiments (Section 5.3), which included how the data was processed (Section 5.3.1) and the experimental setup (Section 5.3.2). All this was necessary to perform experiments that confirmed whether the identified image processing technique was ideal to solve the identified problem. Furthermore, the implementation of the experiments (Section 5.4), the experimental procedure (Section 5.5) and the evaluation plan (Section 5.6) were discussed in this chapter.

The proposed solution discussed in Section 5.2 incorporated the DL CNNs discussed in Section 4.3.3. This continued to answer RQ<sub>4</sub> – demonstrating how an image processing technique can be used appropriately to identify defective PV cells from EL images. Furthermore, the proposed solution leads to the experimental design (Section 5.3). This section discussed the hardware and software requirements (Section 5.3.2.1) for the different experiments, as well as the data requirements (Section 5.3.2.2). This was essential for the data allocation in fulfillment of the research strategy (Figure 5-1).

The experiment implementation was discussed in Section 5.4, and the different hyperparameters were defined. Not all DL CNNs architectures identified in Section 4.3.3 were implemented; however the four DL CNNs that were implemented were listed in this section. The following section then discussed the experimental procedure (Section 5.5) and discussed the different learning techniques that were used for the experiments. The variables that were controlled and how they



were controlled was discussed in this section. This included altering input image dimensions and introducing ImageNet weights to the experimental procedure (TL).

The performance history of the two phases of experiments (binary and multi-class classification) were discussed in Sections 5.5.2 and 5.5.3. This provided an initial confirmation that DL was an appropriate image processing technique to be used to identify defective PV cells from EL images.

Lastly, the evaluation plan discussed in Section 5.6 outlined a plan on how the dependent variables will be tested from the adaptive models obtained from the experiments designed in this chapter. The following chapter will discuss results obtained from the evaluation of the adaptive models that was planned in Section 5.6.

## 6 EXPERIMENTAL RESULTS

### 6.1 Introduction

Experiment design of all experiments conducted in this research were discussed in the previous chapter (Section 5.3). This chapter discusses results obtained from evaluating models trained in the second phase of experiments (Section 5.5.3) to determine how effectively the models trained for this research could classify PV cell EL images. These results include classification results of models trained from scratch (Section 6.2.1), models trained using transferred learning (Section 6.2.2), and the evaluation of the different models (Section 6.2.3).

This chapter aims to answer the fifth research question:

*RQ<sub>5</sub>: How effectively can the chosen image processing technique identify defective PV cells?*

The findings of this chapter are also used to examine the main research question:

***MRQ: How can an image processing technique be used to effectively identify defective polycrystalline PV cells from EL images of such cells?***

Figure 6-1 depicts the deliverables of this chapter and how this chapter forms part of the overall process research. Furthermore, Figure 6-1 shows how this chapter fits within the research approach (Section 2.2.2).

The results discussed in this chapter are a result of the variables that were tested in the previous chapter.

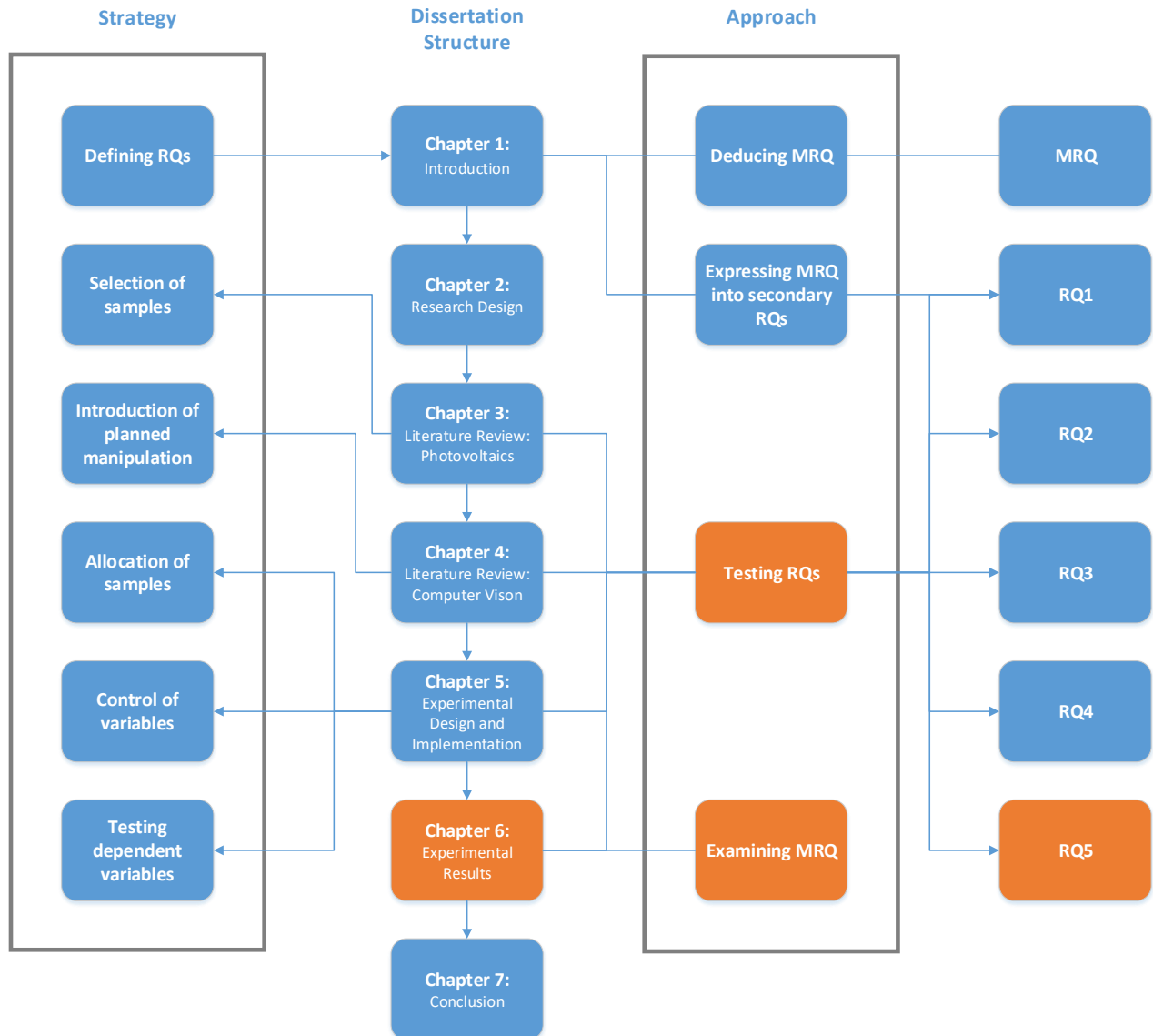


**Figure 6-1: Chapter overview**

The following sections aid in answering the last research question to conclude the answering process of all the defined research questions. The results discussed in this chapter contribute to answering of the main research question.

## 6.2 Image Classification Results

Image classification was discussed in Section 4.3.3, which lead to the experiments designed in the previous chapter (Section 5.3). The experiments were conducted to obtain adaptive models that could be used to classify EL images of PV cell. The classification results discussed in this section will determine how effectively PV cell EL images could be classified into the four identified classes; Normal, uncritical, critical and very critical (Section 3.6). The effectiveness of the identified images processing technique (which leads to the examining of the MRQ) was evaluated by how well the

different adaptive models (LeNet, MobileNet and Xception) could classify the EL images. The following section discusses the results of the multi-class classification experiments designed in the previous chapter; specifically, those experiments that required models to be trained from scratch.

### 6.2.1 Training from Scratch

Three Datasets (A, B and C) of EL images were used for the experiments that conducted in the second phase of experiments (Section 5.3.2.2). An aspect that was examined in the second phase of experiments included determining how altering different variables affected how effectively different adaptive models identified defective PV cells (Section 5.5).

Dataset A was used to decide which models could be used to effectively identify defective PV cells from EL images (Section 5.3.2.2 and 5.5). This enabled elimination of the VGG CNN architecture from further experiments, even though it was experimented on later on to validate whether the conclusion was still true under different circumstances. Figure 6-2 depicts the performance history obtained when an attempt was made to train the VGG architecture using Dataset B. The validation accuracy remained constant at 25% which indicated that no learning occurred during training. The low validation accuracy may be due to the datasets used (Datasets A and B). Even though the data sets were different based on the number of classes and images, it may be that the datasets were not large enough. The resulting classification models after training the VGG architecture thus has no ability to distinguish PV cell images from the four classes. Furthermore, the data represented by the PV cell images could have not been suitable for the model in question to classify; VGG classifier might have better object recognition capabilities than pattern recognition.

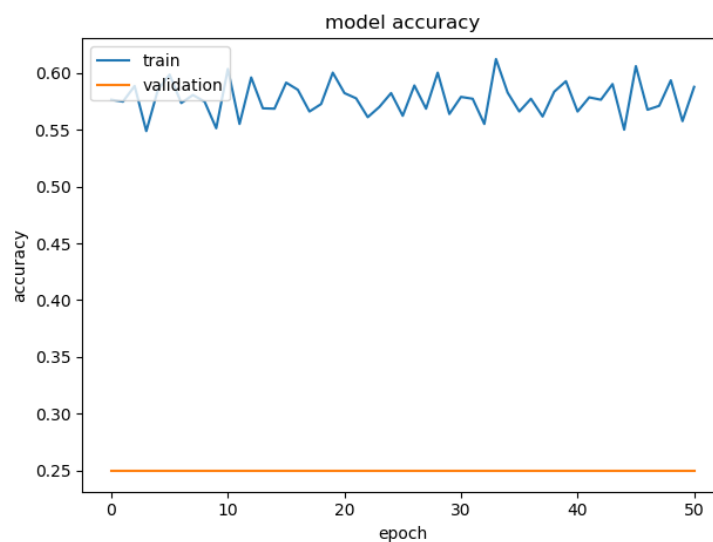


Figure 6-2: VGG performance history on Dataset B

Therefore, the results discussed in this section were of the LeNet, Xception and MobileNet model architectures. These results were obtained when experiments were performed using Datasets B and C based on the experimental procedure discussed in Section 5.5.

### 6.2.1.1 Results - Dataset B

This section discusses the image classification results obtained from experiments performed using Dataset B. The results in Table 6-1 were of experiments performed on Dataset B while maintaining the original dimensions of the input images. The loss, accuracy, validation loss and validation accuracy are compared to identify the best model to use to identify defective PV cells from EL images, bearing in mind that the same image processing technique was used across all experiments. The number of epochs varied because of the use of early stopping. This is the case for all discussed performance results in this chapter.

**Table 6-1: Performance results Dataset B (150 x 150 pixels)**

Model	Loss	Accuracy	Validation Loss	Validation Accuracy
LeNet (epochs = 30)	0.5989	0.7288	0.9589	0.6400
MobileNet (epochs = 150)	0.3043	0.9012	1.0946	0.7035
Xception (epochs = 75)	0.2683	0.9150	1.8879	0.5176

Early stopping (Section 5.5) was incorporated when the experiments of which results are tabulated in Table 6-1, were performed. This was to ensure that models with the most optimal weights were evaluated. The Xception model emerged as the best performing model. The Xception model had the lowest loss (0.2683) and the highest accuracy (0.9150). However, the MobileNet model had the highest validation accuracy (0.7035). The MobileNet model obtained from the performance results tabulated in Table 6-1 was not the best MobileNet classifier across all experiments. The different models were further evaluated to confirm the tabulated results by plotting confusion matrices. The different confusion matrices compared in Appendix B – Results.

The results in Table 6-2 were of experiments performed using Dataset B, after scaling up the dimensions of the input images to 200 by 200 pixels. Just as with the results in Table 6-1, the loss, accuracy, validation loss, and validation accuracy of the different models are compared to determine which model most effectively identifies defective PV cells from EL images.

**Table 6-2: Performance results Dataset B (200 x 200 pixels)**

Model	Loss	Accuracy	Validation Loss	Validation Accuracy
LeNet (epochs = 30)	0.4866	0.7925	1.0164	0.6635
MobileNet (epochs = 150)	0.2345	0.9112	1.0026	0.6988
Xception (epochs = 80)	0.1517	0.9500	1.2121	0.6847

The Xception model had the lowest loss (0.1517) and the highest accuracy (0.9500), and yet the MobileNet model had the lowest validation loss (1.0026) and the highest validation accuracy (0.6988). Furthermore, the LeNet classifier obtained when experiments were performed on Dataset B, with input images scaled up to 200 by 200 pixels was the best performing LeNet classifier obtained across all experiments.

The next section discusses the classification results obtained from experiments performed on Dataset C.

### 6.2.1.2 Results - Dataset C

The results in Table 6-3 were of experiments performed on Dataset C while maintaining the original image dimensions of 150 x 150. The outcomes of these experiments were to determine how a differently sized dataset affect how effectively the resulting models could identify defective PV cells from EL images. The loss, accuracy, validation loss and validation accuracy of the different model architectures are compared to determine which model could effectively identify defective PV cells.

**Table 6-3: Performance results on Dataset C (150 x 150 pixels)**

Model	Loss	Accuracy	Validation Loss	Validation Accuracy
<b>LeNet (epochs = 25)</b>	0.2887	0.8968	0.8996	0.6588
<b>MobileNet (epochs = 100)</b>	<b>0.0720</b>	<b>0.9726</b>	0.8427	<b>0.8047</b>
<b>Xception (epochs = 75)</b>	0.0919	0.9658	<b>0.6665</b>	0.7953

The results tabulated in Table 6-3 were from the most optimal weights before any overfitting because early stopping was incorporated in all the experiments that were performed for this research. MobileNet emerged as the best performing model to attempt to identify defective PV cells from EL images effectively. MobileNet had the lowest loss (0.0720), the highest training accuracy (0.9726) and the highest validation accuracy (0.8047). However, the MobileNet validation loss was not the lowest.

The results in Table 6-4 were of experiments performed on Dataset C after scaling up the dimensions of the input images to 200 by 200 pixels. The outcomes of this experiments were to deduce how scaling up input images dimensions of training data which was unbalanced, affected the performance of adaptive models. The loss, accuracy, validation loss and the validation accuracy of the different models were then compared to identify the best performing model.

**Table 6-4: Performance results on Dataset C (200 x 200 pixels)**

Model	Loss	Accuracy	Validation Loss	Validation Accuracy
<b>LeNet (epochs = 25)</b>	0.2727	0.9003	0.9630	0.6165
<b>MobileNet (epochs = 100)</b>	0.0871	0.9675	0.5635	0.8447
<b>Xception (epochs = 65)</b>	0.0697	0.972	0.9205	0.7624

The Xception model had the lowest loss (0.0697) and the highest accuracy (0.972), and yet the MobileNet model had the lowest validation loss (0.5635) and the highest validation accuracy (0.8447). The next section discusses results obtained after TL was incorporated into the experiments.

## 6.2.2 Transfer Learning (TL)

The Xception and the MobileNet architectures were the only architectures that had ImageNet resources available in the Keras<sup>11</sup> repository. Therefore, the TL evaluation was only viable for Xception and MobileNet models. TL on the MobileNet and Xception architecture using ImageNet weights only permits certain input image dimensions. The permitted image dimensions were: {128;160;192;224}. As a result, experiments were performed using dimensions closest to those of the original images which were 160 x160. The following sections discuss the performance results of the Xception and the MobileNet models, having incorporated TL into the experiments.

### 6.2.2.1 Transfer Learning (TL) Results - Dataset B

Table 6-5 contains Dataset B results obtained from the TL experiments. The results include loss, accuracy, validation loss, and validation accuracy of the Xception and MobileNet models. These results are compared to determine whether the models performed better than the same models trained from scratch, and to determine which of the two models can most effectively identify defective PV cells.

**Table 6-5: TL performance results on Dataset B (160 x 160 pixels)**

Model	Loss	Accuracy	Validation Loss	Validation Accuracy
<b>MobileNet (epochs = 95)</b>	0.0278	0.9912	1.2048	0.7835
<b>Xception (epochs = 60)</b>	0.0765	0.9687	1.0867	0.7812

The MobileNet model emerged as the best performing model from the results tabulated in Table 6-5. The MobileNet model had the lowest loss (0.0278), the highest accuracy (0.9912) and the highest validation (0.7835

<sup>11</sup> <https://keras.io/applications/#applications>

### 6.2.2.2 Transfer Learning (TL) Results - Dataset C

Table 6-6 contain results after performing TL experiments on Dataset C. The results were used to determine which models could most effectively determine defective PV cells. This was achieved by comparing the loss, accuracy, validation loss, and validation accuracy obtained after performing TL experiments on the Xception and MobileNet models.

**Table 6-6: TL Performance results on Dataset C (160 x 160 pixels)**

Model	Loss	Accuracy	Validation Loss	Validation Accuracy
<b>MobileNet (epochs = 90)</b>	0.0379	0.9812	<b>0.8586</b>	<b>0.8353</b>
<b>Xception (epochs = 55)</b>	0.0379	<b>0.9855</b>	1.1349	0.8094

The results tabulated in Table 6-6 indicated that the MobileNet model performed better than the Xception model. Besides both models attaining the same loss of 0.0379, the MobileNet model had a lower validation loss (0.8586) and the highest validation accuracy (0.8356). Similarly to the previous TL experiments, the validation accuracy did improve slightly. This confirmed that weights obtained from a completely different problem can help the model's classification ability. Furthermore, the classifier obtained from the Xception architecture after incorporating TL was compared with classifiers obtained from other Xception experiments. This was depicted in Figure B-4 (Appendix B – Results). The classifier as a result of TL performed better than those classifiers that were not exposed to ImageNet weight during training.

The evaluation of the best performing models from each of the experiments will be discussed in the following section.

### 6.2.3 Model Evaluation

This section explicitly evaluates how effectively the different models could identify defective PV cells from EL images. This was achieved by plotting a confusion matrix (Section 5.6) using the different models trained in the experiments that were performed for this research. A confusion matrix is a table that is used to visually describe the performance of a classification system (Deng et al., 2016). A confusion matrix contains information about actual and predicted classifications done by a classification model. Figure 6-3 to Figure 6-5 depict confusion matrices plotted from predictions made by either the LeNet, MobileNet or Xception models. One of each of these models (LeNet, MobileNet and Xception) discussed in Section 6.2.1, and 6.2.2 was evaluated to plot a confusion matrix. The models that were evaluated were selected based on which of the models attained the best validation accuracy after the different experiments.

The LeNet model that was used to perform this evaluation was obtained from the experiments that were performed using Dataset B that was trained using images with an input image dimension



of 200 by 200 pixels. The classification results of the model are in Table 6-2. Figure 6-3 was the confusion matrix that was obtained from the evaluation of a test dataset. The diagonal of the confusion matrix in Figure 6-3 indicates the accuracies which the LeNet model predicted each of the classes. The normal and critical were predicted with an accuracy of 29%, which was better than the LeNet could predict any other class by this classifier. A conclusion was drawn from these results, that the performance of the LeNet models was better when larger input images were used to train the model, as a larger Dataset C did not yield a better performing classifier. Furthermore, different classifiers obtained from models trained on Dataset B and C were compared in Figure B-1 (Appendix B – Results), to visualise how differently the LeNet models performed.

The rest of the values of the confusion matrix in Figure 6-3 were used to calculate measurements ( $F_1$  – score, recall and precision) on the model. These measurements were defined in Section 5.6 and the resulting measurements of the LeNet model are tabulated in Table 6-7.

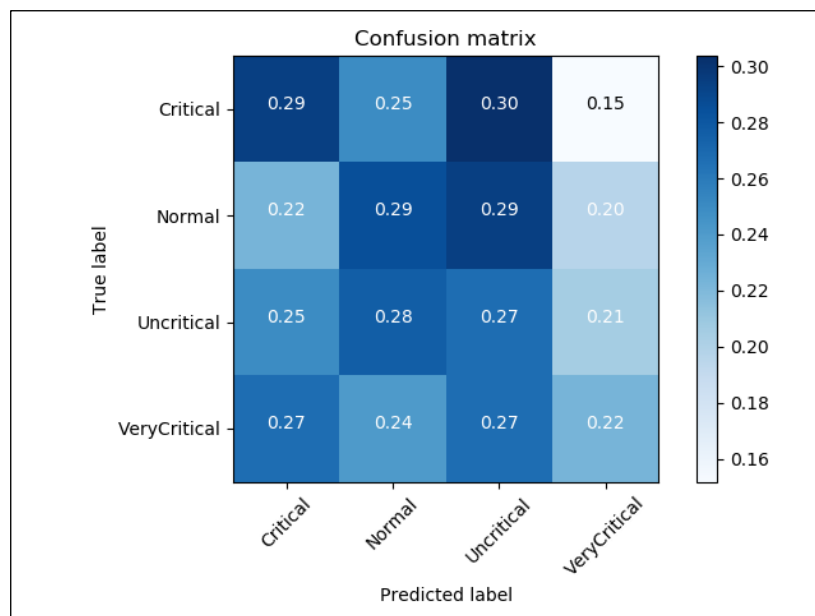


**Figure 6-3: LeNet confusion matrix**

The MobileNet model with the best validation accuracy was obtained when experiments were performed using Dataset C, and the images had an input dimension of 160 by 160 pixels. The classification results of this model are tabulated in Table 6-4. After that, the model was evaluated, and a confusion matrix was plotted and is depicted in Figure 6-4. The values from Figure 6-4 were used to calculate measurements which are tabulated in Table 6-7. Furthermore, it was noted that the MobileNet performance improved by scaling up the input images and indicated that the size of the dataset did affect the performance of the model. The confusion matrices depicted in Figure B-2 (Appendix B – Results), are a visual representation

of how the mentioned factors affected the resulting classifiers having trained the MobileNet on Dataset B and C.

The diagonal of the confusion matrix (Figure 6-4) indicates the accuracies which the MobileNet model predicted each of the classes. Normal PV cells were predicted accurately 42% (0.42) of the time using the MobileNet model and was the highest for the model. However, the desired result would have been a 1 (representing 100% accuracy) across the diagonal of the confusion matrix, which would represent an ideal MobileNet model which is able to classify PV cells from EL images correctly each time.

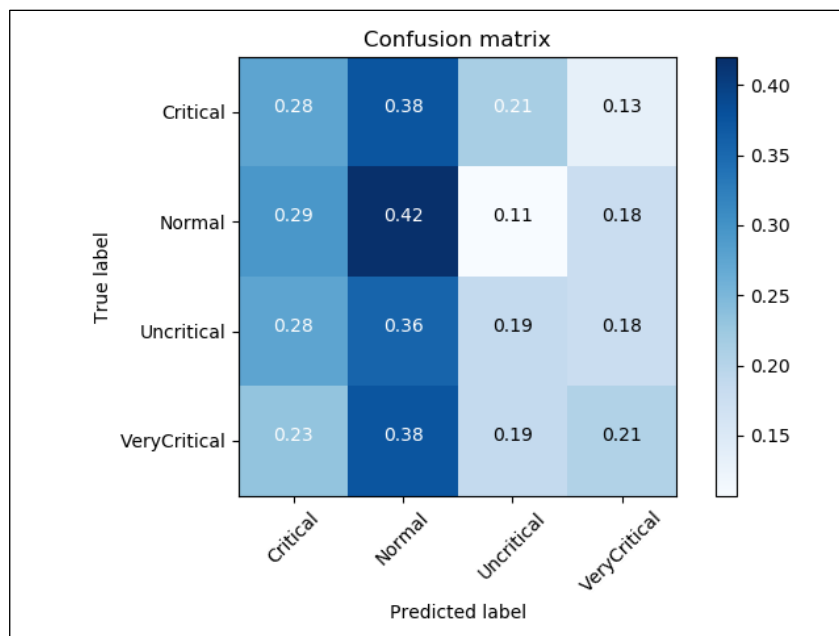


**Figure 6-4: MobileNet confusion matrix**

The best models while performing experiments using the Xception architecture was obtained when TL was employed to the experiments. The performance results for the model that was used to plot the confusion matrix (Figure 6-5) were tabulated in Table 6-6. Figure 6-5 shows percentage distribution of prediction of samples. The highest scores were expected along the diagonal, which indicates how accurately the model makes prediction. The Xception model predicted uncritical PV cells better than any other class with an accuracy of 41%.

In addition, a comparison of the confusion matrix before and after TL was done. Not only did the models converge quicker during training as per Table 6-6, but the resulting model was a better classifier. This was depicted in Figure B-4 (Appendix B – Results). This indicated that inductive TL does improve the classification ability if a model in some cases. Furthermore, the Xception architecture trained on Dataset C produced a better classifier than that trained on Dataset B. This is depicted in Figure B-3 (Appendix B – Results).

The rest of the values from the confusion matrix (Figure 6-5) were used to calculate measurements that were introduced in Section 5.6 and the resulting measurements are tabulated in Table 6-7.

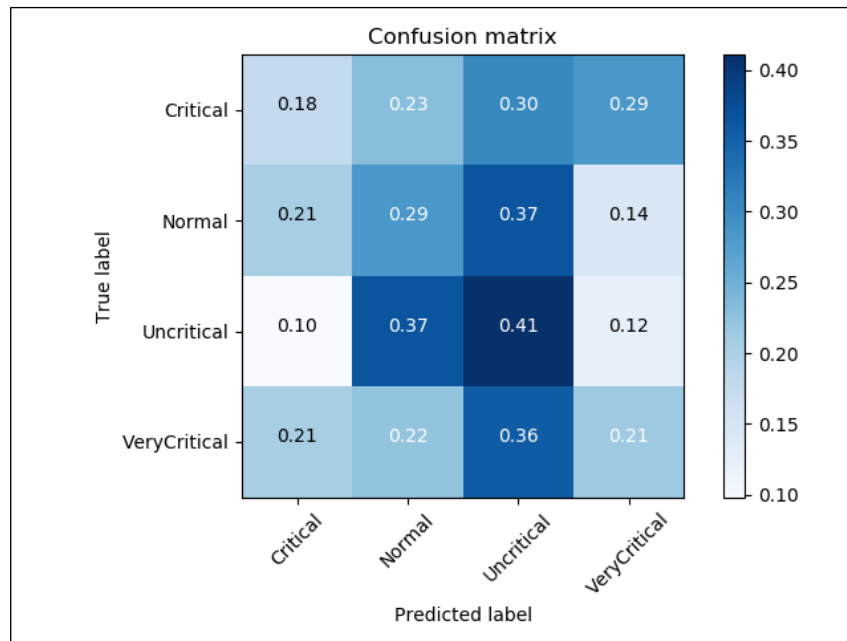


**Figure 6-5: Xception confusion matrix**

There were different conclusions that were drawn from the results obtained from this project. Upon analysing the results, different factors were noted that may have affected the obtained results. This included the difference in datasets used to train the adaptive models, the size of the input images used for training, and TL.

Different datasets were used to test how the size of the dataset used to train the different network architectures affected the resulting classifier. In case of the Xception and MobileNet architectures, increasing the dataset improved the performance of the classifiers. Therefore, increasing the size of the dataset might affect the resulting classifiers even further.

Furthermore, an unbalanced dataset was used to utilise all the images made available for this project and to test how an unbalanced dataset would affect results. There were more normal PV cells than defective cells obtain from the data provided for this research. Experiments on Dataset C were performed to take advantage of this fact, by not disregarding images that would result in excessive images in a single class. The results obtained from experiments performed on Dataset C appeared to have improved the classification ability of the Xception and MobileNet adaptive models.

Scaling up the input images was another factor that affected the performance of the resulting classifiers from the experiments. In the case of the MobileNet, the size of the input images improved the performance of the resulting classifier.

It was observed from the analysis of the results obtained that different factors affected the resulting adaptive models used for classification differently. For instance, the LeNet architecture trained better on a balanced dataset as expected and based on theory. The MobileNet produced a better classifier having trained on dataset C with scaled up input images. And lastly, the Xception model produced a better classifier when an inductive TL was incorporated into the experiments.

Lastly, theory suggested that TL can be used to improve the performance of a classifier even if the intended solutions of the models to be trained and the solution from which weights are obtained are different. ImageNet weights were introduced to Xception and MobileNet. However, only the Xception model produced a better classifier when inductive TL was incorporated to the experiments, but both the Xception and MobileNet architecture exhibited faster convergence during training.

### Evaluation Results

Table 6-7 tabulates the evaluation measurements (Section 5.6) calculated for the best performing adaptive models obtained from the different experiments. The best adaptive models were used to plot a confusion matrix from which the measurements; precision, recall and  $F_1$  – score were calculated.

**Table 6-7: PV cell classification measurements**

Model	Precision	Recall	F1 - score
LeNet	0.268	0.248	0.258
MobileNet	0.275	0.289	0.282
Xception (TL)	0.273	0.238	0.254

Overall, the MobileNet model performed better than the LeNet and Xception model. The MobileNet model had the highest precision, recall and  $F_1$  – score. However, from inspecting the confusion matrices, different models predicted certain classes better than others.

The obtained results were not the most ideal results. This may be due to the data within the different classes appearing to be very closely related, making it difficult for the classifiers to distinguish between the different classes. However further refinement to the model architectures can be incorporated in future research, to determine whether the data within the four classes can be modelled accordingly.

The following section will provide a conclusion to the findings of this chapter based on the different results discussed in this chapter.

### 6.3 Conclusion

This chapter presented the results of the classification of PV cell EL images into four different classes namely; normal, uncritical, critical and very critical (Section 6.2). The classification experiments were of models trained from scratch and through transferred learning. The result from these experiments were discussed in Sections 6.2.1 and 6.2.2 respectively.

The classification results that were discussed in Section 6.2 were obtained from the three models that were identified in Section 5.5.3 namely; LeNet, Xception and MobileNet. The classification results suggested that all three models could classify PV cell from EL images. TL was applied to the experiments to investigate further what impact TL had on the experiments, and the result were discussed in Section 6.2.2. The findings were used to conclude that the Xception model performed better when TL was applied to experiments. In addition, it could further be concluded that weights obtained from different classification tasks can be used to improve the performance of completely different classification tasks.

The models obtained from the image classification experiments were evaluated in Section 6.2.3. This was to determine how effectively DL, an image processing technique, could identify defective PV cells (RQ<sub>5</sub>). The results, however, indicated that the models struggled to precisely make predictions and recall which class a PV cell EL image belongs to if the models have not been previously exposed to the EL image. It was also noted that different models could classify certain classes better than others.

The different aspects discussed in this chapter were required to answer RQ<sub>5</sub> and to examine the MRQ. DL as an image processing technique could be used to effectively identify defective PV cells from EL images, however, the precision at which defective EL images were classified was low indicating that the accuracy at which specific classes were predicted was poor. Even though the results were poor, it was a step in the right direction as at the point when this work was done, no existing systems to classify EL images of PV cells, as documented in this project, could be found. The manual system can currently be viewed as a better alternative, but the results from the experiments carried out in this project can be used to further investigate different ways in which DL can be used to effectively identify defective PV cells. Therefore, DL need not to be disregarded in future as an approach of identifying defective PV cells.

The following chapter discusses the conclusion to this research.

## 7 CONCLUSION

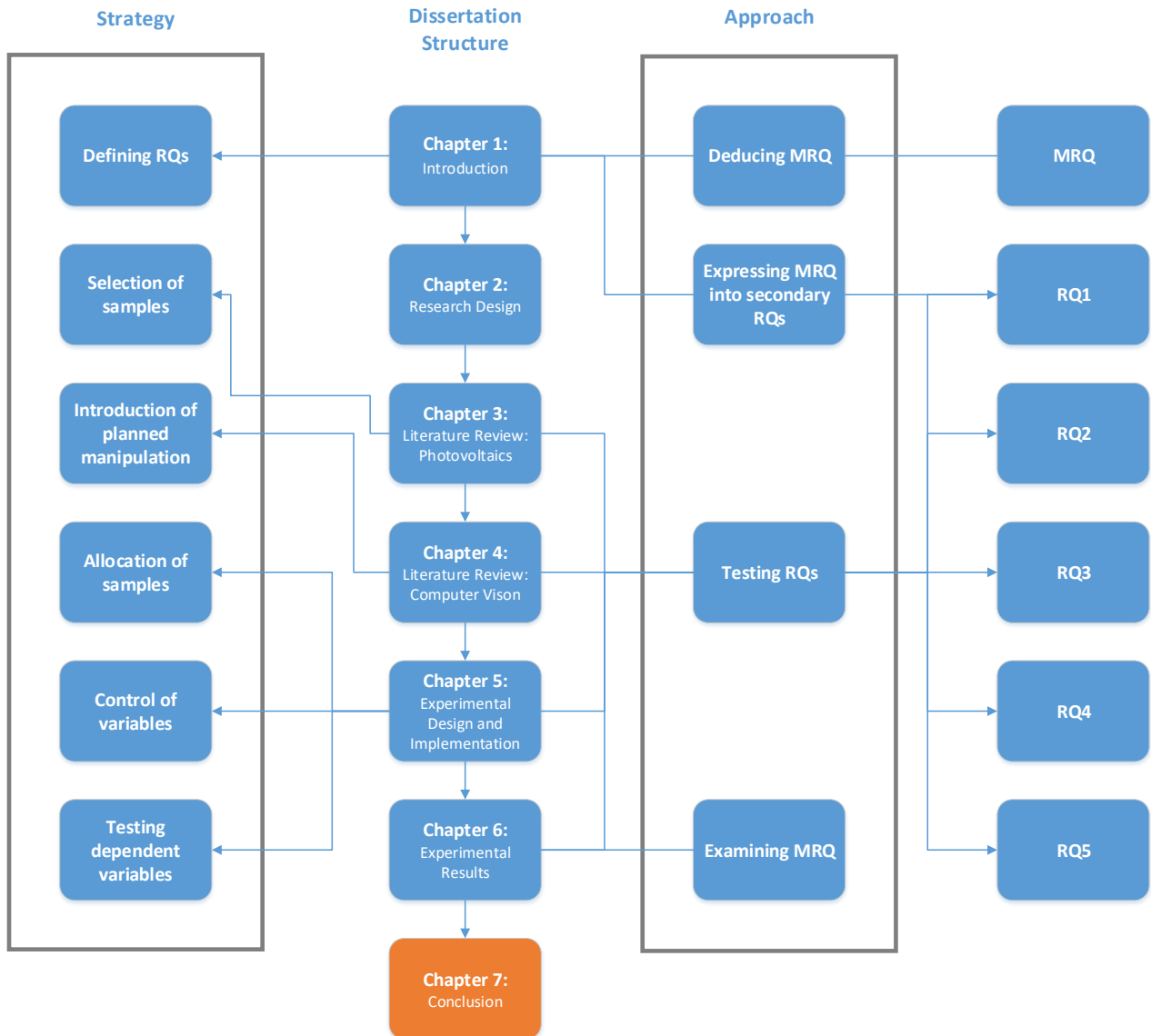


Figure 7-1: Dissertation structure

### 7.1 Introduction

Image processing is said to be used to transform, manipulate or analyse digital images (Fu & Rosenfeld, 1976). It was discovered through literature that image processing is used in, amongst others, the medical and the automotive industry to analyse images. Image processing has been used in the medical field for diagnosis and image processing has been incorporated to driver assist system in the automotive industry. This is accomplished by extracting features from an image in order to complete a task. This research investigated whether image processing can be used in photovoltaics to identify defective PV cells from EL images of these cells.

This chapter will provide a summary of this research. This will be achieved by discussing the research achievements (Section 7.2), the contribution of this research (Section 7.3), problems encountered in this research (Section 7.4) and limitations and recommendation for future research (Section 7.5). Lastly, a final summary will be provided in Section 7.6.

## 7.2 Research Achievements

It was identified in Chapter 1 (Section 1.2) that there was no automated way to identify defective PV cells from EL images effectively. The proposal to this project suggested the use of image processing to identify defective PV cells. The PV cells in question were of polycrystalline PV modules. The goal of this project is to identify defective polycrystalline solar cells from EL images effectively. In addition, the identified defects will be based on standards defined in Section 3.6.

The way in which to effectively identify defective PV cells from EL modules was highly experimental; thus, it was decided that the experimental research methodology would be applied to this research. Furthermore, the deductive approach (Section 2.2.2) and experimental strategy (Section 2.2.3) were applied to the dissertation structure, which helped deduce which chapters addressed the different research questions (Table 7-1). The research questions were derived from the MRQ:

***How can an image processing technique be used to effectively identify defective polycrystalline PV cells from EL images of such cells?***

Therefore, the findings of this research answered the MRQ.

**Table 7-1: Research Questions and Chapters**

<b>Research Question</b>	<b>Chapter</b>
<b>RQ<sub>1</sub>: What are the existing methods for examining PV cell defects?</b>	3
<b>RQ<sub>2</sub>: What are the constraints on existing methods of identifying PV cell defects in polycrystalline solar modules using EL images?</b>	3
<b>RQ<sub>3</sub>: How can an image processing technique be used to assist in identifying defects in polycrystalline PV cells using EL images of the PV cells?</b>	4
<b>RQ<sub>4</sub>: How can an image processing technique be used appropriately to identify defective PV cells?</b>	4, 5
<b>RQ<sub>5</sub>: How effectively can the chosen image processing technique identify defective PV cells?</b>	6

The first research question, RQ<sub>1</sub>, was answered through the review of literature in Chapter 3 (Section 3.5). In addition, the different constraints of identifying defective PV cells from existing

methods was revealed, which answered the second research question, RQ<sub>2</sub>. Furthermore, Chapter 3 provided support to use EL images to automate the process of identifying PV cells.

Answering RQ<sub>3</sub> required identifying an image processing technique that can be used to identify defective PV cells from EL images automatically. This was achieved through the review of literature on image processing (Section 4.3). It was deduced that NNs and consequently DL (Section 4.3.2) was the most suitable image processing technique that could be used to identify defects in polycrystalline PV cells from EL images of the PV cells.

RQ<sub>4</sub> was answered in Chapter 4, alongside RQ<sub>3</sub>. The literature reviewed on image classification and pattern recognition (Sections 4.3.3 and 4.3.4) and the related work reviewed (Section 4.4) revealed how the image processing technique identified could be used appropriately to identify defective PV cells from EL images.

Chapter 5 continued to address RQ<sub>4</sub> by proposing a solution (Section 5.2) based on the findings of Chapter 4. Experiments were designed (Section 5.3) and implemented (Section 5.4) to demonstrate how appropriately the identified image processing could be used to identify defective PV cells from EL images.

RQ<sub>5</sub> was answered in Chapter 6. An evaluation plan discussed in Section 5.6 was used to evaluate the adaptive models (Section 6.2.3) obtained from the experiments conducted in this research. The models to evaluate were deduced from the image classification results discussed in Section 6.2. The results from the evaluation were used to deduce how effectively the chosen image processing technique identified defective PV cells from the EL images.

The MRQ: ***How can an image processing technique be used to effectively identify defective polycrystalline PV cells from EL images of such cells?*** was addressed by answering the different RQs. This indicated that the thesis statement: *Image processing can be used to identify patterns that may indicate PV cell defects in polycrystalline solar modules from EL images. The identified defects can be used to determine the state of the PV cell* – was proved. However, the effectiveness at which the defective PV cells were identified were not as desired as the adaptive models from the classification experiments exhibited a low precision and recall (Section 5.6). The following section discusses the contribution of this research.

### **7.3 Contribution of Research**

The contribution of this research to the body of knowledge is a result of a lack of research to use image processing in photovoltaics. No evidence was found of the use of image processing in



photovoltaics to effectively identify defective PV cell defects from EL images. This research had a theoretical and a practical contribution which are discussed in Sections 7.3.1 and 7.3.2 respectively.

### **7.3.1 Theoretical Contributions**

This research proposed the use of image processing to identify defective polycrystalline PV cells from EL images. The theoretical contributions made by this research are:

- The use of image processing in photovoltaics
- DL, an image processing technique can be used on EL images

The literature reviewed in Chapter 3 provided evidence of constraints in ways that are currently used to examine EL images to identify defective PV cells. The constraints were overcome by proposing the use of image processing in photovoltaics to identify defective PV cells from EL images.

The literature reviewed in Chapter 4 indicated that image processing, a task within computer vision can be used to for different image classification tasks. This research provided evidence that DL CNNs, can be used to identify defective PV cells.

This research aimed at effectively identifying defective polycrystalline PV cells from EL images. This research has contributed to the body of knowledge in the use of DL, an image processing technique, in photovoltaics to identify defective PV cells. The following section will discuss the practical contributions of this research.

### **7.3.2 Practical Contributions**

This research also made a practical contribution. The practical contributions that have been identified for this research are:

- The creation of PV cell EL image dataset
- A classified dataset of EL images of PV cells.
- Trained image classification models that can be used to classify EL images of PV cells.
- Image classification results after evaluating the models.

The EL images received from the Physics Department at NMU was of PV modules, however, it was explained in Section 2.2.4.1 that the analysis of the images will be done on a cell level (Section 2.2.4.1). Therefore, the EL images were pre-processed to obtain PV cell EL image (Section 5.3.1). This enabled the creation of a dataset containing PV cell EL images.

The PV cell EL images obtained in Section 5.3.2.2 were then classified. The PV cell EL images were initially classified using a binary classifier to represent normal and defective PV cells (Section

5.3.2.2). The EL images were further classified using a multi-class classifier into four classes namely; normal, uncritical, critical and very critical (Section 5.3.2.2). This provided the classified dataset of EL images of PV cells.

Trained image classification models that can be used to classify EL images of PV cells were a contribution of this research. The image classification models were obtained from the experiments that were performed in this research (Section 5.5). It was identified in Section 5.4 to use the LeNet, MobileNet and Xception DL CNN architectures for this research.

The final practical contribution of this research were the image classification results after evaluating the adaptive models. The result suggested that an image processing technique can indeed be used to identify defective PV cells from EL images, but not yet as effectively as possible. The following section will discuss the problems and limitation encountered in this research.

## **7.4 Problems Encountered**

Several problems were encountered throughout this project. One of these problems was that the number of normal samples outweighed the number of defective samples from the EL images. Data augmentation was incorporated into the implementation of the experiments to help mitigate this problem. Furthermore, the initial dataset that was obtained from the initial set of images received was not sufficient. Therefore, more images had to be requested from the Physics Department at NMU.

Another problem that was encountered in the early stages of this research was a lack of computation power, as experiments were performed on a PC CPU. However, a GPU was provided by the Computing Sciences Department at NMU which resulted in experiments being performed much faster.

## **7.5 Limitation and Recommendations for Future Research**

This section will discuss the limitations of this research and recommendations for possible future research. Ideally, experiments should be conducted on all existing DL CNN architectures. Therefore, I would recommend exploring more DL CNNs to deduce which adaptive models would attain a higher precision and recall and alternatively more accurately identify defective PV cells from EL images. Furthermore, research can be conducted to develop a DL CNN that can be specifically designed to cater for photovoltaics.

Secondly, the proposed solution (Section 5.2) did not cater for defects of abnormalities that occur in PV cell materials but do not affect the performance of the PV cell. This would require further refinement of the classified dataset that emerged from this research.

Furthermore, the adaptive models obtained from various experiments can be incorporated into systems used to take EL images. The resulting EL images from the system could be labelled according to the nature of each cell in the PV module. However, the adaptive models would have to be robust enough to ensure that defects are identified, regardless of the orientation in which the EL image is taken. In addition, further research can be conducted to improve the effectiveness of the adaptive models that were obtained in this research.

Lastly, other defect detection techniques can be investigated to determine whether they are able to identify defective PV cells from EL images more effectively. Specifically, techniques that do not require a large dataset to produce an effective EL image classifier could be investigated.

## 7.6 Summary

The focus of this research was to investigate whether image processing can be used to identify defective PV cells from EL images effectively. This research addressed the issue that no automated process could be found whereby defective polycrystalline PV cells are classified, according to known standards from EL images. The outcome of this research was adaptive models that can be used to classify EL images of PV cells.

The positivist philosophy, deductive approach and experimental strategy were applied to this research (Section 2.2). These choices were influenced by the experimental research methodology (Section 2.3) that was utilised by this research. The experiments that were designed in this research (Section 5.3) as a result of the research methodology were used to study causal links between variables within EL images.

Existing techniques of identifying defective PV cells (Section 3.5) were reviewed which revealed the constraints that exist within these techniques. It was revealed that EL images were analysed manually in order to identify defects which is a tedious process. Integration between an existing method of identifying PV cell defects and computer vision was therefore proposed (Section 3.6) to automate the process of identifying defective PV cells from EL images.

Image processing was a task within computer vision that was identified to be used for the proposed integration between photovoltaics and computer vision. Through a literature review on image processing (Section 4.3), it was identified that DL was the image processing techniques that was suitable for this research. It was later revealed through literature (Sections 4.3.3 and 4.3.4) and

related work (Section 4.4) how DL can be used appropriately to identify defective PV cells from EL images. Furthermore, experiments were conducted to demonstrate the appropriate use of the image processing technique identified (Section 5.4).

The outcomes of the experiments were adaptive models that can be used to classify EL images of PV cells. The adaptive models were used to answer the MRQ:

***How can an image processing technique be used to effectively identify defective polycrystalline PV cells from EL images of such cells?***

It was concluded that an image processing technique can be used to identify defective polycrystalline PV cells from EL images of such cells.

## REFERENCES

- Acharya, T., & Ray, A. K. (2005). *Image Processing: Principles and Applications*. Hoboken: John Wiley & Sons. <http://doi.org/10.1117/1.2348895>
- Affonso, C., Rossi, A. L. D., Vieira, F. H. A., & de Carvalho, A. C. P. de L. F. (2017). Deep learning for biological image classification. *Expert Systems with Applications*, *85*, 114–122. <http://doi.org/10.1016/j.eswa.2017.05.039>
- Aggarwal, S. (2004). Principles of remote sensing. In *Satellite Remote Sensing and GIS Applications in Agricultural Meteorology* (pp. 23–38). India: World Meteorological Organisation. <http://doi.org/doi:10.1201/b10155-2>
- Al-doski, J., Mansor, S. B., Zulhaidi, H., & Shafri, M. (2013). Image Classification in Remote Sensing. *Journal of Environment and Earth Science*, *3*(10), 141–148.
- Alom, Z., Taha, T. M., Yakopcic, C., Westberg, S., Sidike, P., Nasrin, M. S., ... Asari, V. K. (2018). The History Began from AlexNet: A Comprehensive Survey on Deep Learning Approaches. [http://doi.org/10.1016/S0011-9164\(00\)80105-8](http://doi.org/10.1016/S0011-9164(00)80105-8)
- Alonso-García, M. C., Ruiz, J. M., & Chenlo, F. (2006). Experimental study of mismatch and shading effects in the I-V characteristic of a photovoltaic module. *Solar Energy Materials and Solar Cells*, *90*(3), 329–340. <http://doi.org/10.1016/j.solmat.2005.04.022>
- Ansari, M. A., Kurchaniya, D., & Dixit, M. (2017). A Comprehensive Analysis of Image Edge Detection Techniques. *International Journal of Multimedia and Ubiquitous Engineering*, *12*(11), 1–12. <http://doi.org/10.14257/ijmue.2017.12.11.01>
- Askari, M. B., Abadi, V. M. M., & Mirhabibi, M. (2015). Types of Solar Cells and Application. *American Journal of Optics and Photonics*, *3*(5), 94. <http://doi.org/10.11648/j.ajop.20150305.17>
- Balci, B., Saadati, D., & Shiferaw, D. (2017). Handwritten Text Recognition using Deep Learning. *Journal of Computing and Information Technology*, 1–18. <http://doi.org/10.1053/otsm>
- Banda, P., & Barnard, L. (2018). A deep learning approach to photovoltaic cell defect classification. In *Proceedings of the Annual Conference of the South African Institute of Computer Scientists and Information Technologists - SAICSIT '18, September 26-28* (pp. 215–221). Port Elizabeth: ACM Press. <http://doi.org/10.1145/3278681.3278707>
- Bergmann, R. B., Berge, C., Rinke, T. J., Schmidt, J., & Werner, J. H. (2002). Advances in monocrystalline Si thin film solar cells by layer transfer. *Solar Energy Materials and Solar Cells*, *74*(1–4), 213–218. [http://doi.org/10.1016/S0927-0248\(02\)00070-3](http://doi.org/10.1016/S0927-0248(02)00070-3)
- Bhardwaj, S., & Mittal, A. (2012). A Survey on Various Edge Detector Techniques. *Procedia Technology*, *4*, 220–226. <http://doi.org/10.1016/j.protcy.2012.05.033>
- Bhargava, A., & Bansal, A. (2018). Fruits and vegetables quality evaluation using computer vision: A review. *Journal of King Saud University - Computer and Information Sciences*, *30*(4), 431–

560. <http://doi.org/10.1016/j.jksuci.2018.06.002>
- Bishop, C. M. (2013). *Pattern Recognition and Machine Learning. Journal of Chemical Information and Modeling* (Vol. 53). Singapore: Springer. <http://doi.org/10.1117/1.2819119>
- Bothe, K., Sinton, R., & Schmidt, J. (2005). Fundamental boron-oxygen-related carrier lifetime limit in mono- And multicrystalline silicon. *Progress in Photovoltaics: Research and Applications*, 13(4), 287–296. <http://doi.org/10.1002/pip.586>
- Brownlee, J. (2016). *Deep Learning with Python*. Melbourne: Machine Learning Mastery.
- Budhraj, V. (2012). *Influence of Defects and Impurities on Solar Cell Performance*. New Jersey Institute of Technology. Retrieved from [https://books.google.co.za/books/about/Influence\\_of\\_Defects\\_and\\_Impurities\\_on\\_S.html?id=tcYjwEACAAJ&redir\\_esc=y](https://books.google.co.za/books/about/Influence_of_Defects_and_Impurities_on_S.html?id=tcYjwEACAAJ&redir_esc=y)
- Canny, J. (1986). A Computational Approach to Edge Detection. *IEEE Transactions on Pattern Analysis and Machine Intelligence*, PAMI-8(6), 679–698. <http://doi.org/10.1109/TPAMI.1986.4767851>
- Cha, Y. J., Choi, W., & Büyüköztürk, O. (2017). Deep Learning-Based Crack Damage Detection Using Convolutional Neural Networks. *Computer-Aided Civil and Infrastructure Engineering*, 32(5), 361–378. <http://doi.org/10.1111/mice.12263>
- Chandwadkar, R., Dhole, S., Gadewar, V., Raut, D., & Tiwaskar, S. (2013). Comparison Of Edge Detection Techniques. In *6th Annual Conference of IRAJ* (pp. 133–136). New Delhi. <http://doi.org/10.13140/RG.2.1.5036.7123>
- Chen, C., Seff, A., Kornhauser, A., & Xiao, J. (2015). DeepDriving: Learning Affordance for Direct Perception in Autonomous Driving. In *2015 IEEE International Conference on Computer Vision (ICCV)* (pp. 2722–2730). Las Condes: IEEE. Retrieved from <http://deepdriving.cs.princeton.edu/>
- Chollet, F. (2017). Xception: Deep learning with depthwise separable convolutions. In *Proceedings - 30th IEEE Conference on Computer Vision and Pattern Recognition, CVPR 2017* (Vol. 2017–Janua, pp. 1800–1807). Honolulu: IEEE. <http://doi.org/10.1109/CVPR.2017.195>
- Choras, R. S. (2007). Image feature extraction techniques and their applications for CBIR and biometrics systems. *International Journal of Biology and Biomedical Engineering*, 1(1), 6–16.
- Cireşan, D., Meier, U., & Schmidhuber, J. (2012). Multi-column Deep Neural Networks for Image Classification. In *Proceedings of the IEEE Computer Society Conference on Computer Vision and Pattern Recognition* (pp. 3642–3649). Providence: IEEE. <http://doi.org/10.1109/CVPR.2012.6248110>
- Creswell, J. (2010). *Research design: Qualitative, quantitative, and mixed method. Research design Qualitative quantitative and mixed methods approaches*. SAGE Publications. <http://doi.org/10.1088/1751-8113/44/8/085201>
- Crozier, J. (2012). *Characterization of cell mismatch in photovoltaic modules using*

- electroluminescence and associated electro- optic techniques*. Nelson Mandela Metropolitan University.
- Crozier, J., & Dyk, E. E. Van. (2015). Identification and characterisation of performance limiting defects and cell mismatch in photovoltaic modules. *Journal of Energy in Southern Africa*, 26(3), 19–26.
- de Bruijne, M. (2016). Machine learning approaches in medical image analysis: From detection to diagnosis. *Medical Image Analysis*, 33, 94–97. <http://doi.org/10.1016/j.media.2016.06.032>
- de Villiers, M. R. (2005). Interpretive research models for Informatics: action research, grounded theory, and the family of design- and development research. *Alternation*, 12.2(2), 10–52. Retrieved from [http://alternation.ukzn.ac.za/Files/docs/12.2/02 deV.pdf](http://alternation.ukzn.ac.za/Files/docs/12.2/02%20deV.pdf)
- Deng, L. (2014). A tutorial survey of architectures, algorithms, and applications for deep learning. *Sip*, 3(2), 1–29. <http://doi.org/10.1017/ATSIP.2013.99>
- Deng, L., & Yu, D. (2013). Deep Learning: Methods and Applications. *Foundations and Trends® in Signal Processing*, 7(3–4), 197–387. <http://doi.org/10.1136/bmj.319.7209.0a>
- Deng, X., Liu, Q., Deng, Y., & Mahadevan, S. (2016). An improved method to construct basic probability assignment based on the confusion matrix for classification problem. *Information Sciences*, 340–341, 250–261. <http://doi.org/10.1016/j.ins.2016.01.033>
- Dexter, D. L. (1953). A theory of sensitized luminescence in solids. *The Journal of Chemical Physics*, 21(5), 836–850. <http://doi.org/10.1063/1.1699044>
- Do, H. (2007). Image Recognition Technique using Local Characteristics of Sub-sampled Images. *Digital Image Processing*, 1–5.
- Donolato, C. (1983). Theory of beam induced current characterization of grain boundaries in polycrystalline solar cells. *Journal of Applied Physics*, 54(3), 1314–1322. <http://doi.org/10.1063/1.332205>
- Dutt, V., Chaudhry, V., & Khan, I. (2012). Pattern Recognition: an Overview. *American Journal of Intelligent Systems*, 2(1), 23–27. <http://doi.org/10.5923/j.ajis.20120201.04>
- Engelbrecht, A. P. (2007). *Computational Intelligence: An Introduction: Second Edition*. John Wiley & Sons. West Sussex: John Wiley & Sons. <http://doi.org/10.1002/9780470512517>
- Ferreira, A., & Giraldi, G. (2017). Convolutional Neural Network approaches to granite tiles classification. *Expert Systems with Applications*, 84, 1–11. <http://doi.org/10.1016/j.eswa.2017.04.053>
- Friedrichsková, K., & Horák, B. (2013). A measuring system for monitoring error artefacts in photovoltaic solar cells by the electroluminescence method. *IFAC Proceedings Volumes*, 46(28), 444–448. <http://doi.org/10.3182/20130925-3-CZ-3023.00090>
- Fu, K.-S., & Rosenfeld, A. (1976). Pattern recognition. *IEEE Transactions on Computers*, C-25(12), 1336. <http://doi.org/10.1016/j.patcog.2012.09.015>

- Fuyuki, T., Kondo, H., Yamazaki, T., Takahashi, Y., & Uraoka, Y. (2005). Photographic surveying of minority carrier diffusion length in polycrystalline silicon solar cells by electroluminescence. *Applied Physics Letters*, *86*(26), 1–3. <http://doi.org/10.1063/1.1978979>
- García-Pulido, J. A., Pajares, G., Dormido, S., & de la Cruz, J. M. (2017). Recognition of a landing platform for unmanned aerial vehicles by using computer vision-based techniques. *Expert Systems with Applications*, *76*, 152–165. <http://doi.org/10.1016/j.eswa.2017.01.017>
- Gaur, R., & Chouhan, V. S. (2017). Classifiers in Image processing. *International Journal on Future Revolution in Computer Science & Communication Engineering IJFRCSCCE*, *3*(6), 22–24. Retrieved from <http://www.ijfrcsce.org>
- Glunz, S. W., Rein, S., Warta, W., Knobloch, J., & Wettling, W. (2001). Degradation of carrier lifetime in Cz silicon solar cells. *Solar Energy Materials and Solar Cells*, *65*(1–4), 219–229. [http://doi.org/10.1016/S0927-0248\(00\)00098-2](http://doi.org/10.1016/S0927-0248(00)00098-2)
- Goetzberger, A., Hebling, C., & Schock, H. W. (2003). Photovoltaic materials, history, status and outlook. *Materials Science and Engineering: R: Reports*, *40*(1), 1–46. [http://doi.org/10.1016/S0927-796X\(02\)00092-X](http://doi.org/10.1016/S0927-796X(02)00092-X)
- Goodfellow, I., Bengio, Y., & Courville, A. (2016). Deep Learning. *Nature*, *521*(7553), 800. <http://doi.org/10.1038/nmeth.3707>
- Gray, D. E. (2004). *Doing Research in the Real World*. Sage Publications. London: SAGE.
- Guenounou, A., Malek, A., & Aillerie, M. (2016). Comparative performance of PV panels of different technologies over one year of exposure: Application to a coastal Mediterranean region of Algeria. *Energy Conversion and Management*, *114*, 356–363. <http://doi.org/10.1016/j.enconman.2016.02.044>
- Han, J., Kamber, M., & Pei, J. (2012). *Data Mining: Concepts and Techniques* (Vol. 3). Waltham: Elsevier. <http://doi.org/10.1017/CBO9781107415324.004>
- Haykin, S. (2008). *Neural Networks and Learning Machines* (Vol. 3). New Jersey: Prentice Hall/Pearson. <http://doi.org/978-0131471399>
- He, K., Zhang, X., Ren, S., & Sun, J. (2015). Delving deep into rectifiers: Surpassing human-level performance on imagenet classification. In *Proceedings of the IEEE International Conference on Computer Vision* (Vol. 2015 Inter, pp. 1026–1034). IEEE. <http://doi.org/10.1109/ICCV.2015.123>
- Honsberg, C., & Bowden, S. (2013). Manufacturing Si Cells. Retrieved November 20, 2018, from <https://www.pveducation.org/pvcdrom/welcome-to-pvcdrom/manufacturing-si-cells>
- Howard, A. G., Zhu, M., Chen, B., Kalenichenko, D., Wang, W., Weyand, T., ... Adam, H. (2017). MobileNets: Efficient Convolutional Neural Networks for Mobile Vision Applications. *CoRR*. [http://doi.org/10.1016/S1507-1367\(10\)60022-3](http://doi.org/10.1016/S1507-1367(10)60022-3)
- Hox, J. J., & Boeijs, H. R. (2005). Data Collection, Primary vs. Secondary. In *Encyclopedia of Social Measurement* (pp. 593–599). Elsevier. <http://doi.org/10.1016/B0-12-369398-5/00041-4>



- Huang, H., Xie, Q., Yao, L., Li, Y., & Chen, Q. (2018). Research on a Surface Defect Detection Algorithm Based on MobileNet-SSD. *Applied Sciences*, 8(9), 1678. <http://doi.org/10.3390/app8091678>
- Hulbert, L. (2008). Experimental Research Designs. In *Doing Social Psychology Research* (pp. 10–53). London: Blackwell Publishing Ltd. <http://doi.org/10.1002/9780470776278.ch2>
- Hussain, A., Arif, S. M., & Aslam, M. (2017). Emerging renewable and sustainable energy technologies: State of the art. *Renewable and Sustainable Energy Reviews*, 71, 12–28. <http://doi.org/10.1016/j.rser.2016.12.033>
- Johnston, M. P. (2014). Secondary Data Analysis: A Method of which the Time Has Come. *Qualitative and Quantitative Methods in Libraries (QQML)*, 3, 619–626. <http://doi.org/10.1097/00125817-200207000-00009>
- Kajari-Schröder, S., Köntges, M., Kunze, I., Breitenmoser, X., & Bjørneklett, B. (2010). Quantifying the risk of power loss in PV modules due to micro cracks. In *25th European Photovoltaic Solar Energy Conference and Exhibition* (pp. 6–10). Valencia. <http://doi.org/10.4229/25thEUPVSEC2010-4BO.9.4>
- Kamdi, S., & Krishna, R. K. (2012). Image Segmentation and Region Growing Algorithm. *International Journal of Computer Technology and Electronics Engineering*, 2(1), 2249–6343. <http://doi.org/10.4028/www.scientific.net/AMR.706-708.1799>
- Kaur, D., & Kaur, Y. (2014). Various Image Segmentation Techniques: A Review. *International Journal of Computer Science and Mobile Computing*, 3(5), 809–814. Retrieved from [www.ijcsmc.com](http://www.ijcsmc.com)
- Ker, J., Wang, L., Rao, J., & Lim, T. (2018). Deep Learning Applications in Medical Image Analysis. *IEEE Access*, 6, 9375–9389. <http://doi.org/10.1109/ACCESS.2017.2788044>
- Keras. (2017). Keras Documentation. Retrieved March 29, 2018, from <https://keras.io/>
- Köntges, M., Kurtz, S., Packard, C. E., Jahn, U., Berger, K., Kato, K., ... Van Iseghem, M. (2014). *Review of Failures of Photovoltaic Modules*. IEA-Photovoltaic Power Systems Programme. Emmerthal.
- Kriesel, D. (2005). *A Brief Introduction to Neural Networks*. [www.dkriesel.com](http://www.dkriesel.com). [http://doi.org/10.1016/0893-6080\(94\)90051-5](http://doi.org/10.1016/0893-6080(94)90051-5)
- Krig, S. (1993). Image pre-processing. In *Computer Vision Metrics* (pp. 56–111). Berkeley: Apress. [http://doi.org/10.1007/978-3-319-50490-2\\_3](http://doi.org/10.1007/978-3-319-50490-2_3)
- Krizhevsky, A., Sutskever, I., & Hinton, G. E. (2012). ImageNet Classification with Deep Convolutional Neural Networks. *Communications of the ACM*, 60(6), 84–90. Retrieved from <http://code.google.com/p/cuda-convnet/>
- Langote, V. B., & Chaudhari, D. D. S. (2012). Segmentation Techniques for Image Analysis. *International Journal of Advanced Engineering Research and Studies*, 1(2), 4.

- Latham, B. (2007). Sampling : What is it ? *Quantitative Research Methods ENGL 5377*, 1, 1–12. <http://doi.org/10.1006/cpac.2000.0439>
- LeCun, Y., Bengio, Y., & Hinton, G. (2015). Deep learning. *Nature*, 521(7553), 436–444. <http://doi.org/10.1038/nature14539>
- LeCun, Y., Haffner, P., Bottou, L., & Bengio, Y. (1999). Object Recognition with Gradient-Based Learning. *Journal of Electronic Imaging*, 7(3), 319–345. [http://doi.org/10.1007/3-540-46805-6\\_19](http://doi.org/10.1007/3-540-46805-6_19)
- Leo, M., Medioni, G., Trivedi, M., Kanade, T., & Farinella, G. M. (2017). Computer vision for assistive technologies. *Computer Vision and Image Understanding*, 154, 1–15. <http://doi.org/10.1016/j.cviu.2016.09.001>
- Li, Q., Cai, W., Wang, X., Zhou, Y., Feng, D. D., & Chen, M. (2014). Medical image classification with convolutional neural network. In *2014 13th International Conference on Control Automation Robotics and Vision, ICARCV 2014* (Vol. 4, pp. 844–848). Singapore: IEEE. <http://doi.org/10.1109/ICARCV.2014.7064414>
- Litjens, G., Kooi, T., Bejnordi, B. E., Setio, A. A. A., Ciompi, F., Ghafoorian, M., ... Sánchez, C. I. (2017). A survey on deep learning in medical image analysis. *Medical Image Analysis*, 42(December 2012), 60–88. <http://doi.org/10.1016/j.media.2017.07.005>
- Mahsereci, M., Balles, L., Lassner, C., & Hennig, P. (2017). Early Stopping without a Validation Set. *CoRR*. Retrieved from <http://arxiv.org/abs/1703.09580>
- Mari, B., Ullah, H., & Sanchez Ruiz, L. (2016). Effect of defects on the performance of some photovoltaic solar cells : an introduction to research methods to engineering students. In *44th SEFI Conference* (pp. 12–15). Tampere: Elsevier.
- Mayekar, P., Kotmire, N. J., Wagh, M., & Shinde, N. (2016). Review on the Thermographic analysis of PV panels / system using the infrared thermal cameras. *International Journal of Scientific Engineering and Applied Science*, 2(4), 2–6.
- McGregor, S. L. T., & Murnane, J. A. (2010). Paradigm, methodology and method: intellectual integrity in consumer scholarship. *International Journal of Consumer Studies*, 34(4), 419–427. <http://doi.org/10.1111/j.1470-6431.2010.00883.x>
- Mitchell, T. (1994). *Machine Learning*. New York: McGraw-Hill Education. <http://doi.org/10.1145/242224.242229>
- Nicolosi, L., Abt, F., Blug, A., Heider, A., Tetzlaff, R., & Höfler, H. (2012). A novel spatter detection algorithm based on typical cellular neural network operations for laser beam welding processes. *Measurement Science and Technology*, 23(1). <http://doi.org/10.1088/0957-0233/23/1/015401>
- Nogueira, C. E. C., Bedin, J., Niedzialkoski, R. K., De Souza, S. N. M., & Das Neves, J. C. M. (2015). Performance of monocrystalline and polycrystalline solar panels in a water pumping system in Brazil. *Renewable and Sustainable Energy Reviews*, 51, 1610–1616. <http://doi.org/10.1016/j.rser.2015.07.082>

- Nowotny, J., Dodson, J., Fiechter, S., Gür, T. M., Kennedy, B., Macyk, W., ... Rahman, K. A. (2018). Towards global sustainability: Education on environmentally clean energy technologies. *Renewable and Sustainable Energy Reviews*, 81(June 2016), 2541–2551. <http://doi.org/10.1016/j.rser.2017.06.060>
- OpenCV team. (2018). About - OpenCV library. Retrieved March 29, 2018, from <https://opencv.org/about.html>
- Oquab, M., Bottou, L., Laptev, I., & Sivic, J. (2014). Learning and transferring mid-level image representations using convolutional neural networks. In *Proceedings of the IEEE Computer Society Conference on Computer Vision and Pattern Recognition* (pp. 1717–1724). Columbus: IEEE. <http://doi.org/10.1109/CVPR.2014.222>
- Pan, S. J., & Yang, Q. (2010). A survey on transfer learning. *IEEE Transactions on Knowledge and Data Engineering*, 22(10), 1345–1359. <http://doi.org/10.1109/TKDE.2009.191>
- Patterson, J., & Gibson, A. (2017). *Deep Learning: A Practitioner's Approach*. Newton: O'Reilly Media, Inc. <http://doi.org/10.1016/B978-0-12-391420-0.09987-X>
- Phillips, A. B., Song, Z., Dewitt, J. L., Stone, J. M., Krantz, P. W., Royston, J. M., ... Heben, M. J. (2016). High speed, intermediate resolution, large area laser beam induced current imaging and laser scribing system for photovoltaic devices and modules. *Review of Scientific Instruments*, 87(9). <http://doi.org/10.1063/1.4962940>
- Pierdicca, R., Malinverni, E. S., Piccinini, F., Paolanti, M., Felicetti, A., & Zingaretti, P. (2018). Deep convolutional neural network for automatic detection of damaged photovoltaic cells. *International Archives of the Photogrammetry, Remote Sensing and Spatial Information Sciences - ISPRS Archives*, 42(2), 893–900. <http://doi.org/10.5194/isprs-archives-XLII-2-893-2018>
- Prechelt, L. (2012). Early stopping - But when? In *Neural Networks: Tricks of the Trade* (Vol. 7700, pp. 53–67). Berlin: Springer. <http://doi.org/10.1007/978-3-642-35289-8-5>
- Rabha, M. B., Dimassi, W., Bouaïcha, M., Ezzaouia, H., & Bessais, B. (2009). Laser-beam-induced current mapping evaluation of porous silicon-based passivation in polycrystalline silicon solar cells. *Solar Energy*, 83(5), 721–725. <http://doi.org/10.1016/j.solener.2008.11.002>
- Rao, K. M. M. (2006). Overview of Image Processing. In *Proceedings of 2006 International Conference on Image Processing, Computer Vision, & Pattern Recognition* (pp. 1–7). Las Vegas: CSREA Press.
- Rawat, W., & Wang, Z. (2017). Deep Convolutional Neural Networks for Image Classification: A Comprehensive Review. *Neural Computation*, 29(9), 2352–2449. [http://doi.org/10.1162/neco\\_a\\_00990](http://doi.org/10.1162/neco_a_00990)
- Sahoo, P. K., Soltani, S., & Wong, A. K. C. (1988). A survey of thresholding techniques. *Computer Vision, Graphics and Image Processing*, 41(2), 233–260. [http://doi.org/10.1016/0734-189X\(88\)90022-9](http://doi.org/10.1016/0734-189X(88)90022-9)
- Sahu, M., Saxenaa, A., & Manoria, M. (2015). Application of Feature Extraction Technique : A

- Review. (*IJCSIT International Journal of Computer Science and Information Technologies*, 6(3), 3014–3016.
- Saunders, M., Lewis, P., & Thornhill, A. (2008). *Research Methods for Business Students. Research methods for business students*. London: Pearson Education Ltd. <http://doi.org/10.1007/s13398-014-0173-7.2>
- Saunders, M., Lewis, P., & Thornhill, A. (2009). Understanding research philosophies and approaches. *Research Methods for Business Students* 4, 106–136. <http://doi.org/10.1176/appi.ajp.162.10.1985>
- Schill, C., Brachmann, S., & Koehl, M. (2015). Impact of soiling on IV-curves and efficiency of PV-modules. *Solar Energy*, 112, 259–262. <http://doi.org/10.1016/j.solener.2014.12.003>
- Schmidhuber, J. (2015). Deep Learning in neural networks: An overview. *Neural Networks*, 61, 85–117. <http://doi.org/10.1016/j.neunet.2014.09.003>
- Sharifi, M., Fathy, M., & Mahmoudi, M. T. (2002). A classified and comparative study of edge detection algorithms. In *Proceedings. International Conference on Information Technology: Coding and Computing* (pp. 5–8). Las Vegas. <http://doi.org/10.1109/ITCC.2002.1000371>
- Shen, D., Wu, G., & Suk, H.-I. (2017). Deep Learning in Medical Image Analysis. *Annual Review of Biomedical Engineering*, 19(1), 221–248. <http://doi.org/10.1146/annurev-bioeng-071516-044442>
- Shrivakshan, G. T., & Chandrasekar, D. C. (2012). A Comparison of various Edge Detection Techniques used in Image Processing. *International Journal of Computer Science Issues*, 9(5), 269–276. Retrieved from <http://www.ijcsi.org/papers/IJCSI-9-5-1-269-276.pdf>
- Shu, L., Mclsaac, K., Osinski, G. R., & Francis, R. (2017). Unsupervised feature learning for autonomous rock image classification. *Computers and Geosciences*, 106(May), 10–17. <http://doi.org/10.1016/j.cageo.2017.05.010>
- Simonyan, K., & Zisserman, A. (2015). Very Deep Convolutional Networks For Large-Scale Image Recognition. In *International Conference on Learning Representations*. San Diego: McMillan. Retrieved from <http://www.robots.ox.ac.uk/>
- Sokolova, M., & Lapalme, G. (2009). A systematic analysis of performance measures for classification tasks. *Information Processing and Management*, 45(4), 427–437. <http://doi.org/10.1016/j.ipm.2009.03.002>
- Spampinato, C., Palazzo, S., Giordano, D., Aldinucci, M., & Leonardi, R. (2017). Deep learning for automated skeletal bone age assessment in X-ray images. *Medical Image Analysis*, 36, 41–51. <http://doi.org/10.1016/j.media.2016.10.010>
- Srivastava, N., Hinton, G., Krizhevsky, A., Sutskever, I., & Salakhutdinov, R. (2014). Dropout: A Simple Way to Prevent Neural Networks from Overfitting. *Journal of Machine Learning Research*, 15, 1929–1958. <http://doi.org/10.1214/12-AOS1000>
- Sze, V., Chen, Y., & Yang, T. (2017). Efficient Processing of Deep Neural Networks : A Tutorial and

- Survey. *Proceedings of the IEEE*, 105(12), 2295–2329.
- Szegedy, C., Liu, W., Jia, Y., Sermanet, P., Reed, S., Anguelov, D., ... Rabinovich, A. (2014). Going Deeper with Convolutions. In *2015 IEEE Conference on Computer Vision and Pattern Recognition (CVPR)* (pp. 1–9). Boston: IEEE.
- Tao, X., Xu, D., Ma, W., Zhang, D., & Liu, X. (2018). Automatic Metallic Surface Defect Detection and Recognition with Convolutional Neural Networks. *Applied Sciences*, 8(9), 1575. <http://doi.org/10.3390/app8091575>
- TensorFlow. (2018). Retrieved March 29, 2018, from <https://www.tensorflow.org/>
- Wahab, N., Khan, A., & Lee, Y. S. (2017). Two-phase deep convolutional neural network for reducing class skewness in histopathological images based breast cancer detection. *Computers in Biology and Medicine*, 85(November 2016), 86–97. <http://doi.org/10.1016/j.combiomed.2017.04.012>
- Wu, R., Yan, S., Shan, Y., Dang, Q., & Sun, G. (2015). Deep Image: Scaling up Image Recognition. *CoRR*, (2). <http://doi.org/10.1007/3-540-60220-8>
- Wu, S., Zhong, S., & Liu, Y. (2017). Deep residual learning for image steganalysis. *Multimedia Tools and Applications*, pp. 1–17. <http://doi.org/10.1007/s11042-017-4440-4>
- Zhang Jin-Yu, C. Y. H. X. (2009). Edge detection of images based on improved Sobel operator and genetic algorithms. *2009 International Conference on Image Analysis and Signal Processing*, (3), 31–35. <http://doi.org/10.1109/IASP.2009.5054605>
- Zhang, T., & Yu, B. (2005). Boosting with early stopping: Convergence and consistency. *Annals of Statistics*, 33(4), 1538–1579. <http://doi.org/10.1214/009053605000000255>
- Zheng, Y., Rao, J., & Wu, L. (2010). Edge detection methods in digital image processing. In *Computer Science and Education (ICCSE), 2010 5th International Conference on* (pp. 471–473). Hefei: IEEE.

# APPENDICES

## Appendix A – Article

### A Deep Learning Approach to Photovoltaic Cell Defect Classification

P. Banda

Department of Computing Science,  
Nelson Mandela University  
P.O. Box 77000  
Port Elizabeth, 6031, South Africa  
s212386832@mandela.ac.za

L. Barnard

Department of Computing Science,  
Nelson Mandela University  
P.O. Box 77000  
Port Elizabeth, 6031, South Africa  
Lynette.Barnard@mandela.ac.za

#### ABSTRACT

The aim of this paper is to determine whether photovoltaic (PV) cells can be automatically identified as either defective or normal from electroluminescence (EL) images. This paper utilizes an experimental methodology to address the identified research problem. This paper provides evidence that deep learning (DL) can be used to distinguish between a defective and a normal PV cell. The results of this research confirm that techniques from the Computer Science discipline can be applied in photovoltaics to alleviate the tedious processes used in identifying defective PV cells from EL images.

#### CCS CONCEPTS

• **Computing methodologies** → **Machine learning**; *Machine learning approach* • **Applied computing** → **Physical science and engineering**; Physics

#### KEYWORDS

Deep learning; Machine learning; Photovoltaic; Electroluminescence.

#### ACM Reference format:

Peter Banda and Lynette Barnard. 2018 . A Deep Learning Approach to Photovoltaic Cell Defect Classification. In *Proceedings of SAICSIT '18, Port Elizabeth, South Africa, September 26 – 28, 2018*, 7 pages. <https://doi.org/10.1145/3278681.3278707>

Permission to make digital or hard copies of all or part of this work for personal or classroom use is granted without fee provided that copies are not made or distributed for profit or commercial advantage and that copies bear this notice and the full citation on the first page. Copyrights for components of this work owned by others than ACM must be honored. Abstracting with credit is permitted. To copy otherwise, or republish, to post on servers or to redistribute to lists, requires prior specific permission and/or a fee. Request permissions from [Permissions@acm.org](mailto:Permissions@acm.org).

SAICSIT '18, September 26–28, 2018, Port Elizabeth, South Africa  
© 2018 Association for Computing Machinery.  
ACM ISBN 978-1-4503-6647-2/18/09...\$15.00  
<https://doi.org/10.1145/3278681.3278707>

#### 1 INTRODUCTION

Climate change resulting from the increased use of fossil fuels has resulted in a call for pollutant free technologies that can be used to harness electricity from different energy sources [18]. One device that emerged from this call of pollutant free technologies was a solar or photovoltaic (PV) cell. An array of PV cells forms a PV panel. There are three types of solar cells, single-crystalline, polycrystalline and amorphous silicon [11,15]. This research only takes into account polycrystalline PV cells.

The performance of any type of PV cell is affected by defects [11]. Defective PV cells are a result of cracks in the cell or cells being blocked from the sun's radiation. PV cell defects can be identified using infrared imaging, large-area laser beam induced current, current-voltage (I-V) characteristic or electroluminescence (EL).

EL images were selected as the data that would be analyzed for the purpose of this research. Currently, no stand-alone automated ways of analyzing EL images in order to distinguish between normal and defective PV cells were found. The process of identifying normal and defective PV cells from EL images is a tedious, manual process.

This paper documents aspects of the research that were important in determining which techniques to use to automatically identify if a PV cell is defective. The research design section of this paper reports on the literature and existing systems that were reviewed, as well as the experimental design. The implementation and the experiment results are discussed after the research design section, followed by a discussion of different limitations of the research and a conclusion.

#### 2 RESEARCH DESIGN

The proposed solution is to automate the identification process of PV cell defects using existing image processing techniques. The proposed solution is highly experimental; therefore, an experimental research approach was taken to solve the problem. Identifying causal links between variables is the main focus of an experimental research methodology [27].

experiments. The next sections document the literature and existing systems reviewed and an outline of the experiments that were designed.

## 2.1 Literature Review

This section provides an insight into different techniques that can be used to solve the identified problem for this research through image processing. The proceeding section will discuss image processing techniques and a deep learning approach to image processing.

### 2.1.1 Image Processing

Image processing is the transformation, manipulation or the analysis of digital images [14]. An initial step in preparing images for analysis is referred to as image pre-processing. During this stage, images are either corrected or enhanced.

Image pre-processing is the normalization of an image data set which is essential for different image processing techniques. Image pre-processing usually has a positive effect on results from image analysis tasks [26]. Image pre-processing is done before certain image processing techniques are applied. Image pre-processing is vital in determining areas of interest within images.

Figure 1 shows the schematics of a pattern/image recognition system indicating how image pre-processing is performed on images before feature extraction in an image recognition system. Image recognition is identified as a technique to solve the EL image classification problem present in photovoltaics.

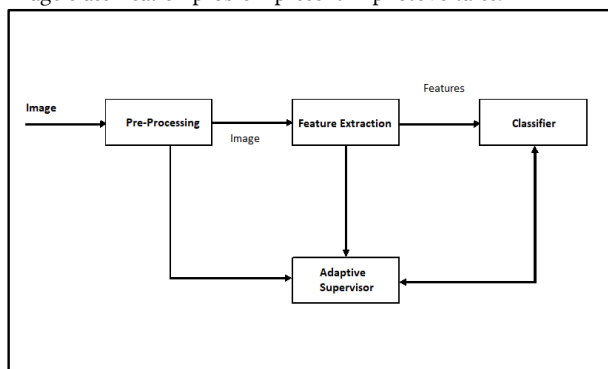


Figure 1: **Pattern/image recognition system schematic** [16].

Image classification is a technique that goes hand in hand with image recognition and was proposed to solve the identified problem. Figure 1 shows that a classifier aspect is included within image recognition systems. Image classification is important for this research, especially when distinguishing between normal and defective PV cells. There are two main types of classification namely, supervised and unsupervised classification [3]. The Deep Learning (DL) approach discussed in Section 2.1.2 utilizes supervised learning which uses similar principles to those in supervised image classification. Image classification can only be carried out after some image processing has been performed on images.

Image processing consists of different techniques that can be performed on images. One of these techniques is feature extraction, which is used in image recognition. Feature extraction is the process of extracting features within the image that best describes the content of the image [8].

Edge detection is another technique within image processing. Edge detection is one of the most basic tasks in image processing and recognition [32]. Edge detection is important for performing image segmentation on images.

Image segmentation is a major problem in image processing and one technique used to solve segmentation is thresholding [20]. Image segmentation is the process of splitting an image into independent regions that can be processed separately.

Computer vision applications utilize most of the above-mentioned techniques. In recent years, deep learning (DL) has been applied to computer vision applications as an alternative to some of the above-mentioned techniques. The following section will discuss a DL approach to image processing and image recognition.

### 2.1.2 Deep Learning Approach

For this paper, image recognition was identified as a technique that could be used for pattern and feature detection in EL images. Image recognition is an aspect of image processing. In essence, image recognition is the identification of features within an image. This is carried out by mapping parts of the image to descriptors of the content within said part [14]. Image and pattern recognition form a branch in machine learning [5].

Machine learning (ML) is defined as the change in a system that carries out tasks related to artificial intelligence (AI) [25]. This gives computer systems the ability to learn from different types of data without being explicitly programmed. More complex problems are attempted using DL [21]. DL is a class within machine learning utilized in this paper to solve the problem of identifying defective cells within the field of photovoltaics. Convolutional neural networks (CNN) are a fundamental part of DL and best describes the learning method within deep learning. CNNs have over the years, become useful in image recognition and image classification [12,22]. In addition, CNN architectures are the best representation of DL methods [1]

Neural networks (NN) are modeled from the human brain and nervous system [17,19]. CNNs use fewer parameters for their learning algorithms in comparison to traditional fully-connected NN. The basic structure of a CNN architecture is described below [13]:

1. **Input layer**: data is fed into the network through this layer. Raw image pixels can form part of this input data.
2. **Convolution layer**: a convolution is an operation on two functions. The convolution layer consists of a function of images input values and filter function. The filter highlights patterns that can be used in characterizing input images. The dot product of the two functions gives an output.

**Rectified Linear Unit (ReLU)**: ReLU layers are used to apply non-linear functions to outputs of previous

1. functions. The functions are used to improve the training performance of CNNs.
2. **Pooling layer** : the pooling layer is found in between convolution and ReLU layers. This is how CNNs result in using fewer parameters in the learning process. As a result, the network only focuses on the most important patterns.
3. **Fully-connected layer**: every neuron from all the other layers is connected in this layer. This is done to get an understanding of all the patterns generated in the preceding layers. This layer computes the possible score for the different classes used to train the network on.
4. **Loss layer**: this is usually the last layer of a network. The aim of this layer is to evaluate how much the predictions from the trained model deviate from the true labels.

One important thing to note is that in DL the feature extraction from the layers mentioned above is not engineered, but rather learned from a general-purpose learning procedure [21]. The following section will discuss areas in which DL has been applied to carry out image processing tasks, including image analysis.

## 2.2 Related Work

This section explores some areas in which DL techniques have been applied to solve problems similar to that of distinguishing between normal and defective PV cells. The preceding sections will discuss the use of DL in medical image analysis and its use in feature learning and image classification.

### 2.2.1 Medical Image Analysis

AI paradigms were adopted as early as the 1970s in medicine [28]. The rise of hand-crafted feature extraction techniques resulted in the use of ML in medical image analysis. The ability of CNNs to recognise and classify images has allowed DL to be one of the leading techniques in medical image classification.

CNNs can be utilized in the case of both 2-dimensional and 3-dimensional structures of organs, in order to distinguish between

tomography (CT) scans, magnetic resonance imaging (MRI), positron emission tomography and retinal photography [22,30].

Based on the images mentioned above, there are a few areas in which DL is continually being used. The ability of CNNs to process 3-D images allows for analysis to be performed on brain images, which are obtained from MRIs [22].

Retinal images are another type of images that have been subjected to CNNs for analysis. As a result, applications have been developed that can detect retinal abnormalities and diagnose eye diseases [22].

The complexity of medical images allows for a DL approach to be taken to automate medical systems that use retinal images and MRIs. These medical systems are usually used to diagnose patients. Existing MRIs and retinal images are used to train CNNs that are incorporated in the medical systems. The resulting models can take in as an input different images and predict a single diagnosis based on the labels of the images used to train the model.

### 2.2.2 Feature Learning and Classification

DL is continually being used to solve pattern/feature extraction, image recognition and classification problems [2]. One area in which feature learning/extraction and classification are being used is handwritten text recognition [4]. Handwritten text recognition poses a challenge due to the variation of writing styles from different writers. CNNs have the ability to learn different handwritten text representations.

Besides handwritten text recognition, CNNs have also been used in the classification of different images. A very common problem solved by CNNs is the cat-vs-dog problem [23]. Figure 2 shows what is involved in training a CNN model and how predictions are made from a test set. The CNN is represented by feature vector space in Figure 2. Similarly to the photovoltaics

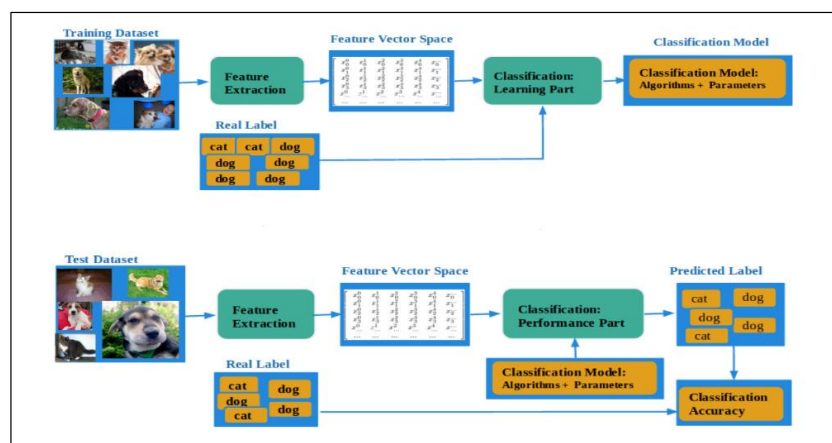


Figure 2: Learning and prediction architecture for the cat-vs-dog problem [23].

normal or abnormal organ structures [29]. Some of the common images used for medical analysis include: X-rays, computed



problem, the cat-vs-dog problem requires a feature extraction component in order to solve it. The proposed solution discussed in this paper needs to have the ability to differentiate between features extracted from normal and defective PV cells.

In the automotive industry, DL allows for the possibility of traffic sign recognition, which is helpful with driver assist technologies [9].

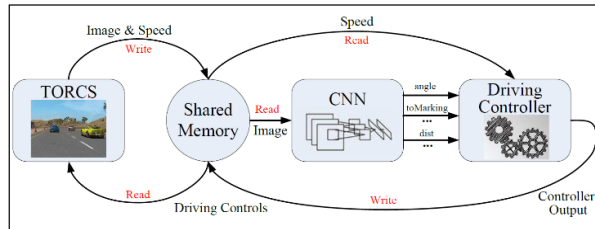


Figure 3: Driver assist system architecture [7].

Figure 3 shows how a captured image is read into a pre-trained CNN (CNN model) and the resulting prediction is responsible for adjusting driving controls. For instance, a speed sign indicating a necessary reduction in speed can trigger an output control to slow down a car. The same principle is applied to the proposed solution in the sense that the trained model makes a prediction responsible for the distinction between normal and defective PV cells.

The next session discusses how experiments for this research were designed based on some of the principles highlighted in this section.

### 2.3 Experimental Design

This section discusses the framework in which the experiments for this research were conducted, based on the reviewed literature and related work. The outcome of the research has to be evaluated from data gathered and from the variables present in the data [10]. This research used EL images that were obtained from the Physics department at Nelson Mandela University.

The EL images were intended to be used to train a CNN and based on the performance, it would then be deduced whether DL could be an appropriate approach to solving the identified problem. The images would have to be augmented during training of the CNN to cater for different possible orientations when testing the model ability to make predictions. This is due to the fact that all obtained images of the initial dataset were of a single orientation. Figure 4 shows samples of the images used for this research. Figure 4-A represents a normal PV cell and Figure 4-B to 4-D represent the different defective cells.

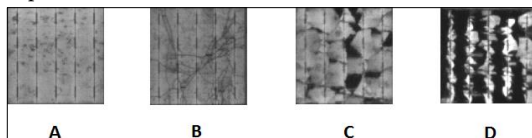


Figure 4: A - normal PV cell; B to D - variation of defective PV cells.

One immediate concern when designing the experiments was the number of images in the dataset obtained from the data provided. The dataset was small, which would most likely lead to overfitting during training. Overfitting is a result of a model overcompensating when determining relationships from training data [31]. This results in noise within the data being considered as useful.

The experiments were used to deduce whether normal or defective PV cells can be distinguished by a DL model using EL images. The image set was split into two classes in order to train the DL model. The two image classes represented normal and defective PV cells.

The experiments and the experiment results are discussed in the next section. The next section also includes a discussion of the different CNN model architectures that were implemented from the experiments.

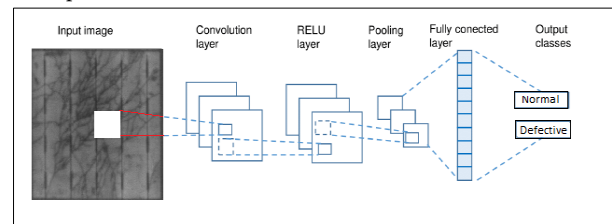


Figure 5: Basic CNN architecture for image classification.

Figure 5 is a visualization of a basic CNN architecture which was discussed in section 2.1.2. This architecture is used as a basis of all the models implemented in the next section.

## 3 IMPLEMENTATION AND EXPERIMENT

The experiments outlined in the previous section were implemented in Python and was coupled with Keras and Tensorflow libraries. The implemented experiments were run on a Mecer Proficient PC, with an i7 - 4790 processor, 3.60 GHz, 16 GB of ram, a Nvidia GeForce GTX 1080 graphics card with 8 GB dedicated memory and running on Windows 10 OS.

The initial experiments were to determine whether DL could be used to solve the problem at hand and whether the data provided was suitable for the experiments. Three model architectures were tested to help confirm whether DL could be used as an approach for automatically identifying defective PV cells from EL images.

EL images of normal and defective PV cells formed the two classes for the initial experiments. A total of 600 images from both classes were used to train the model. An additional 48 images not belonging to the training set were used for validation. The validation data was used to determine and approximate number of epochs to use for training, and the process will be discussed in the following section. And lastly, 10 images not from either the training or validation sets were reserved to test the trained model. An experiment was performed to determine an approximate number of epoch to use for the rest of the experiments. An epoch

is a single pass through the training set while training a model. The number of epochs to use were approximated using a technique known as early stopping. In addition, early stopping ensures that models are trained without overfitting. The validation accuracy from the performance of the model was used to determine the number of epochs.

Early stopping is achieved with the aid of checkpoints which allow for a model to be monitored during training and in turn deduce when the maximum validation accuracy was achieved. The training process (fitness function) was terminated after 149 epochs as depicted in Figure 6. A patience of 50 was used in this case which indicate that the model validation accuracy did not improve after the 99<sup>th</sup> epoch.

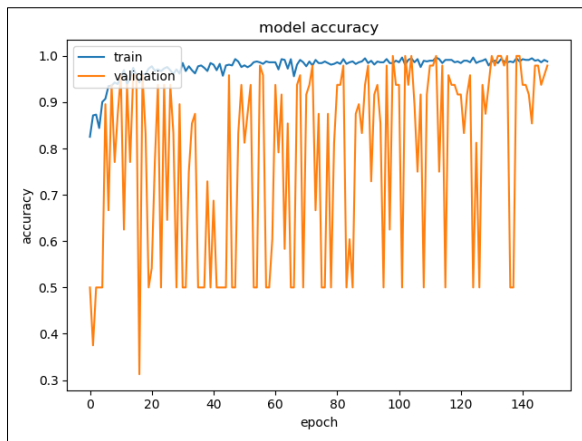


Figure 6: visualizing when training was terminated.

The three model architectures that were used in the initial experiments to help confirm the DL approach were, a simplified adaption of the LeNet, the CifarCNN architecture, and the GoogleNet architecture. Models in Keras use Stochastic gradient descent (SGD) as the training algorithm [6]. In addition, root mean square propagation was used to optimize the learning algorithm.

All three implemented models were run over 100 epochs based on the earlier experiment. Therefore, all three models iterated through all the images in the training set a hundred times before the models were completely trained. The accuracy of all the models trained were plotted in Figures 7-9 below.

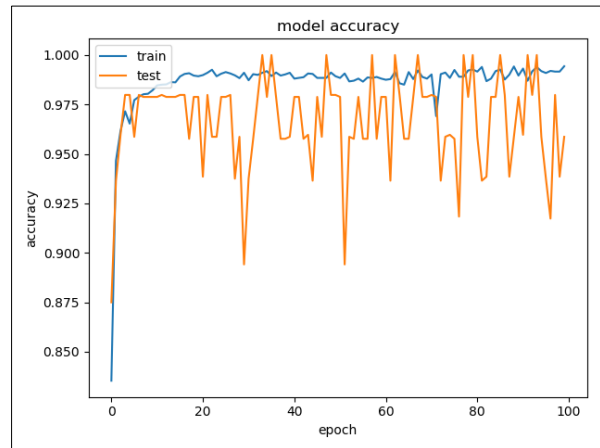


Figure 7: Epoch vs. Accuracy LeNet.

Figure 7 shows the performance accuracy plotted of the model adapted from the LeNet model architecture while it was being trained. The graph above shows that the model had a resulting performance accuracy of 99%.

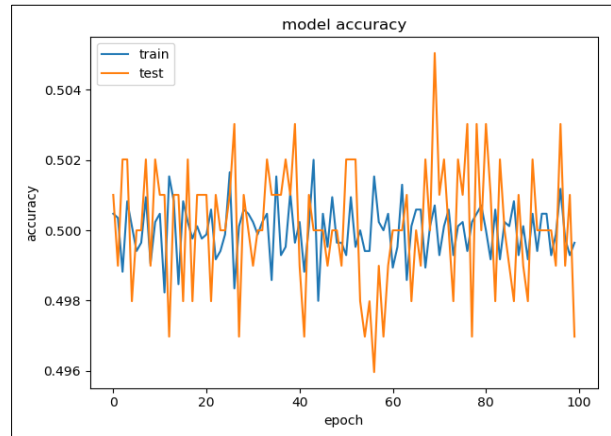


Figure 8: Epoch vs. Accuracy CifarCNN.

Figure 8 shows the performance accuracy of the CifarCNN model architecture for each of the 100 epochs. The training graph in Figure 8 shows that the performance of the model constantly revolved around 50% during the course of the training process.

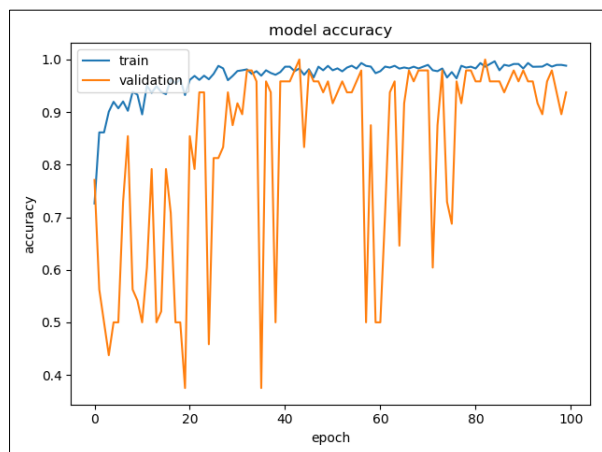


Figure 9: Epoch vs. Accuracy GoogleNet.

Figure 9 shows the performance accuracy of the GoogleNet model during training up until 100 epochs were completed. The training graph in Figure 9 shows that the model had a 98% performance accuracy.

Fortunately, the model adapted from the LeNet architecture and the GoogleNet architecture performed well on the data used to train the models. This provided an initial confirmation that DL could indeed be used to solve the problem at hand and was an appropriate approach to use in solving the problem. The trained models could predict all the images in the test set as being normal or defective correctly. The CifarCNN, did not perform as well as hoped and was crossed off the list of model architectures to use when further refining the proposed solution.

On the other hand, the validation graphs in Figures 7-9 were erratic. This was an indication that the validation set was not large enough. Therefore, the validation data set has to be increased for the refinement of the proposed solution.

The model loss of one of the model architectures that performed well was plotted in Figure 10. The figure was plotted to determine whether overfitting occurred during training.

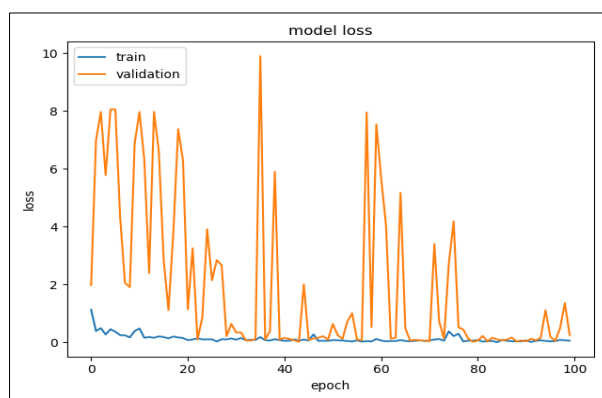


Figure 10: Epoch vs. Loss GoogleNet.

The model loss for the GoogleNet architecture was selected and is depicted in Figure 10. The gradual decrease in the loss present in Figure 10 was an indication that overfitting did not occur. The same erratic behavior present in Figures 7-9 was present in Figure 10, which confirmed that the validation set was indeed not large enough.

#### 4 LIMITATIONS

This paper is part of a research project that aims at classifying PV cells into four MBJ PV cell classes. MBJ is an innovation solutions company that offers different PV related products ranging from sun simulators, EL test systems, and test systems for insulation and ground testing for PV module testing [24]. The four classes mentioned are adopted from the EL test system. The classes represent normal, uncritical, critical and very critical PV cells.

This paper focuses on a binary classification, and the two classes represented normal and defective PV cell as mentioned in Section 2.3. The experimental results confirmed that normal and defective PV cells could be predicted with 98% certainty.

Even though the accuracy from the experiment results were high, it might not be the best representation of what might happen when four classes were taken into account. The differences between the classes might be very difficult to distinguish, resulting in a poor performance of the DL model.

#### 5 CONCLUSIONS

In this paper, a proposal was made to use DL as a technique of automatically identifying defective PV cells. Experiments on different DL model architectures were carried out to confirm whether it was possible to solve the problem using DL and the results indicated that it was possible. Therefore, an extension to the binary classification can be implemented to cater for the four MBJ PV cell defect classes.

#### ACKNOWLEDGMENTS

This work was supported by the PV Research Group at Nelson Mandela University that provided the EL images used for the various experiments.

#### REFERENCES

- [1] Carlos Affonso, André Luis Debiasio Rossi, Fábio Henrique Antunes Vieira, and André Carlos Ponce de Leon Ferreira de Carvalho. 2017. Deep learning for biological image classification. *Expert Syst. Appl.* 85, (2017), 114–122. DOI:<https://doi.org/10.1016/j.eswa.2017.05.039>
- [2] Carlos Affonso, André Luis Debiasio Rossi, Fábio Henrique Antunes Vieira, and André Carlos Ponce de Leon Ferreira de Carvalho. 2017. Deep learning for biological image classification. *Expert Syst. Appl.* 85, (2017), 114–122. DOI:<https://doi.org/10.1016/j.eswa.2017.05.039>
- [3] Jwan Al-doski, Shattri B Mansor, Helmi Zulhaidi, and Mohd Shafri. 2013. Image Classification in Remote Sensing. *J. Environ. Earth Sci.* 3, 10 (2013), 141–148.
- [4] Batuhan Balci, Dan Saadati, and Dan Shiferaw. 2017. Handwritten Text Recognition using Deep Learning. (2017).
- [5] Christopher M Bishop. 2013. *Pattern Recognition and Machine Learning*. DOI:<https://doi.org/10.1117/1.2819119>
- [6] Jason Brownlee. 2016. Deep Learning with Python. 53, 9 (2016), 1689–1699. DOI:<https://doi.org/10.1017/CBO9781107415324.004>
- [7] Chenyi Chen, Ari Seff, Alain Kornhauser, and Jianxiang Xiao. 2018. DeepDriving: Learning Affordance for Direct Perception in

- [1] Carlos Affonso, André Luis Debasio Rossi, Fábio Henrique Antunes Vieira, and André Carlos Ponce de Leon Ferreira de Carvalho. 2017. Deep learning for biological image classification. *Expert Syst. Appl.* 85, (2017), 114–122. DOI:https://doi.org/10.1016/j.eswa.2017.05.039
- [2] Carlos Affonso, André Luis Debasio Rossi, Fábio Henrique Antunes Vieira, and André Carlos Ponce de Leon Ferreira de Carvalho. 2017. Deep learning for biological image classification. *Expert Syst. Appl.* 85, (2017), 114–122. DOI:https://doi.org/10.1016/j.eswa.2017.05.039
- [3] Jwan Al-doski, Shattri B Mansor, Helmi Zulhaidi, and Mohd Shafri. 2013. Image Classification in Remote Sensing. *J. Environ. Earth Sci.* 3, 10 (2013), 141–148.
- [4] Batuhan Balci, Dan Saadati, and Dan Shiferaw. 2017. Handwritten Text Recognition using Deep Learning. (2017).
- [5] Christopher M Bishop. 2013. *Pattern Recognition and Machine Learning*. DOI:https://doi.org/10.1117/1.2819119
- [6] Jason Brownlee. 2016. Deep Learning with Python. 53, 9 (2016), 1689–1699. DOI:https://doi.org/10.1017/CBO9781107415324.004
- [7] Chenyi Chen, Ari Seff, Alain Kornhauser, and Jianxiang Xiao. 2018. DeepDriving: Learning Affordance for Direct Perception in Autonomous Driving. *Princet. Vison&Robotics Figure 1* (2018), 1. Retrieved from <http://deepdriving.cs.princeton.edu/>
- [8] R.S. Choras. 2007. Image feature extraction techniques and their applications for CBIR and biometrics systems. *Int. J. Biol. Biomed. Eng.* 1, 1 (2007), 6–16. Retrieved from <http://www.naun.org/journals/bio/bio-2.pdf>
- [9] Dan Cireşan, Ueli Meier, and Juergen Schmidhuber. 2012. Multi-column Deep Neural Networks for Image Classification. February (2012). DOI:https://doi.org/10.1109/CVPR.2012.6248110
- [10] John W Creswell. 2014. *Research design: Qualitative, quantitative, and mixed method*. DOI:https://doi.org/10.1007/s13398-014-0173-7.2
- [11] Jacqueline Louise Crozier. 2012. Characterization of cell mismatch in photovoltaic modules using electroluminescence and associated electro-optic techniques Magister Scientiae. January (2012), 40.
- [12] Anselmo Ferreira and Gilson Giraldi. 2017. Convolutional Neural Network approaches to granite tiles classification. *Expert Syst. Appl.* 84, (2017), 1–11. DOI:https://doi.org/10.1016/j.eswa.2017.04.053
- [13] Anselmo Ferreira and Gilson Giraldi. 2017. Convolutional Neural Network approaches to granite tiles classification. *Expert Syst. Appl.* 84, (2017), 1–11. DOI:https://doi.org/10.1016/j.eswa.2017.04.053
- [14] King-Sun Fu and Azriel Rosenfeld. 1976. Pattern recognition. *Ieee Trans. Comput.* C-25, 12 (1976), 1336. DOI:https://doi.org/10.1016/j.patcog.2012.09.015
- [15] A Goetzberger, C Hebling, and H W Schock. 2003. Photovoltaic materials, history, status and outlook. *Mater. Sci. Eng. R Reports* 40, 1 (2003), 1–46. DOI:https://doi.org/10.1016/S0927-796X(02)00092-X
- [16] Ernest L Hall, Richard P Kruger, J Samuel, David L Hall, Robert W McLaren, and Gwilym S Lodwick. 1971. Survey of Preprocessing and Feature Extraction Techniques for Radiographic Images. c, 9 (1971).
- [17] S. Haykin. 2008. *Neural Networks and Learning Machines*. DOI:https://doi.org/978-0131471399
- [18] Akhtar Hussain, Syed Muhammad Arif, and Muhammad Aslam. 2017. Emerging renewable and sustainable energy technologies: State of the art. *Renew. Sustain. Energy Rev.* 71, December 2016 (2017), 12–28. DOI:https://doi.org/10.1016/j.rser.2016.12.033
- [19] David Kriesel. 2005. A Brief Introduction to Neural Networks. Retrieved August (2005), 244. DOI:https://doi.org/10.1016/0893-6080(94)90051-5
- [20] Scott Krig. 1993. Image pre-processing. *Comput. Vis. Metrics* (1993), 56–111. DOI:https://doi.org/10.1007/978-3-319-50490-2\_3
- [21] Yann Lecun, Yoshua Bengio, and Geoffrey Hinton. 2015. Deep learning. *Nature* 521, 7553 (2015), 436–444. DOI:https://doi.org/10.1038/nature14539
- [22] Geert Litjens, Thijs Kooi, Babak Ehteshami Bejnordi, Arnaud Arindra Adiyoso Setio, Francesco Ciompi, Mohsen Ghafoorian, Jeroen A.W.M. van der Laak, Bram van Ginneken, and Clara I. Sánchez. 2017. A survey on deep learning in medical image analysis. *Med. Image Anal.* 42, December 2012 (2017), 60–88. DOI:https://doi.org/10.1016/j.media.2017.07.005
- [23] Bang Liu, Yan Liu, and Kai Zhou. Image Classification for Dogs and Cats. 1–10.
- [24] MBJ Group. 2018. MBJ Solutions. Retrieved June 29, 2018 from <https://www.mbj-solutions.com/en/about-mbj/about-us/>
- [25] T Mitchell. 2012. Machine Learning. *Mach. Learn.* X (2012), 639–644. DOI:https://doi.org/10.1145/242224.242229
- [26] K.M.M. Rao. 2006. Overview of Image Processing. *Proc. a Work. image Process. pattern Recognit.* (2006), 1–7.
- [27] Mark Saunders, Philip Lewis, and Adrian Thornhill. 2008. *Research Methods for Business Students*. DOI:https://doi.org/10.1007/s13398-014-0173-7.2
- [28] Dinggang Shen, Guorong Wu, and Heung-Il Suk. 2017. Deep Learning in Medical Image Analysis. *Annu. Rev. Biomed. Eng.* 19, 1 (2017), 221–248. DOI:https://doi.org/10.1146/annurev-bioeng-071516-044442
- [29] Dinggang Shen, Guorong Wu, and Heung-Il Suk. 2017. Deep Learning in Medical Image Analysis. *Annu. Rev. Biomed. Eng.* 19, 1 (2017), 221–248. DOI:https://doi.org/10.1146/annurev-bioeng-071516-044442
- [30] C. Spampinato, S. Palazzo, D. Giordano, M. Aldinucci, and R. Leonardi. 2017. Deep learning for automated skeletal bone age assessment in X-ray images. *Med. Image Anal.* 36, (2017), 41–51. DOI:https://doi.org/10.1016/j.media.2016.10.010
- [31] Nitish Srivastava, Geoffrey Hinton, Alex Krizhevsky, Ilya Sutskever, and Ruslan Salakhutdinov. 2014. Dropout: A Simple Way to Prevent Neural Networks from Overfitting. *J. Mach. Learn. Res.* 15, (2014), 1929–1958. DOI:https://doi.org/10.1214/12-AOS1000
- [32] Chen Yan Huang Xian-xiang Zhang Jin-Yu. 2009. Edge detection of images based on improved Sobel operator and genetic algorithms. *2009 Int. Conf. Image Anal. Signal Process.* 3 (2009), 31–35. DOI:https://doi.org/10.1109/IASP.2009.5054605

## Appendix B – Results

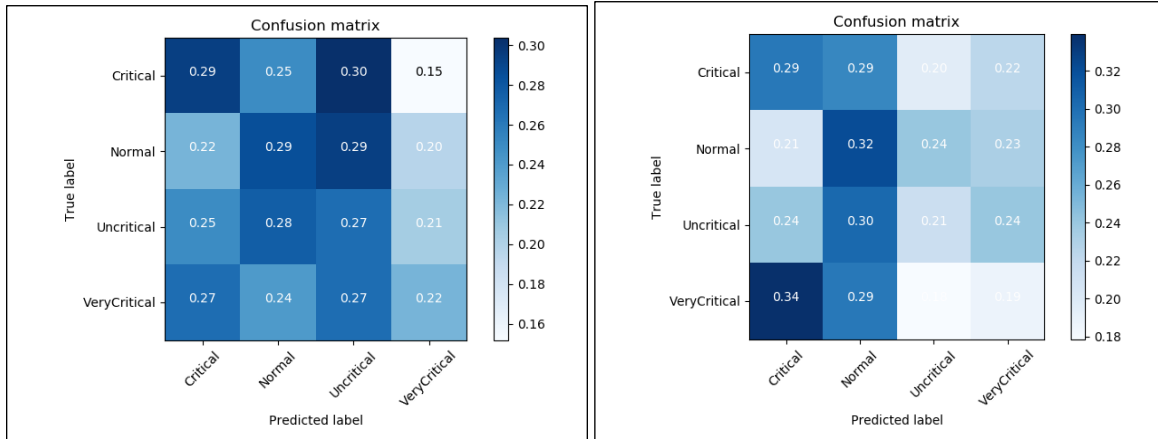


Figure B-1: LeNet – Dataset B vs. Dataset C

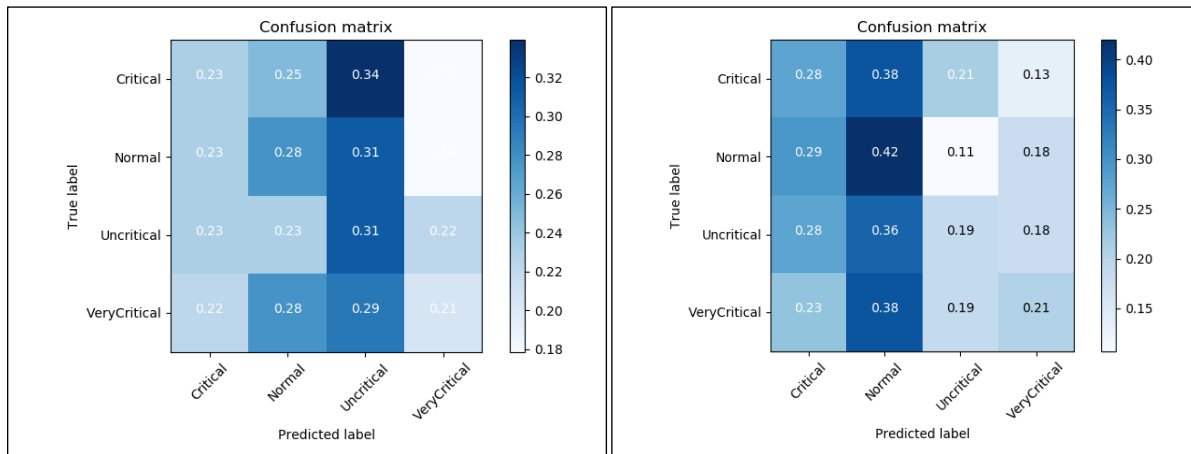


Figure B-2: MobileNet – Dataset B vs. Dataset C

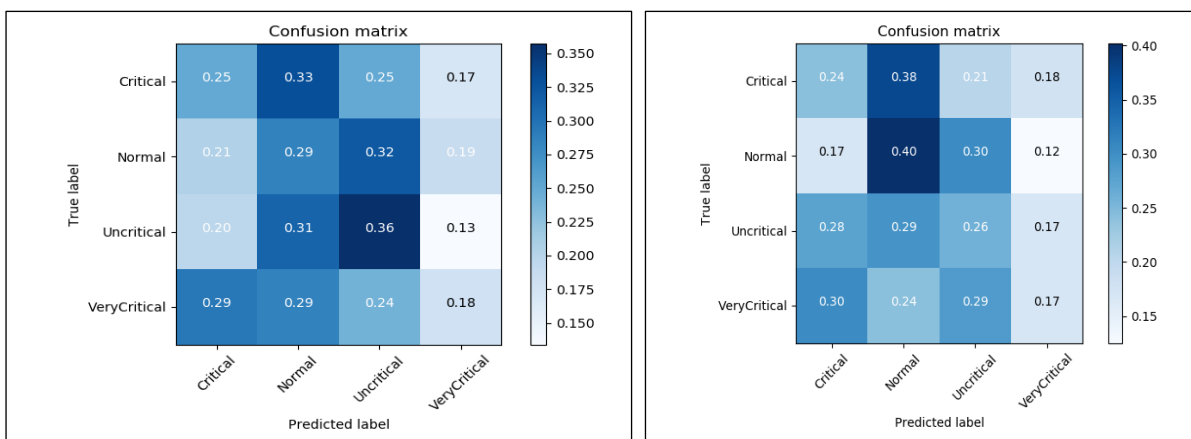
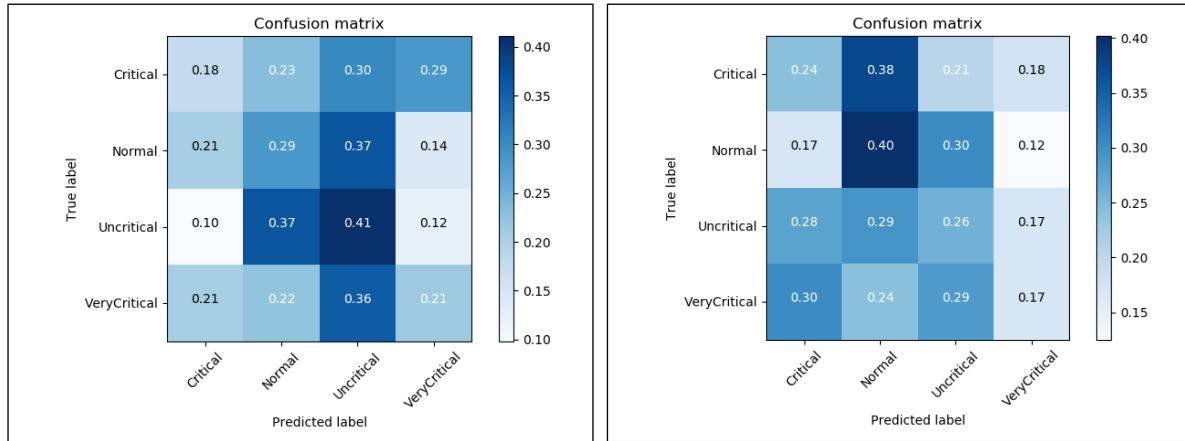


Figure B-3: Xception – Dataset B vs. Dataset C



**Figure B-4:TL Xception – Dataset C vs. Xception - Dataset C**